SAND REPORT
SAND2002-1577
Unlimited Release
Printed September 2002

Dynamic Properties of Concrete through Particle Velocity Profile Measurements

Lalit C. Chhabildas, Dennis E. Grady, Clint A. Hall, William D. Reinhart, and Gregory A. Mann

Prepared by
Sandia National Laboratories
Albuquerque, New Mexico 87185 and Livermore, California 94550

Sandia is a multiprogram laboratory operated by Sandia Corporation, a Lockheed Martin Company, for the United States Department of Energy under Contract DE-AC04-94AL85000.

Sandia National Laboratories

Issued by Sandia National Laboratories, operated for the United States Department of Energy by Sandia Corporation.

Available to DOE and DOE contractors from
U.S. Department of Energy
Office of Scientific and Technical Information
P.O. Box 62
Oak Ridge, TN 37831

Telephone: (865)576-8401
Facsimile: *(865)576-5728*
E-Mail: reports@adonis.osti.gov
Online ordering: http://www.doe.gov/bridge

Available to the public from
U.S. Department of Commerce
National Technical Information Service
5285 Port Royal Rd
Springfield, VA 22161

Telephone: (800)553-6847
Facsimile: (703)605-6900
E-Mail: orders@ntis.fedworld.gov
Online order: http://www.ntis.gov/help/ordermethods.asp?loc=7-4-0#online

SAND2002-1577
Unlimited Release
Printed September 2002

Dynamic Properties of Concrete through Particle Velocity Profile Measurements

Lalit C. Chhabildas, Dennis E. Grady, Clint A. Hall, William D. Reinhart, and Gregory A. Mann
Shock Physics Applications Department
Sandia National Laboratories
P.O. Box 5800
Albuquerque, NM 87185-1181

Abstract

Controlled gun impact and high-resolution velocity interferometery has been used to investigate a wide range of dynamic strength and equation-of-state properties of concrete. Principal Hugoniot, compression and release isentrope, and compression and tensile strength properties has been measured. The present report summarizes key findings and provides a database of velocity profile measurements. (Report and papers that address in more detail the material response issues are provided in the references.)

Intentionally Left Blank

CONTENTS

LIST OF FIGURES

Intentionally Left Blank

Executive Summary

1.0 Introduction

Planar impact experiments provide the backbone data for the development of dynamic material response models used in computational simulation and engineering analysis of the high velocity interaction of materials and structures. While such techniques do not exhaustively examine the stress-strain-time states achieved in high velocity impact events, they do target the high-confining-stress and high-strain-rate deformation characteristics of such interactions. In addition, the technology of planar impact, material response studies, and the concomitant high-resolution diagnostics of such technology have achieved maturity not available in other dynamic test methods.

Over the past several years, the DOD/DOE MOU effort at Sandia National Laboratories has actively pursued a study of the dynamic mechanical and equation-of-state properties of concrete through controlled launch impact experiments. A large number of experiments have been completed under a range of material and impact loading conditions. As these data unfold, the critical material response features are emerging, and results are impacting the development of constitutive models for concrete. High-resolution wave profile measurements have been provided exclusively by time-resolved interferometry (VISAR) diagnostics. Through novel implementation of such experiments, the critical features concerning dynamic compressibility, strength, flow, and fracture are being explored. Some unique examples of important effects revealed through shock profile studies on concrete materials include:

- Hugoniot properties that are bi-linear in their shock-velocity-versus-particle-velocity transition from pore and lattice crushing to equation-of-state dominated compliance with increasing pressure.
- Irreversible void and cementations lattice collapse with Hugoniot pressure that governs character of decompression release paths in concrete.
- A dilatancy behavior observed in release curves from higher pressures theorized to reflect crystalline elastic anisotropy during decompression.
- Finite dynamic compression and spall strength.
- Effects of aggregate size scale in the shock and release response of concrete.
- Effects of aggregate size scale in the shock and spall response of concrete.

The features noted above and other physical features of concrete materials being extracted from wave-profile measurements are providing both insights into dynamic response and critical data for constitutive model development. Reports and papers that address in more detail the material response issues outlined above are provided in the references.

It is not the intention of the authors to explore the very rich dynamic properties of concrete materials, as revealed by shock wave experiments. Rather, we seek to document the extensive database of wave profile measurements, which have been made on concrete materials, and to make this data available for the development of material response models and the validation of predictive computational codes.

This report is organized as follows: After this introduction, the next section discusses, in some detail, the experimental impact procedures and the VISAR diagnostic methods used to acquire the wave profile data. Major sections in which specific features of the dynamic response of concrete are reported follow this. Since differing techniques were used to measure each feature, a description of the experimental method, and materials involved, is included in each major section.

2.0 Experimental Methods

Controlled planar impact experiments were used in all cases to obtain the wave-profile data provided in this report. Variations in both impact geometry and in ancillary impact, materials were often used to achieve specific loading conditions or to enhance profile features characteristics of particular deformation properties of the target material. Uniaxial-strain, compressive shock, and release waves were produced in the concrete test samples. The launchers used were a single-stage compressed air gun or a powder gun. In particular, an 89 mm (inner-bore diameter), smoothbore, powder gun with a velocity range of 0.4-2.4 km/s was used for the largest portion of the shock-wave tests presented in this report.

Three electrical self-shorting pins were used to measure the velocity of the projectile at impact. Accuracy of the velocity measurement for these experiments was typically .2 % or better. Four similar pins were mounted flush to the impact plane and were used to monitor the planarity of impact. These pins were also used to trigger diagnostic equipment, including transient digitizers and counters. Deviations from planarity at impact were typically about 10^{-3} radians.

Specific target configurations are shown in the subsequent sections. Either a disc of the concrete being tested or another material of known shock properties is mounted on the projectile, and it is typically backed by (and sometimes preceded by) a lower shock impedance material. To provide an impact surface for the shorting pins within the impact plane when the impactor is less than full projectile diameter, an aluminum ring that encircles the impactor was used.

In one configuration, a disc of the concrete was mounted in a stationary supporting target fixture. An optical-quality disc of transparent window material was intimately bonded, with epoxy, to the back of this concrete sample. All critical surfaces were lapped and polished, and they were typically flat to within a few bands of sodium light. The bonding surface of the window material was first lightly diffused, and then plated by vapor-deposition with about 100 nm of aluminum. The epoxy bond between the concrete sample and the window was typically 10 to 20 nm.

In another very effective technique, a thin disc of metal (typically aluminum or copper) was mounted in the target and provided a stationary medium that introduced an impact shock into the projectile concrete.

Using laser velocity interferometry techniques (VISAR Barker and Hollenbach, 1972), the shock wave behavior was measured by monitoring the time-resolved longitudinal motion at the center of the target disc either at a free surface or at the interface between the target and the window material. Typically, the illuminated spot size of the incoming laser beam was 50 to 100 μm in diameter. Transient digitizers (with a sample period of 0.742 ns per point) were used to record the measurements. Polymethyl-methacrylate (PMMA) was the window material of choice when used. The interference fringes measured by the VISAR system were converted to time-resolved histories of the velocity of the interface using the method originally developed by Barker and Hollenbach (1972). Amplitude resolution was approximately 2% for one fringe. Typically, two to three fringes were achieved in the interface acceleration through the compressive shock front. Occasionally, shock jumps exceed the frequency response of the VISAR instrumentation, and the fringes corresponding to the velocity change are not recorded. These points are easily recognized by contrast dips in the VISAR reduction process. Integral fringes (typically one or two fringes) are added at these points to accommodate missing jumps in velocity. The required, approximate, amplitude of the missing velocity jump must be determined from other experimental and physical constraints. The high-resolution motion histories monitored by the VISAR instrumentation are frequently only indirectly related to the intrinsic concrete dynamic properties sought. Consequently, numerical simulations are commonly used to complement the data reduction process. More specific experimental details will be provided in the subsequent sections.

Impact Compression Properties of Concrete

1.0 Introduction

Controlled impact experiments have been performed on concrete to determine dynamic material properties. The properties assessed include the high-strain rate-yield strength (Hugoniot elastic limit), and details of the inelastic dynamic stress versus strain response of the concrete. The latter features entail the initial void-collapse modules, the high-stress limiting void collapse strain, and the stress amplitude dependence of the deformational wave, which loads the concrete from the elastic limit to the maximum dynamic stress state. Dynamic stress versus strain data are reported over the stress range of the data, from the Hugoniot elastic limit to, in excess of, 4 GPa.

In this study, controlled impact experiments were performed which were intended to reveal the response of concrete to transient loading conditions, and to provide a base of dynamic compression and strength data for developing constitutive response models. Specifically, a smoothbore gas gun was used to perform planar impact experiments on concrete. A maximum velocity of 2.2 km/s constrained the range of impact test data to below approximately 4.0 Gpa compressive stress. Within this stress range, statistically significant data describing the dynamic strength, compressibility and deformational wave speed of aggregate concrete were obtained.

Further discussion and analysis of this data can be found in Grady (1993a, 1993b).

2.0 Material Description

Concrete tested in the present study (SAC-5 concrete) was prepared and supplied by the Army Waterways Experimental Station (WES) (Ergott, 1993). A 15-cm by 30-cm core of concrete obtained from a larger body of material was machined to precise cylindrical dimensions. Density and ultrasonic measurements were performed on the cylinder before further machining to impact specimen dimensions was performed. Bulk densities of 2263 kg/m^3, and a longitudinal and shear elastic wave velocity of 4.45 km/s and 2.68 km/s, respectively, were determined. Ultrasonic measurements both along and across the cylindrical axis indicated isotropic elastic behavior. Density and ultrasonic properties are in good agreement with independent measurements at WES (Egrott, 1992). A crystal density of about 2550-2680 kg/m^3 and free water content of 4.1-4.8% by weight are reported for this concrete (Ergott, 1992).

3.0 Experimental Method – Reverse Ballistic Configuration

Impact experiments were performed with a single-stage light-gas gun of 100 mm inner-bore diameter capable of achieving controlled velocities over a range of approximately 50 m/s to 1 km/s. Higher-pressure experiments were performed using an 89 mm powder gun capable of impact velocities to 2.4 km/s. A reverse ballistic configuration was created (Grady and Furnish, 1988) using a disc-shaped specimen of the test concrete mounted in the projectile that underwent planar impact with a stationary diagnostic target. The principal component of the stationary target was a large poly-methyl methacrylate (PMMA) disc with an interior-reflecting interface (vapor-deposited aluminum). A diffused laser velocity interferometer (Barker and Hollenbach, 1972) was used to measure the time-resolved motion as shock waves caused by the planar impact traversed the recording interface. The impact experimental configuration is illustrated in Figure 1.

This configuration was used in this study because the method effectively averages the measured dynamic compression state over a sensibly large volume of the test sample. This feature is attractive in

heterogeneous samples such as the present aggregate concrete. A representative VISAR measurement of the interface velocity profile is illustrated in the first velocity profile. The initial velocity amplitude reflects only the impact of the projectile and target PMMA buffer plates. The second velocity amplitude is determined by the dynamic compression properties of the concrete. However, release waves from this interface do not reach the recording interface before the VISAR recording time is exceeded. Pertinent experimental dimensions are provided in Table 1 and with each profile. The concrete discs were approximately 10 cm in diameter. The target buffer and window assemblies were approximately 15 cm in diameter.

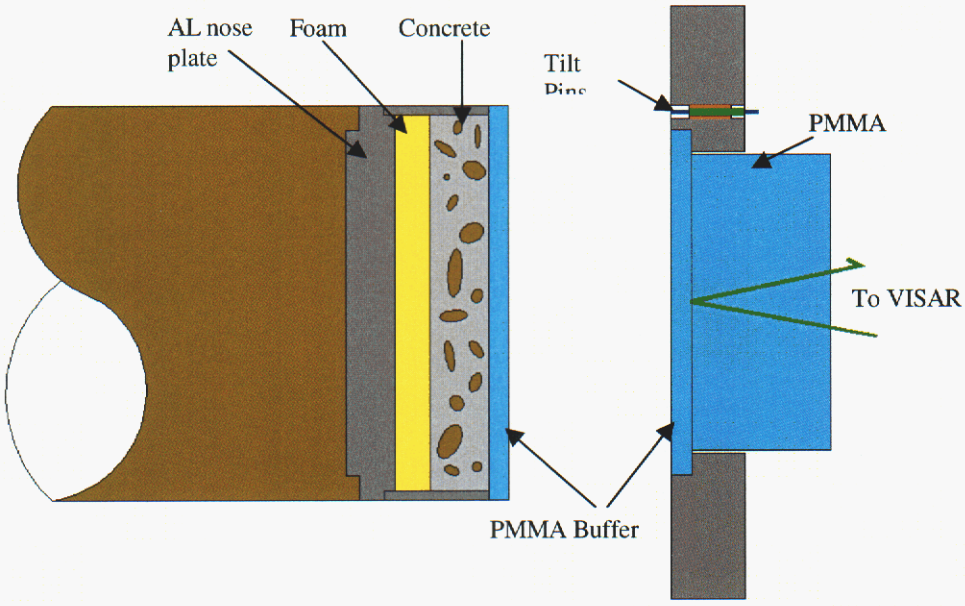

Figure 1. Experimental configuration for compression studies of concrete.

Test	Density (kg/m^3)	Concrete Thick. (mm)	Projectile PMMA Thick. (mm)	Target PMMA Thick. (mm)	Window PMMA Thick. (mm)	Impact Velocity (km/s)	Particle Velocity (km/s)	Shock Velocity (km/s)
JC1	2234	15.23	4.80	4.76	35.7	.264	.132	3.09
JC2	2261	15.25	4.80	4.76	35.4	.442	.221	3.20
JC3	2216	15.20	4.82	4.76	36.0	.596	.298	3.26
JC4	2247	15.26	4.82	4.76	35.6	.656	.328	3.27
JC5	2225	15.23	4.82	4.78	35.5	.892	.446	3.33
JC6	2216	15.19	4.80	4.78	35.7	.730	.365	3.29
JC7	2225	15.25	4.80	4.77	36.3	.304	.152	3.13
JC8	2202	15.24	4.80	4.76	36.0	.450	.225	3.20
JC9	2209	15.20	4.80	4.77	35.3	.780	.390	3.30
JC10	2239	15.26	4.80	4.76	35.6	.860	.430	3.32

Table 1. Summary of compression experiments

4.0 Results for Velocity Profiles

Shot Number: JC1

Impact Velocity: 0.264 km/s
Concrete Density: 2234 kg/m^3

	Material	Thickness (mm)
Concrete	WES	15.23
Impactor Buffer	PMMA	4.80
Target Buffer	PMMA	4.76
VISAR Window	PMMA	35.7

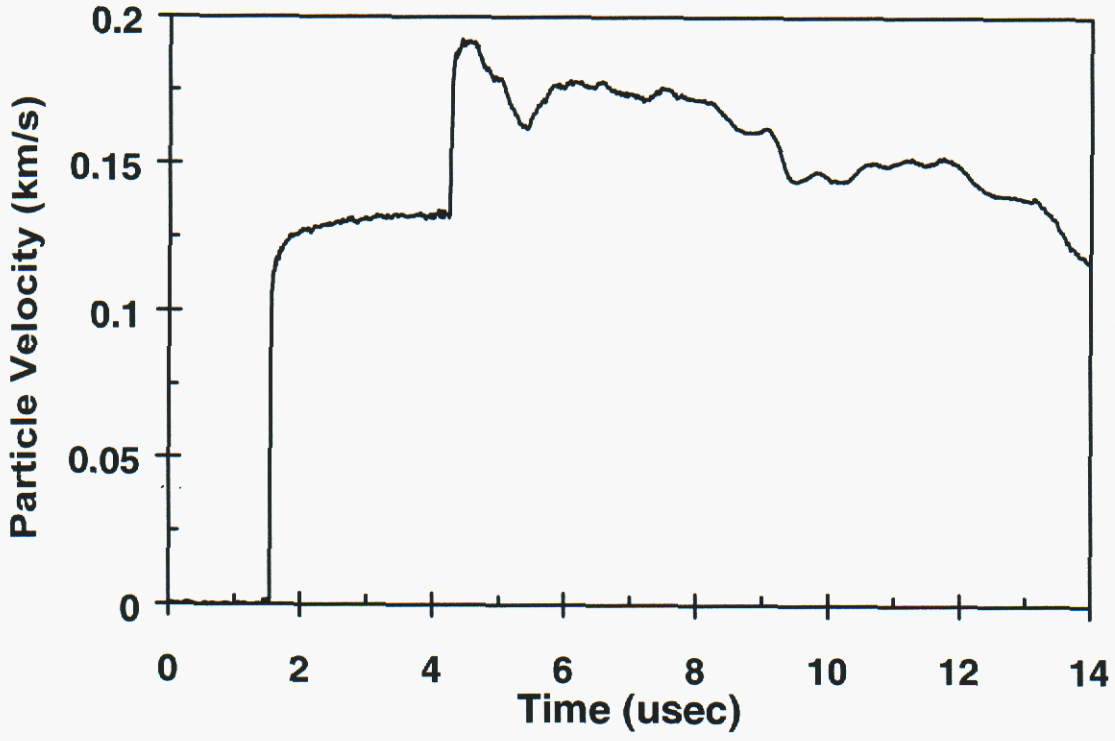

Figure 2. Shot Number: JC1

Shot Number: JC2

Impact Velocity: 0.442 km/s
Concrete Density: 2261 kg/m^3

	Material	Thickness (mm)
Concrete	WES	15.25
Impactor Buffer	PMMA	4.80
Target Buffer	PMMA	4.76
VISAR Window	PMMA	35.4

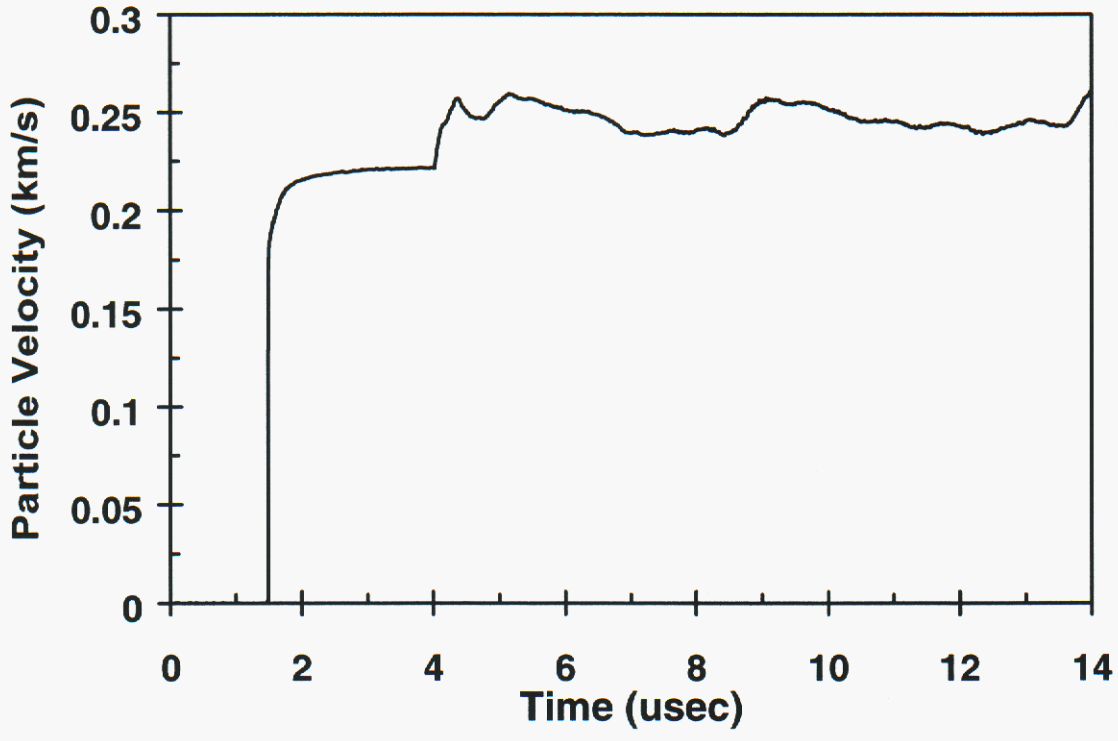

Figure 3. Shot Number: JC2

Shot Number: JC3

Impact Velocity: 0.596 km/s
Concrete Density: 2216 kg/m^3

	Material	Thickness (mm)
Concrete	WES	15.20
Impactor Buffer	PMMA	4.82
Target Buffer	PMMA	4.76
VISAR Window	PMMA	36.0

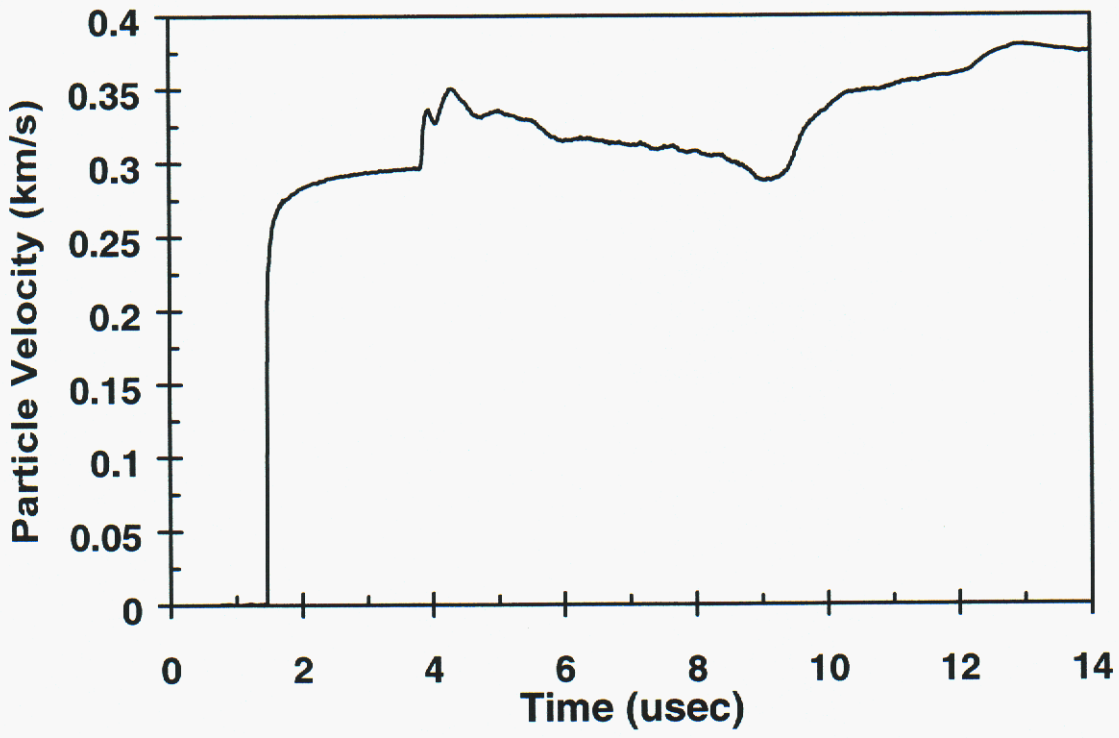

Figure 4. Shot Number: JC3

Shot Number: JC4

Impact Velocity: 0.656 km/s
Concrete Density: 2247 kg/m^3

	Material	Thickness (mm)
Concrete	WES	15.26
Impactor Buffer	PMMA	4.82
Target Buffer	PMMA	4.76
VISAR Window	PMMA	35.6

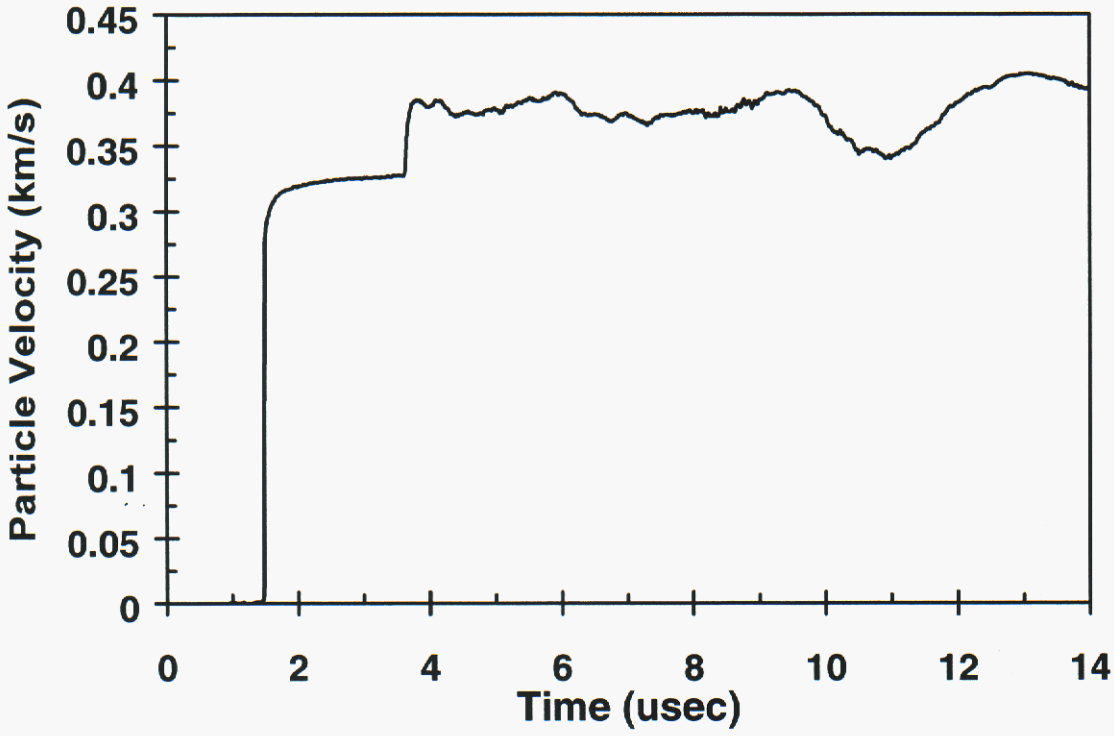

Figure 5. Shot Number:JC4

Shot Number: JC5

Impact Velocity: 0.892 km/s
Concrete Density: 2225 kg/m^3

	Material	Thickness (mm)
Concrete	WES	15.23
Impactor Buffer	PMMA	4.82
Target Buffer	PMMA	4.78
VISAR Window	PMMA	35.5

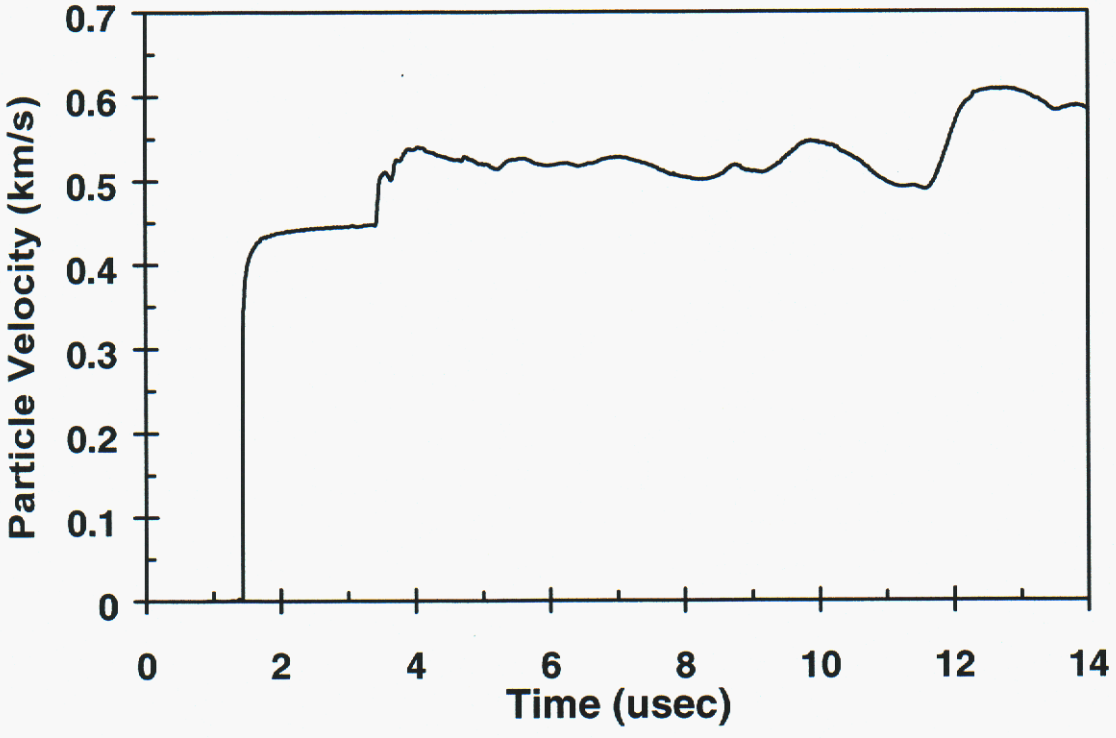

Figure 6. Shot Number: JC5

Shot Number: JC6

Impact Velocity: 0.730 km/s
Concrete Density: 2216 kg/m^3

	Material	Thickness (mm)
Concrete	WES	15.19
Impactor Buffer	PMMA	4.80
Target Buffer	PMMA	4.78
VISAR Window	PMMA	35.7

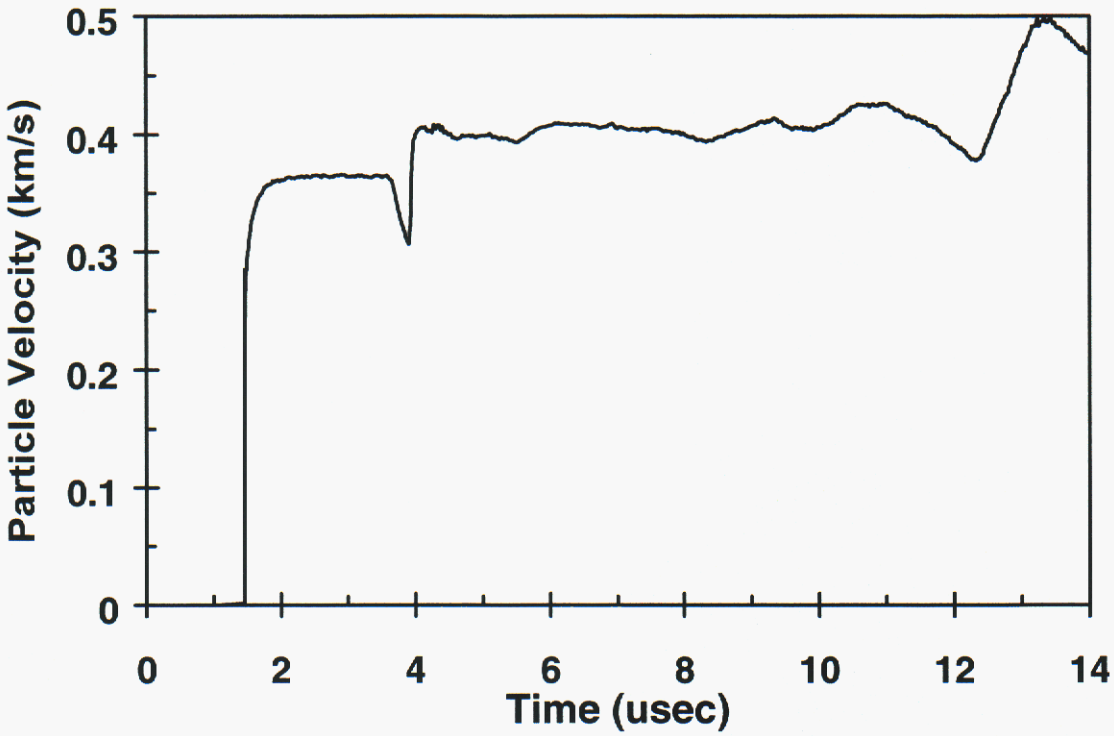

Figure 7. Shot Number: JC6

Shot Number: JC7

Impact Velocity: 0.304 km/s
Concrete Density: 2225 kg/m^3

	Material	Thickness (mm)
Concrete	WES	15.25
Impactor Buffer	PMMA	4.80
Target Buffer	PMMA	4.77
VISAR Window	PMMA	36.3

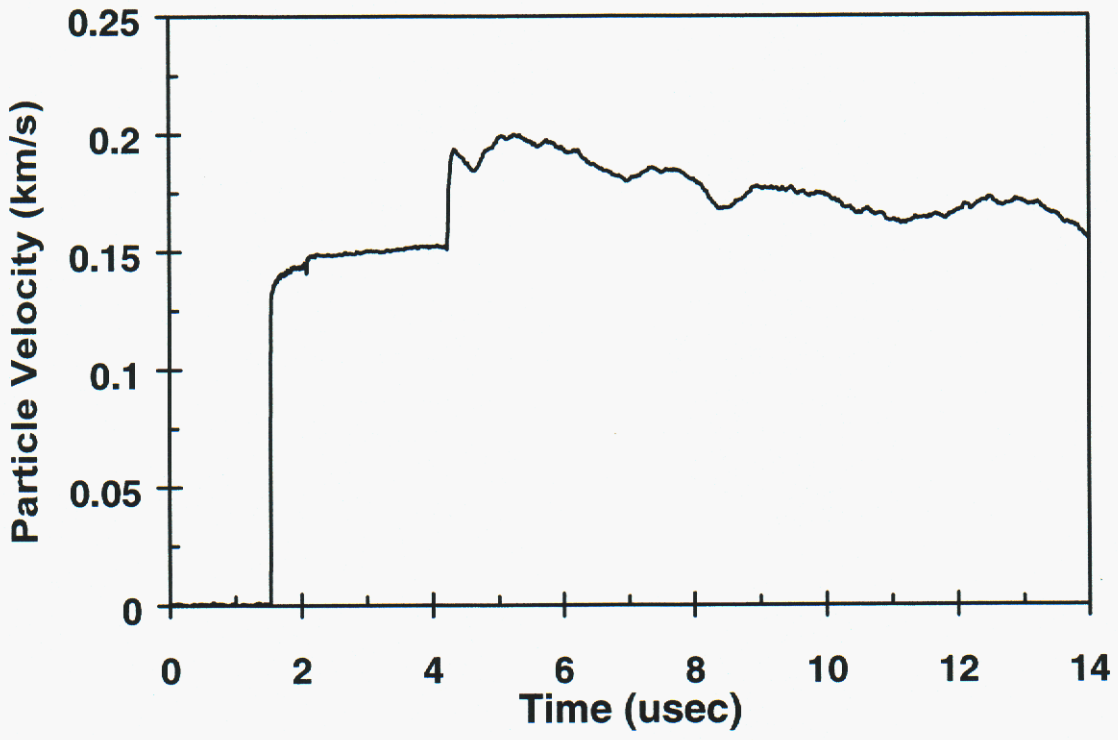

Figure 8. Shot Number: JC7

Shot Number: JC8

Impact Velocity: 0.450 km/s
Concrete Density: 2202 kg/m^3

	Material	Thickness (mm)
Concrete	WES	15.24
Impactor Buffer	PMMA	4.80
Target Buffer	PMMA	4.76
VISAR Window	PMMA	36.0

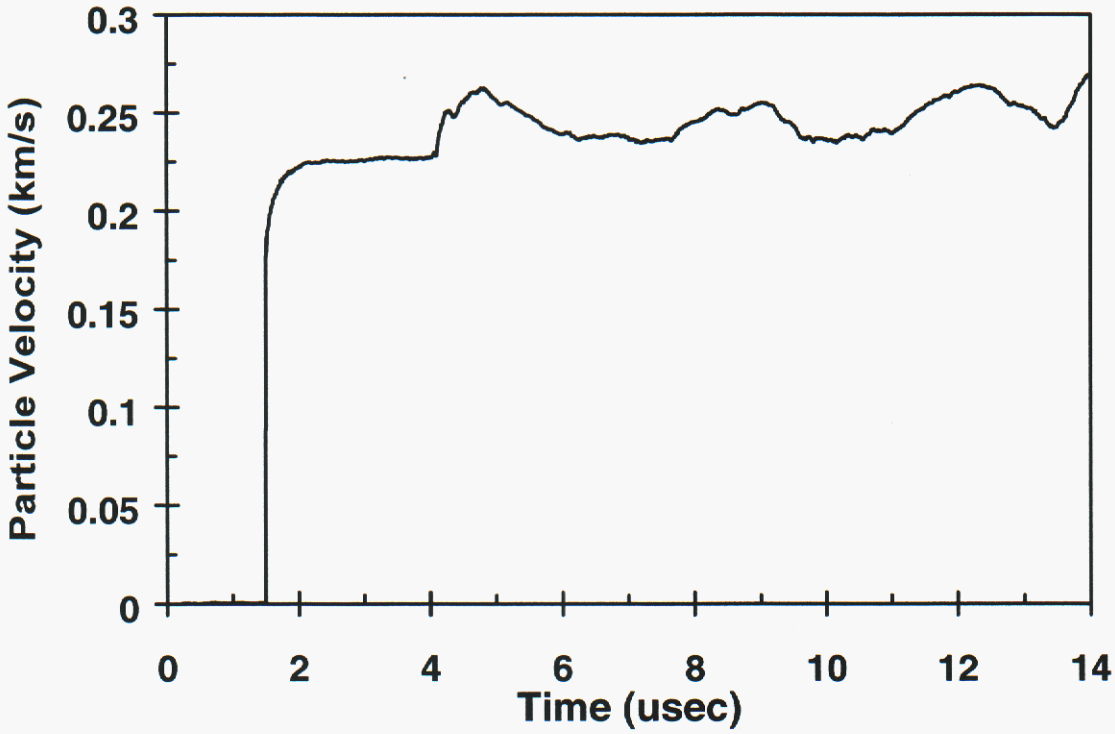

Figure 9. Shot Number: JC8

Shot Number: JC9

Impact Velocity: 0.780 km/s
Concrete Density: 2209 kg/m^3

	Material	Thickness (mm)
Concrete	WES	15.20
Impactor Buffer	PMMA	4.80
Target Buffer	PMMA	4.77
VISAR Window	PMMA	35.3

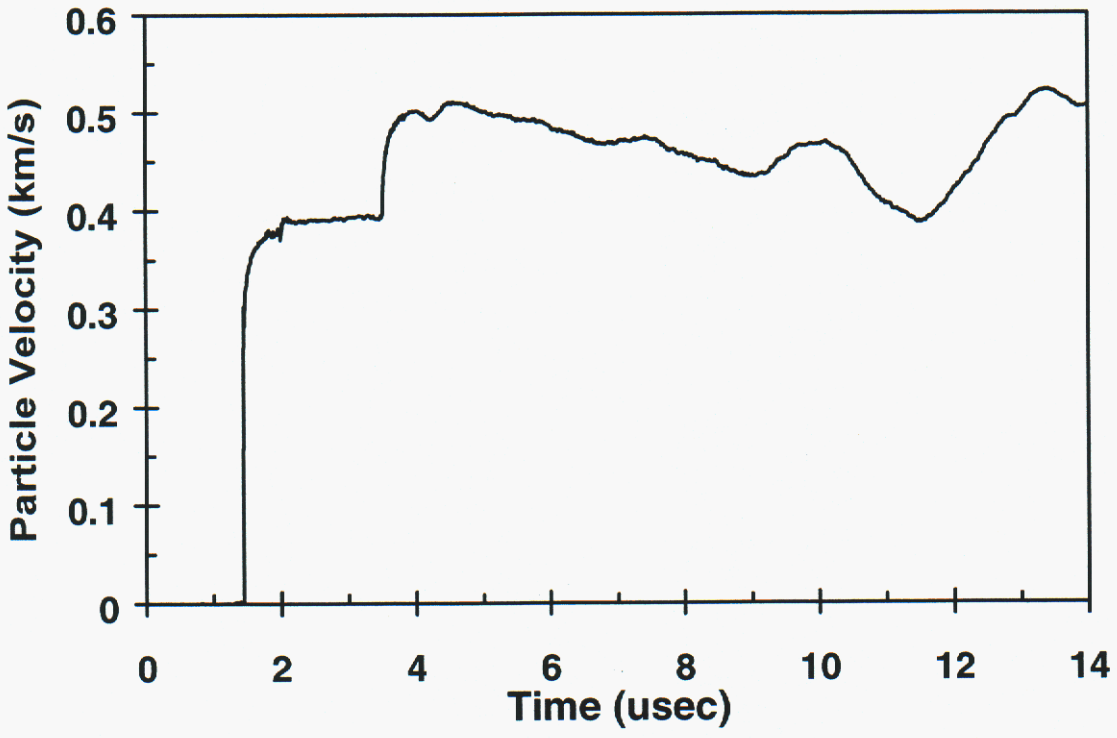

Figure 10. Shot Number: JC9

Shot Number: JC10

Impact Velocity: 0.860 km/s
Concrete Density: 2239 kg/m^3

	Material	Thickness (mm)
Concrete	WES	15.26
Impactor Buffer	PMMA	4.80
Target Buffer	PMMA	4.76
VISAR Window	PMMA	35.6

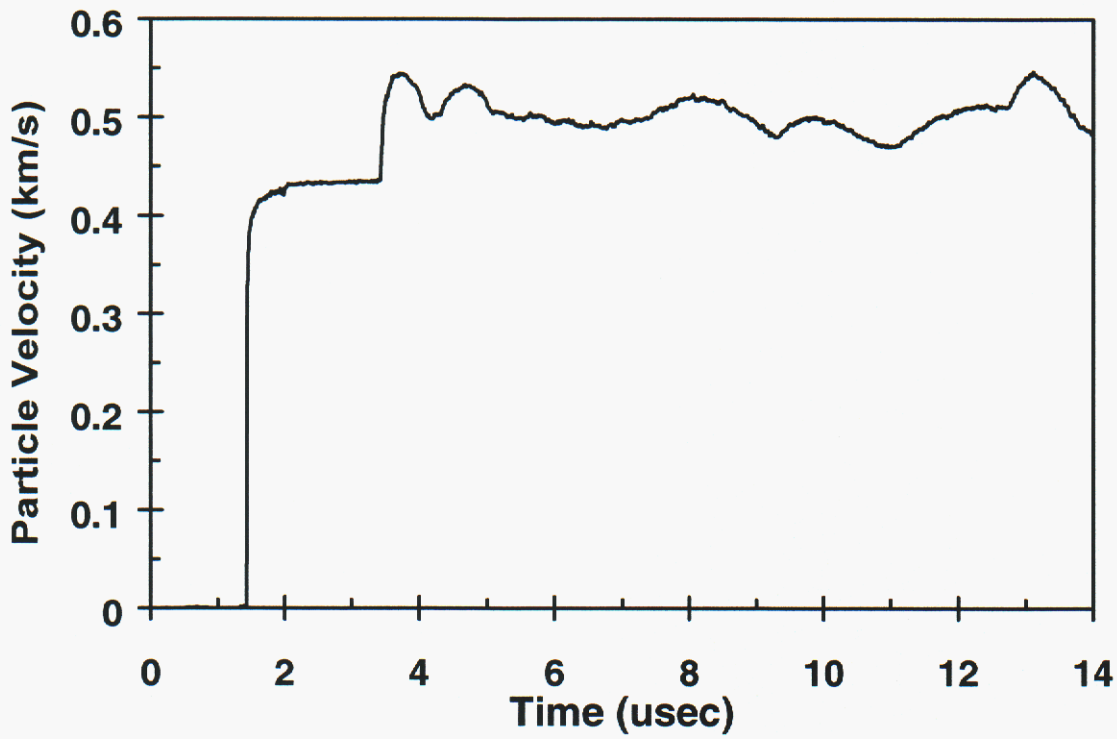

Figure 11. Shot Number: JC10

Shock Wave Compression Profiles of Concrete

1.0 Introduction

Stationary sample discs of SAC-5 concrete were impacted with thin discs of fused-silica to produce transmission compressive shock-wave profiles for dynamic property measurements and computational model validation studies (Grady, 1993c). Two experiments have been performed at impact velocities of 0.53 and 0.72 km/s. A dual VISAR system was used to assess statistical differences in shock profile characteristics. On each experiment, two VISARs measuring transmitted particle velocity profiles, at different lateral positions, showed statistically significant differences due to the heterogeneous structure of the aggregate concrete. Input stress amplitudes of approximately 2 GPa and 3 GPa, respectively, for the two experiments were observed to attenuate to stress levels of about 0.7 GPa and 0.9 GPa upon transmission through the sample thickness. Such rapid attenuation indicates substantial shock wave dissipation in the concrete. Compression profiles do not show an abrupt compressive yield (Hugoniot elastic limit). Rather, the data indicate initial yield at a very low stress level, which increased continuously with increasing dynamic stress. The dynamic compression curve converges continuously with the lower end of previous Hugoniot measurements.

2.0 Material Description

Tests were performed on the same SAC-5 concrete provided by Waterways Experimental Station (WES) (Ergott, 1993) that was described in the previous section.

3.0 Experimental Technique

In the projectile, fused silica, which is well characterized and remains elastic within the present range of impact velocities (Barker and Hollenbach, 1970), was used as the impact material. The fused silica was backed by low-density polyurethane foam, which provided for a release wave and followed the initial compression wave through the concrete sample. The concrete sample was mounted in the stationary target assembly. The transmitted shock and release wave profile was measured at an interface forward of a PMMA window 50.7 mm in diameter and behind a thin (2mm) PMMA buffer plate as shown in **Figure 12**. Two VISARs were used in these experiments to sample statistical variations in the transmitted wave profile at different lateral positions at the recording interface. VISAR #1 (designated by A in the wave profiles) was focused on a point ~ 6.3 mm from the centerline. VISAR #2 (B in the wave profiles) was located ~ 12.7 mm from the centerline. Consequently, the two VISAR beams recorded the normal motion at separate points 19 mm apart. Critical experimental dimensions and impact velocities for these tests are provided in profile tables.

Experiments JC-21 and JC-22 were performed at impact velocities of 0.53 and 0.72 km/s, respectively. As noted earlier, the "A" profiles correspond to the VISAR beam focused at a point closest to the centerline of the target; the "B" profiles, the furthest. The spike in the data, just past 5 us for Test JC-21, and at about 2 us for JC-22, is a timing fiducial. Profiles are aligned so that impact occurs at the time zero and wave arrival times correspond to transit through the concrete samples plus the PMMA buffer (see **Figure 12**).

Significant differences in wave arrivals at the two VISAR stations are expected due to the coarse structure of the nominal 3/8-inch aggregate concrete. Based on a shock velocity of 3.0 km/s at the present particle velocity amplitude in PMMA (Barker and Hollenbach, 1970) to account for the transit time in the 2-mm PMMA buffer, wave velocities for each profile were calculated. Velocities for both first arrival (foot of

the wave), and the wave midpoint were determined. Statistically significant differences between tests JC-21 and JC-22 were not observed. It is important to note that the average foot velocity is in good agreement with the ultrasonic longitudinal wave velocity of 4.45 km/s for SAC-5 concrete (Grady 1993a).

The profiles provide measured VISAR motion until abrupt loss of light occurs (~10 μs) corresponding approximately to shock arrival at the back of the PMMA window. Note that one-dimensional (uniaxial strain) motion is not maintained throughout the full recording time due to the finite diameter of the concrete sample and PMMA window. Again, differences in A and B profiles is attributed to the heterogeneous nature of the concrete aggregate.

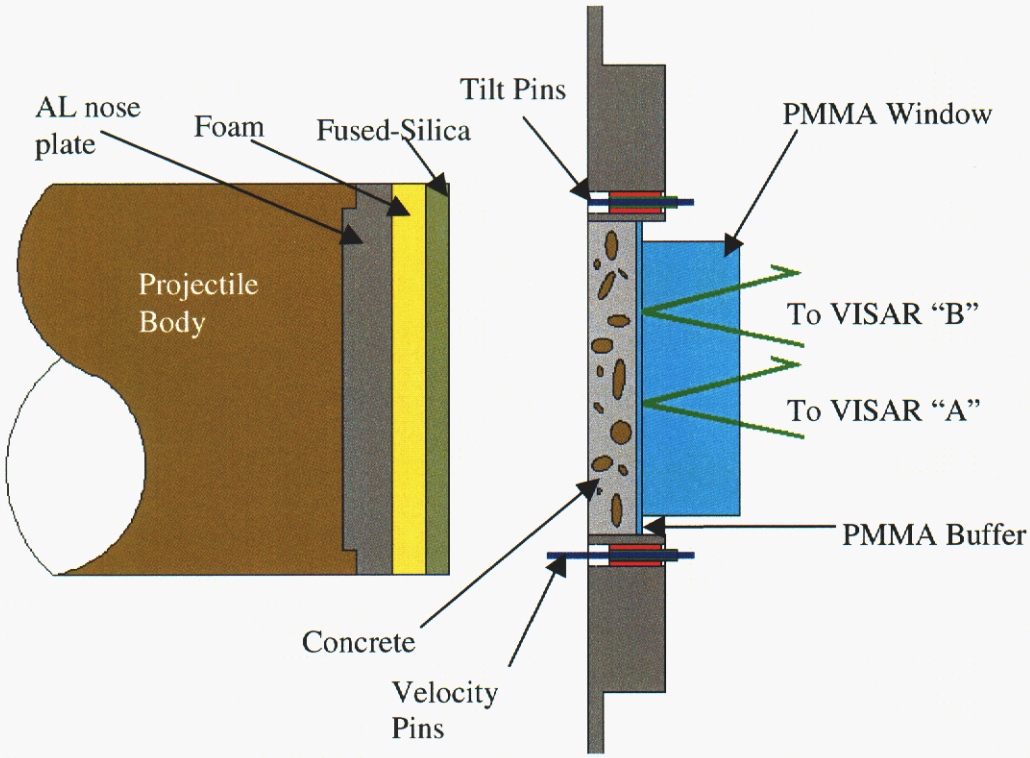

Figure 12. Experimental configuration for impact shock compression measurements of concrete.

4.0 Velocity Profiles

Shot Number:JC21A

Impact Velocity: 0.530 km/s
Concrete Density: 2220 kg/m^3

	Material	Thickness (mm)
Concrete	SAC5	12.01
Impactor	Fused Silica	6.40
Target Buffer	PMMA	2.03
VISAR Window	PMMA	24.2

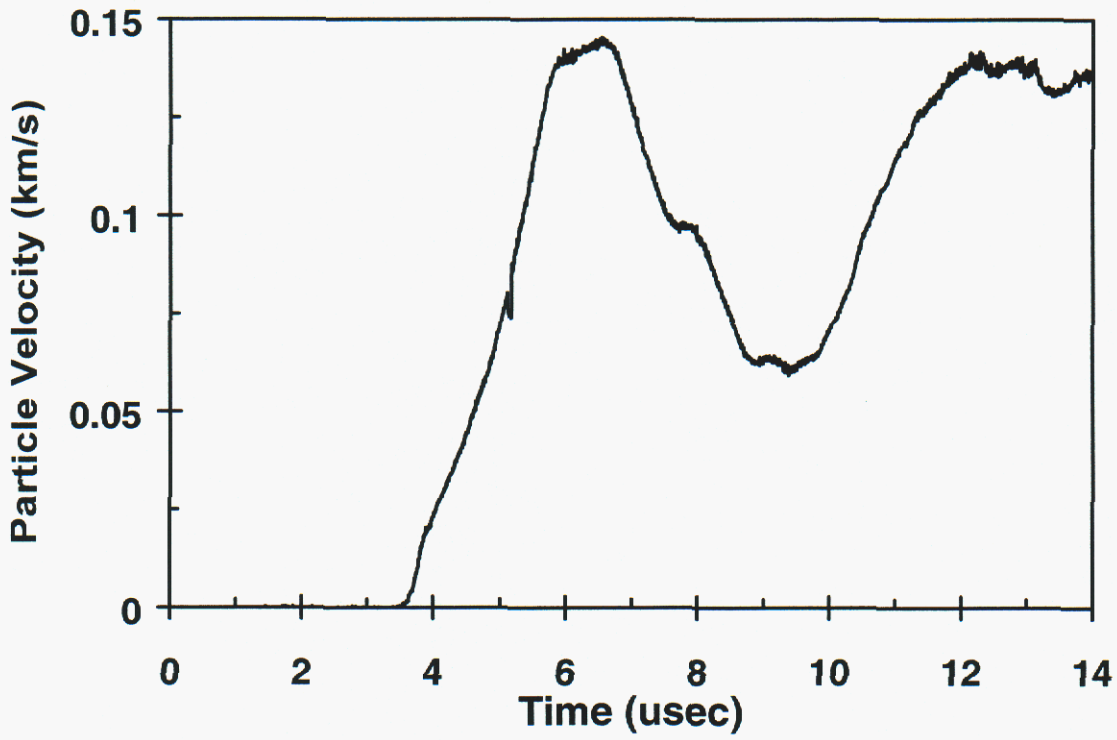

Figure 13. Shot Number: JC21A

Shot Number:JC21B

Impact Velocity: 0.530 km/s
Concrete Density: 2220 kg/m^3

	Material	Thickness (mm)
Concrete	SAC5	12.01
Impactor	Fused Silica	6.40
Target Buffer	PMMA	2.03
VISAR Window	PMMA	24.2

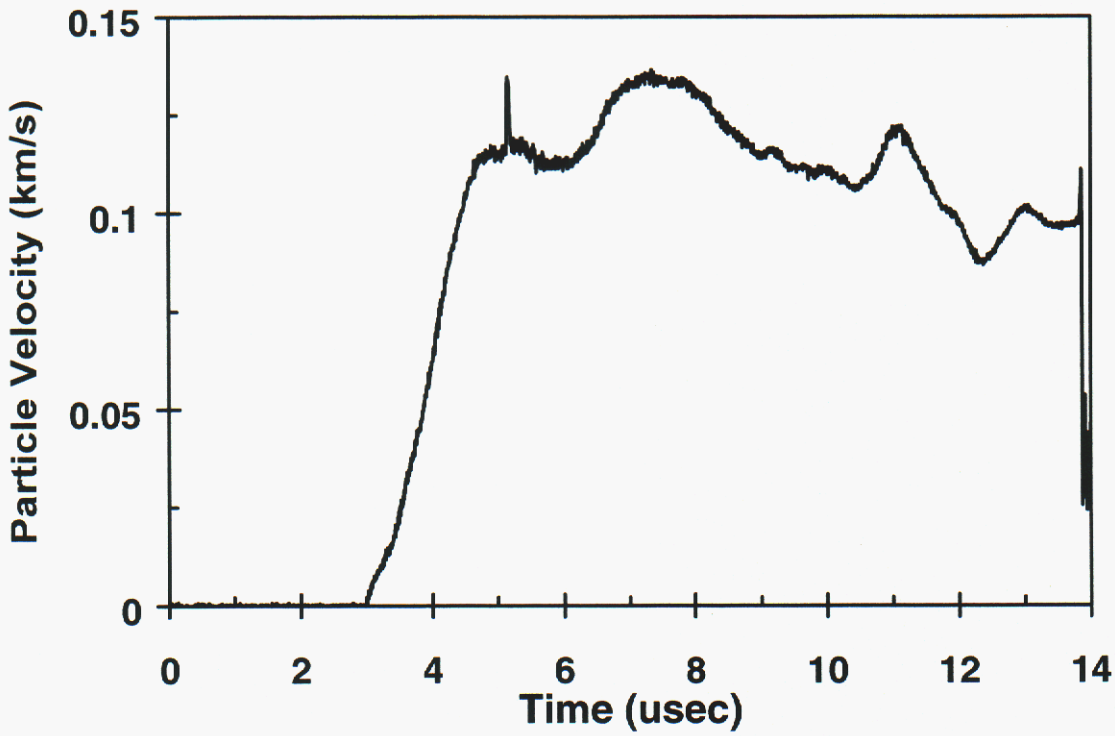

Figure 14. Shot Number: JC21B

Shot Number:JC22A

Impact Velocity: 0.720 km/s
Concrete Density: 2240 kg/m^3

	Material	Thickness (mm)
Concrete	SAC5	11.99
Impactor	Fused Silica	6.37
Target Buffer	PMMA	2.03
VISAR Window	PMMA	24.1

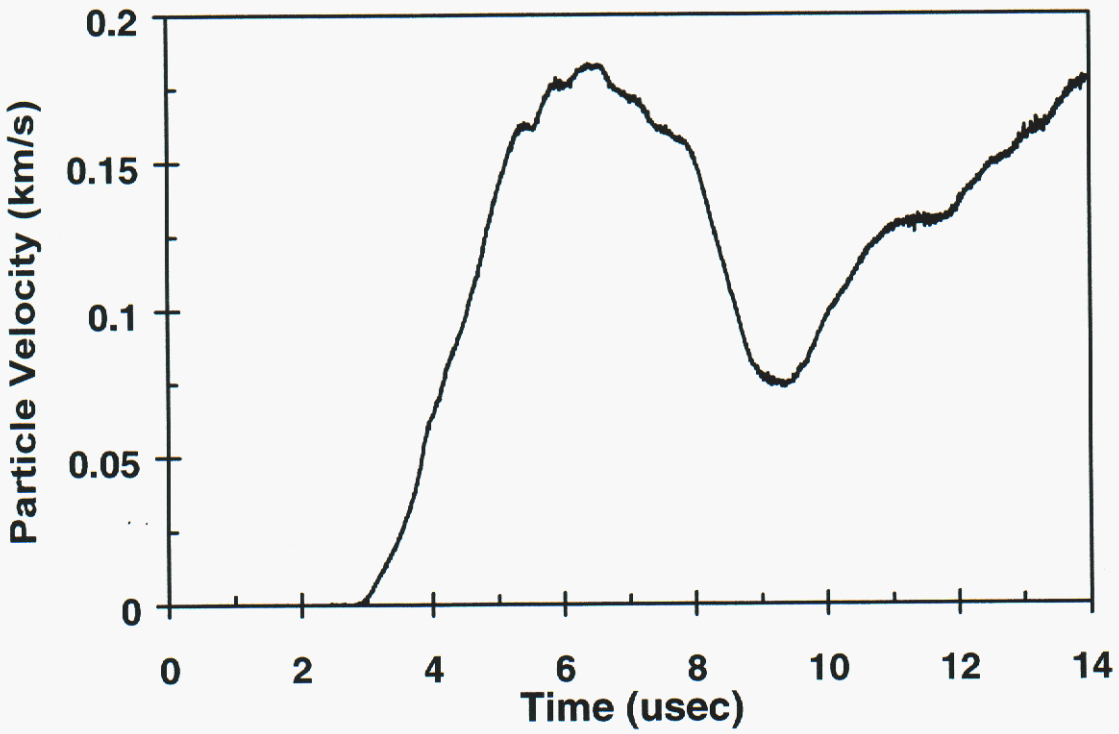

Figure 15. Shot Number: JC22A

Shot Number:JC22B

Impact Velocity: 0.720 km/s
Concrete Density: 2240 kg/m^3

	Material	Thickness (mm)
Concrete	SAC5	11.99
Impactor	Fused Silica	6.37
Target Buffer	PMMA	2.03
VISAR Window	PMMA	24.1

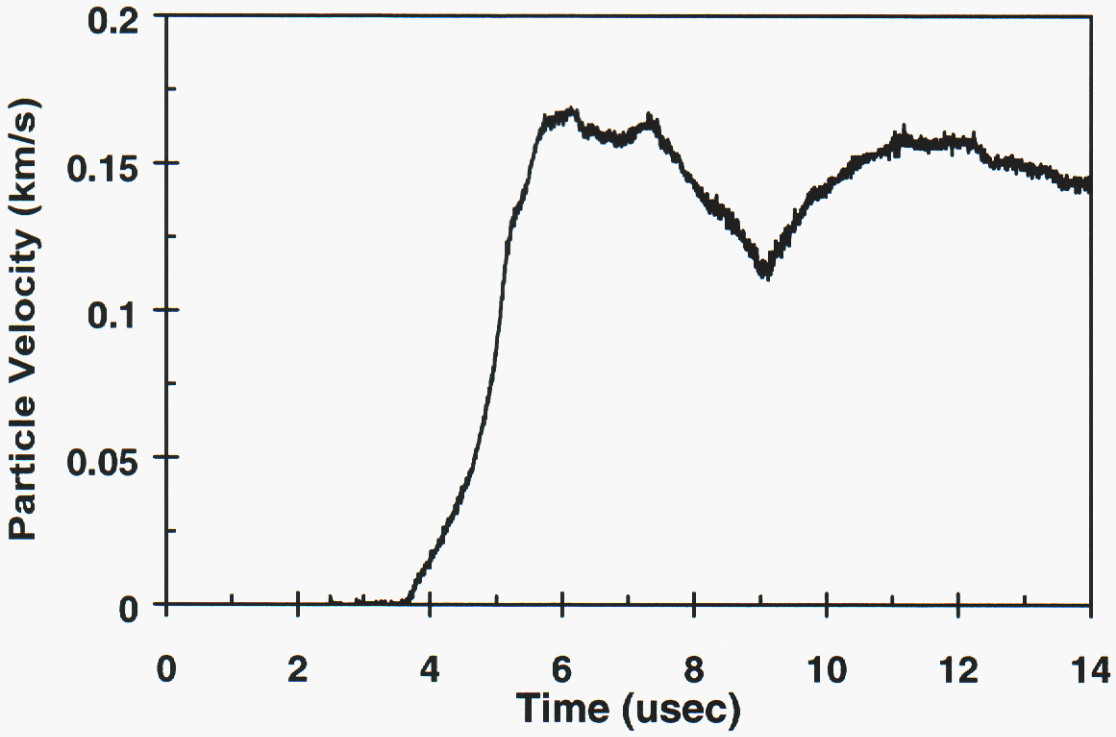

Figure 16. Shot Number: JC22B

Shock and Release Properties of Concrete

1.0 Introduction

Experimental shock and adiabatic release data have been determined for concrete over a shock pressure range of approximately 3-25 GPa. In the experimental method a concrete sample (disc) was mounted in a projectile and underwent planar impact on a thin disc of metal (copper or tantalum). Subsequent acceleration of the metal plate is monitored with diffused-surface velocity interferometry – VISAR (Barker and Hollenbach, 1972). Velocity histories are determined with a VISAR analysis and optimization program (Crawford, 1994). A single measured acceleration history establishes both the initial shock compression Hugoniot state, and states on the decompression adiabat from that specific Hugoniot state.

Dynamic unloading properties of concrete are not well understood. Such properties are critical to the impact response of concrete because of the complex compaction and uncertain void volume in the cementatious component of the aggregate concrete. The experiments pursued in this study offered a technique for measuring dynamic release properties of this complicated heterogeneous material. Rosenberg and Ahrens (1966), Lysne et al. (1969), and Chhabildas and Grady (1984) have reported previous applications of the impact-plate acceleration method. Preliminary developmental work using the present technique on concrete has been reported in Grady (1993c). Earlier dynamic and quasistatic material property data for the same materials have also been reported (Ehrgott, 1993; Olson, 1993; Grady, 1993a,b,c).

Following initial shock compression, subsequent acceleration histories of the metal witness plates to nearly 10 μs recording time provide decompression data from the Hugoniot state down to near zero pressure. This data can be used directly to constrain computational models for concrete [Silling, 1995; Sinz, 1995]. Analytic methods can also be used to determine dynamic pressure-versus-particle-velocity and pressure-versus-volume release data from the acceleration histories. Static and low-pressure shock data indicate substantial volume compaction in the concrete. Marked flattening of the Hugoniot immediately above the HEL (~0.5 GPa) before stiffening to a compressibility more characteristic of the solid rock component is common to the dynamic compaction of a porous material. Release paths from Hugoniot states in the range of 3-5 GPa indicate a 10-11% irrecoverable volume change consistent with compaction measurements under static loading. Shock compression and release measurements to Hugoniot states in excess of 5 GPa and up to about 25 GPa indicate a decreasing irrecoverable volume strain.

There are several possible explanations for this behavior. One possibility is thermal expansion on shock recovery due to the extensive shock heating during the dynamic compaction event. This possibility was pursued and found capable of explaining about half of the recovery strain. Uncertainties concerning distribution of the shock dissipation energy in the heterogeneous material remains. A further mechanism for strain recovery during decompression from the shocked state can be traced to the anisotropic elastic compliance of the material. Compaction and inelastic shear during the shock compression process eliminates all, or most, of the initial void volume; however, dilatant void can be generated during release. A model of this dilatancy process indicates a recovery strain of the same order as thermal expansion. Together the two mechanisms are capable of explaining the anomalous recovery strain on shock decompression of concrete.

2.0 Material Description

The primary material tested in the present study was SAC-5 concrete (Ehrgott, 1993) with a nominal density of 2260 kg/m^3. Two additional experiments reported in this work were performed on a conventional strength Portland cement concrete with a density of 2290 kg/m^3, similar to the SAC-5 material. Hugoniot states and release paths for the concrete showed negligible differences. Additional experiments were conducted to determine the Hugoniot states and release paths differentiated by aggregate sizes. The material description is given in the section on page 13.

3.0 Experimental Method

Measurement of dynamic unloading properties by conventional forward ballistic wave propagation experiments (Grady et al, 1977), or by reverse ballistic Hugoniot and decompression methods (Grady and Furnish, 1988) is made very difficult because of the extremely low shock (deformation) wave velocities for concrete in this regime. Another technique, referred to as the plate reverberation method, which has been developed in earlier studies (e.g., Chhabildas and Grady, 1984), is potentially better suited to the measurement of dynamic unloading properties for the present material.

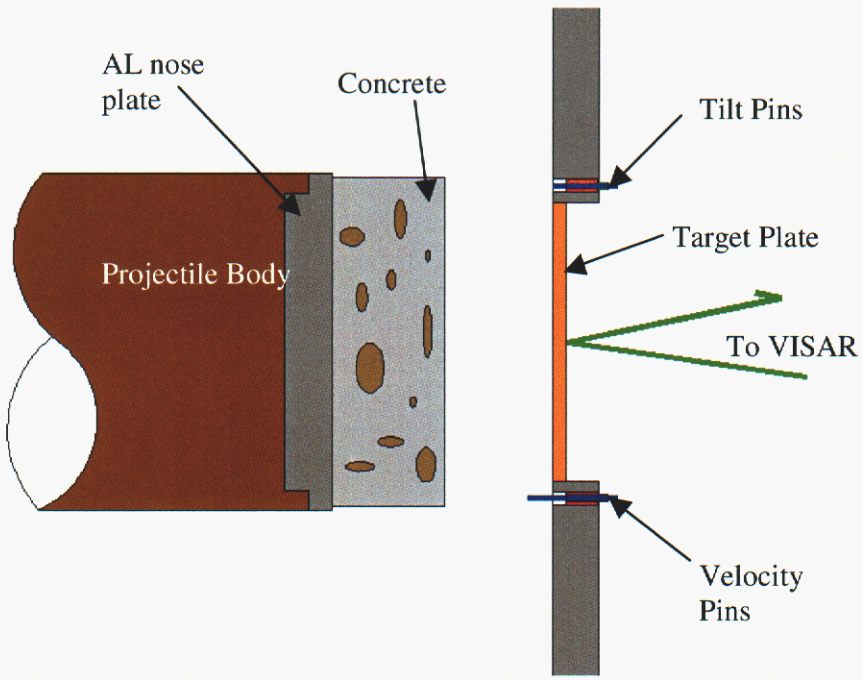

Figure 17. Experimental configuration for shock compression and release measurements of concrete.

The shock compression and release experiments were performed on a single stage 89 mm diameter smoothbore powder gun capable of controlled impact velocities over 0.5-2.5 km/s. The reverse ballistics experimental configuration used to determine shock compression and release properties of SAC-5 concrete is illustrated in **Figure 17**. The concrete sample is mounted in the projectile as shown. A metal plate (disc) is mounted in a stationary target assembly and back-surface motion of the plate is measured by VISAR methods. In this study both copper and tantalum were used as metal plate material. Higher shock impedance of the tantalum results in higher Hugoniot pressures at a specified impact velocity. Pertinent experimental parameters for the tests are provided in Table 2 and with each profile.

The stress states and motion histories induced by the impact in the present experimental configuration are pictured as follows. The initial impact of concrete on metal causes both samples to achieve their Hugoniot states. The subsequent arrival and reflection of the shock wave at the back free surface of the metal witness plate provides the initial measured acceleration. Experimental determination of the Hugoniot state in the concrete is established from the amplitude of the first velocity plateau and the measured projectile velocity. Subsequent reverberations of the wave through the plate alternately decompress the plate to zero stress on the concrete unloading curve. The experimental pressures versus specific volume release characteristics (isentrope) of the concrete are determined from the subsequent motion history of the metal witness plate. Thus, the acceleration history of the metal witness plate contains detailed experimental information regarding the shock compression and dynamic release properties of the concrete material.

Test	Density (kg/m^3)	Concrete Thickness (mm)	Impact Velocity (km/s)	Target Plate Material	Target Thickness (mm)	Free Surface Velocity (km/s)	Target Shock Velocity (km/s)
JC23	2260 (SAC-5)	12.0	0.523	Copper	3.11	0.145	4.048
JC24	2290 (Portland)	12.0	0.524	Copper	3.18	0.145	4.048
JC25	2260 (SAC-5)	15.2	0.774	Copper	3.11	0.240	4.119
JC26	2290 (Portland)	15.0	0.775	Copper	3.14	0.255	4.130
CON-1	2332 (SAC-5)	25.4	2.15	Copper	2.39	0.93	4.633
CON-2	2325 (SAC-5)	25.3	2.14	Copper	2.36	na	
CON-3	2328 (SAC-5)	25.4	1.74	Copper	2.33	0.79	4.529
CON-4	2327 (SAC-5)	25.3	1.71	Copper	2.39	0.80	4.536
CON-5	2363 (SAC-5)	25.4	1.33	Copper	2.36	0.49	4.305
CON-6	2323 (SAC-5)	25.4	1.32	Copper	2.34	0.56	4.357
CON-7	2337 (SAC-5)	25.4	2.27	Tantalum	1.53	0.70	3.830
CON-8	2320 (SAC-5)	25.4	2.20	Tantalum	1.52	0.79	3.884
CON-9	2315 (SAC-5)	25.4	2.09	Copper	2.41	0.85	4.573
CON-10	2314 (SAC-5)	25.4	1.71	Copper	2.36	0.71	4.469

Table 2. Summary of plate reverberation experiments

4.0 Velocity Profiles

Shot Number: JC23

Impact Velocity: 0.523 km/s
Concrete Density: 2260 kg/m^3

	Material	Thickness (mm)
Concrete	SAC5	12.0
Target	Copper	3.11

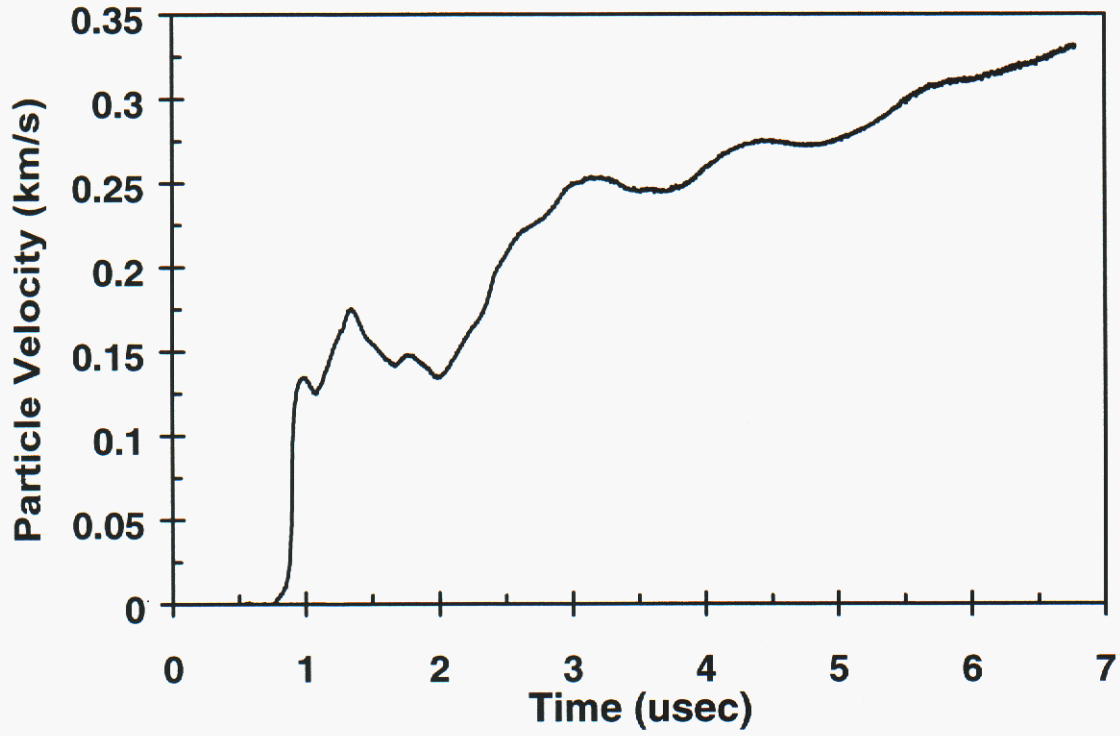

Figure 18. Shot Number: JC23

Shot Number: JC24

Impact Velocity: 0.524 km/s
Concrete Density: 2290 kg/m^3

	Material	Thickness (mm)
Concrete	Portland	12.0
Target	Copper	3.18

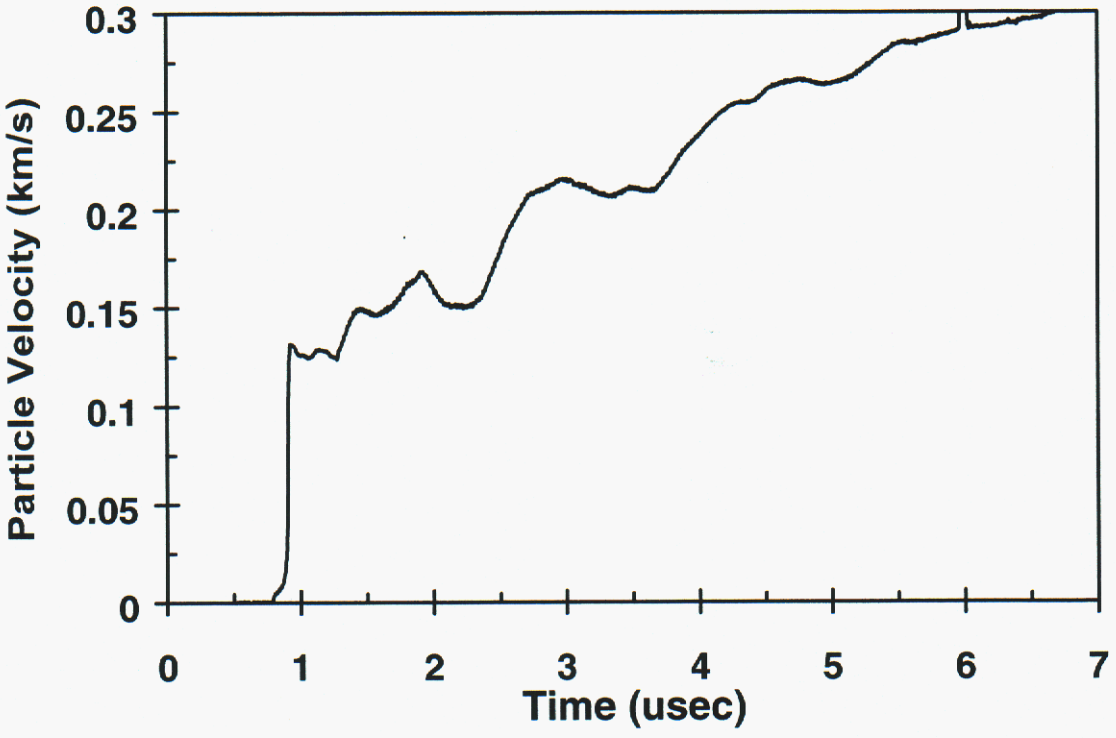

Figure 19. Shot Number: JC24

Shot Number: JC25

Impact Velocity: 0.774 km/s
Concrete Density: 2260 kg/m^3

	Material	Thickness (mm)
Concrete	SAC5	15.2
Target	Copper	3.11

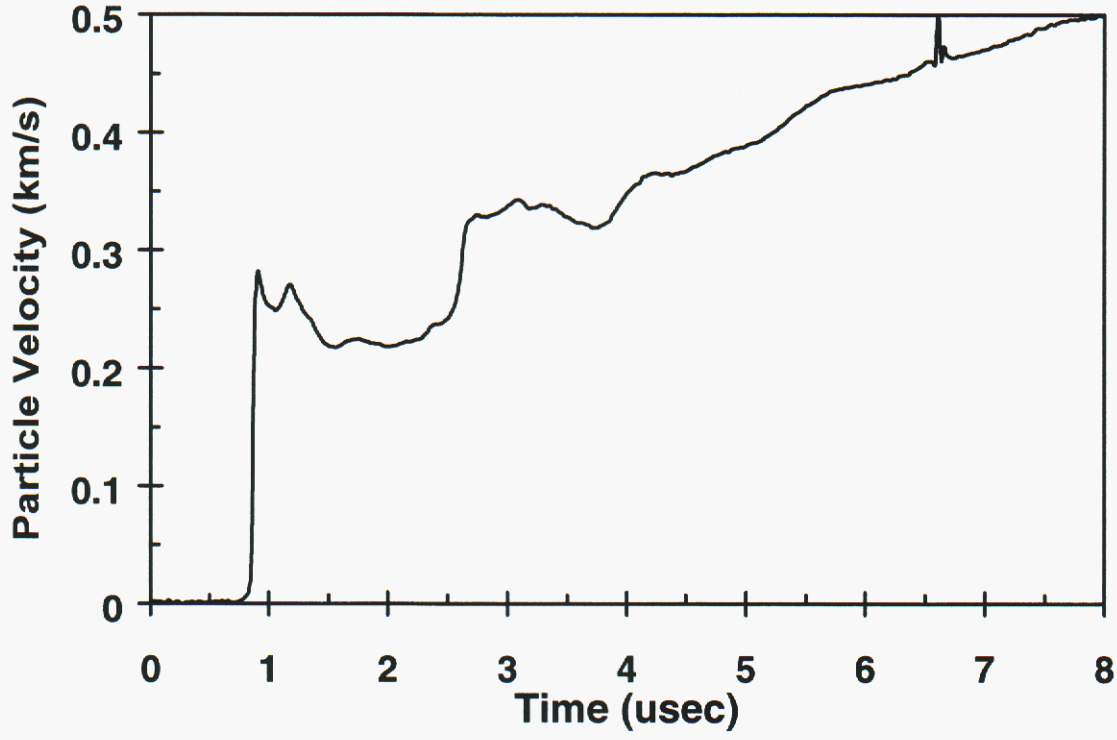

Figure 20. Shot Number: JC25

Shot Number: JC26

Impact Velocity: 0.775 km/s
Concrete Density: 2290 kg/m^3

	Material	Thickness (mm)
Concrete	Portland	15.0
Target	Copper	3.14

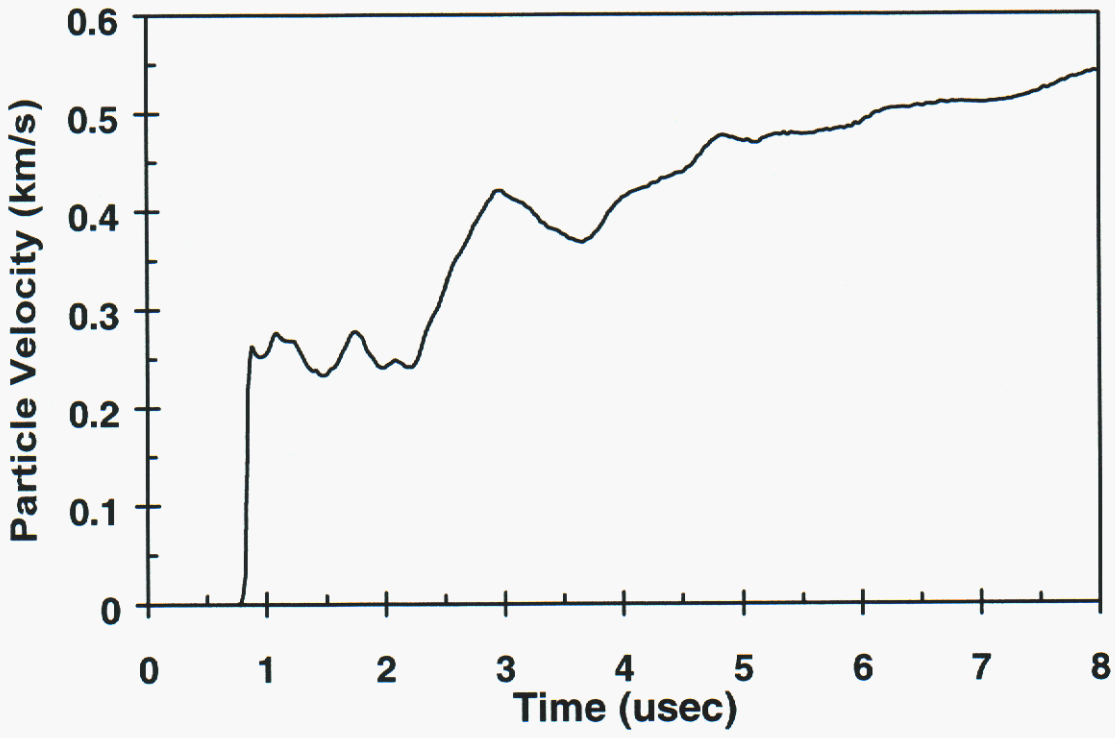

Figure 21. Shot Number: JC26

Shot Number:CON1

Impact Velocity: 2.15 km/s
Concrete Density: 2332 kg/m^3

	Material	Thickness (mm)
Concrete	SAC5	25.4
Target	Copper	2.39

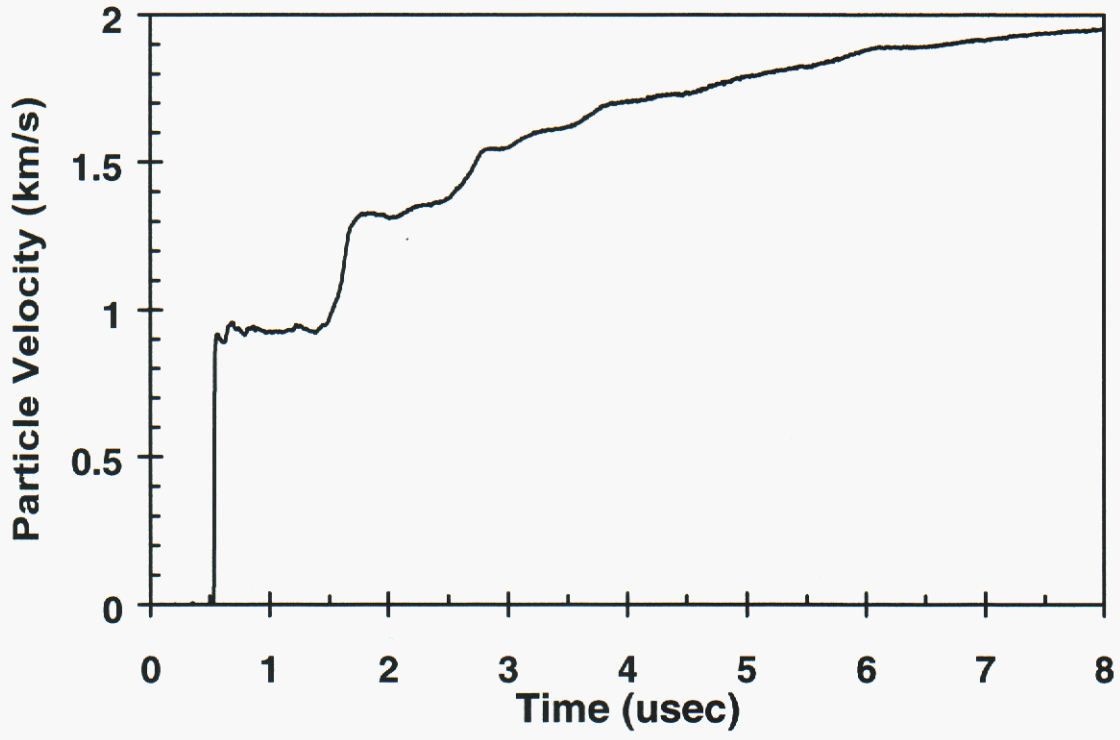

Figure 22. Shot Number: CON1

Shot Number:CON2

Impact Velocity: 2.14 km/s
Concrete Density: 2325 kg/m^3

	Material	Thickness (mm)
Concrete	SAC5	25.3
Target	Copper	2.36

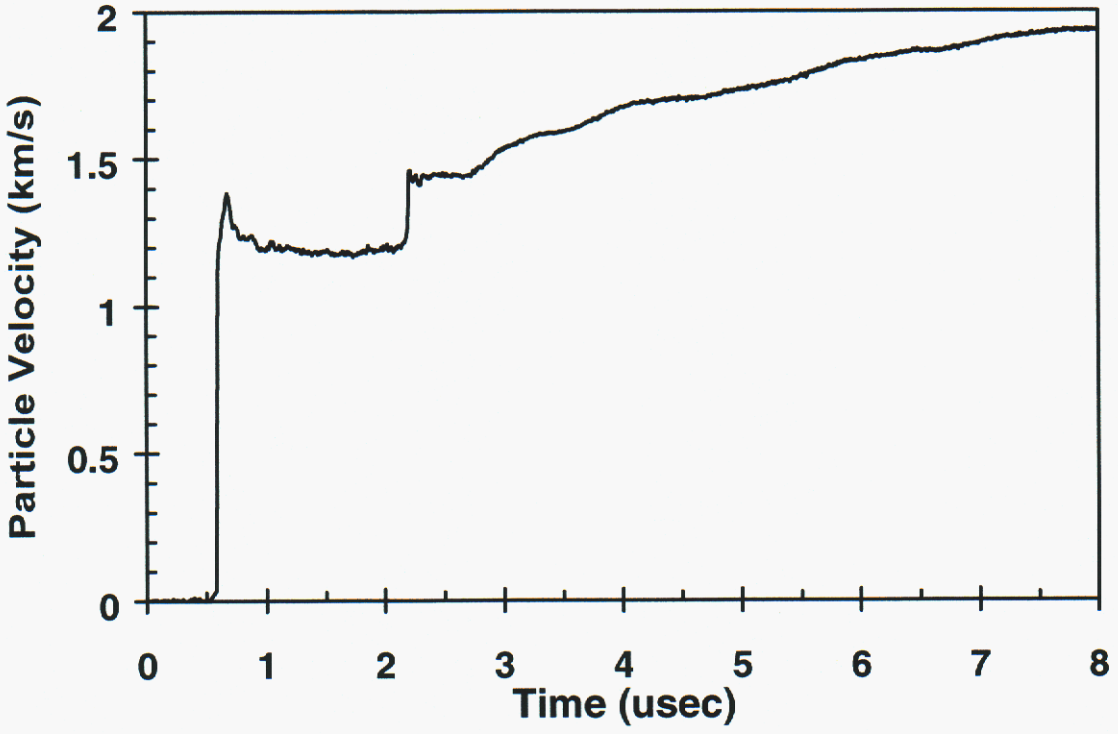

Figure 23. Shot Number: CON2

Shot Number:CON3

Impact Velocity: 1.74 km/s
Concrete Density: 2328 kg/m^3

	Material	Thickness (mm)
Concrete	SAC5	25.4
Target	Copper	2.33

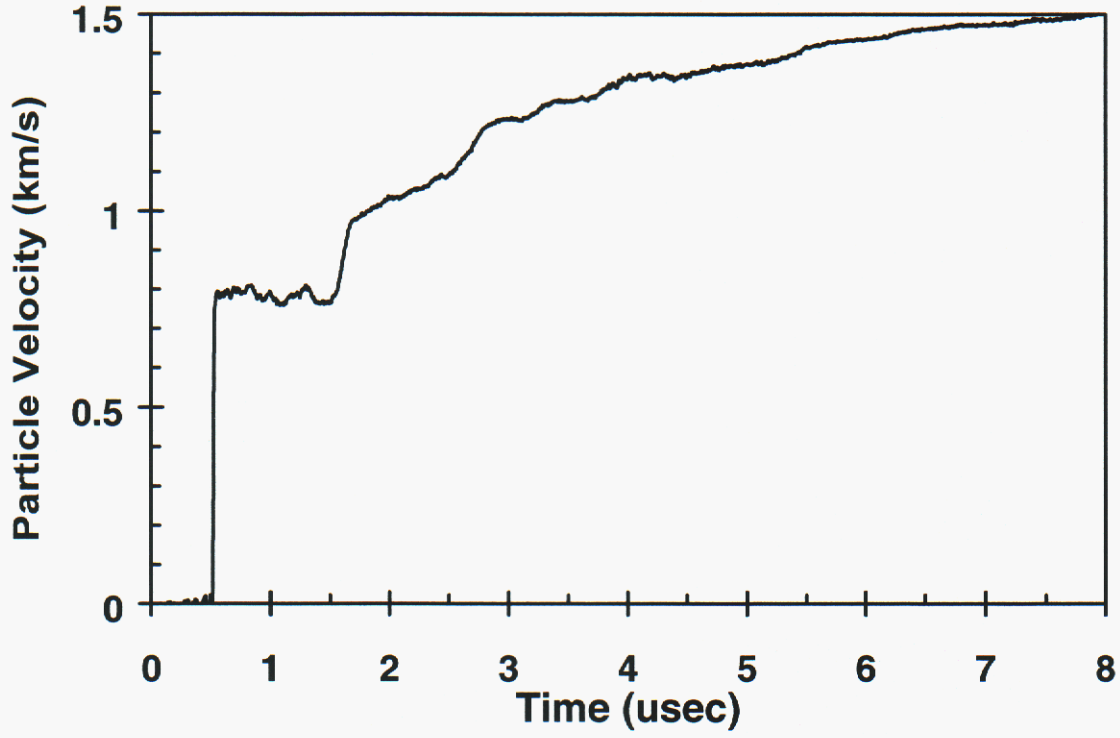

Figure 24. Shot Number: CON3

Shot Number:CON4

Impact Velocity: 1.71 km/s
Concrete Density: 2327 kg/m^3

	Material	Thickness (mm)
Concrete	SAC5	25.3
Target	Copper	2.39

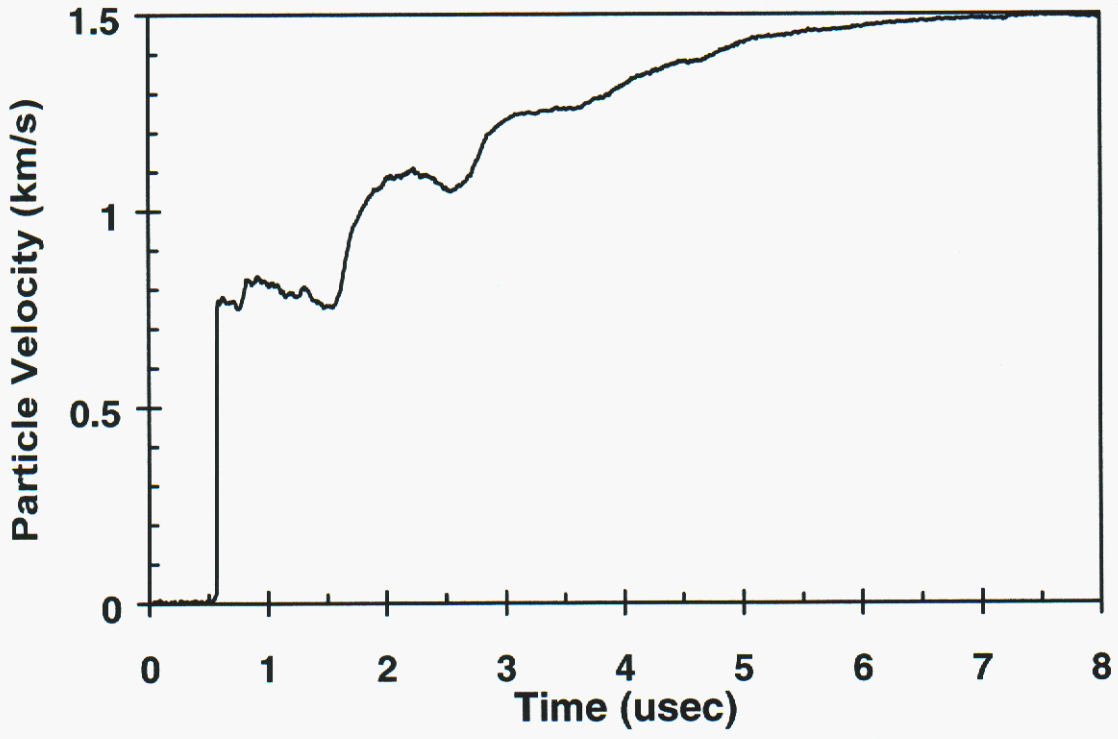

Figure 25. Shot Number: CON4

Shot Number:CON5

Impact Velocity: 1.33 km/s
Concrete Density: 2363 kg/m^3

	Material	Thickness (mm)
Concrete	SAC5	25.4
Target	Copper	2.36

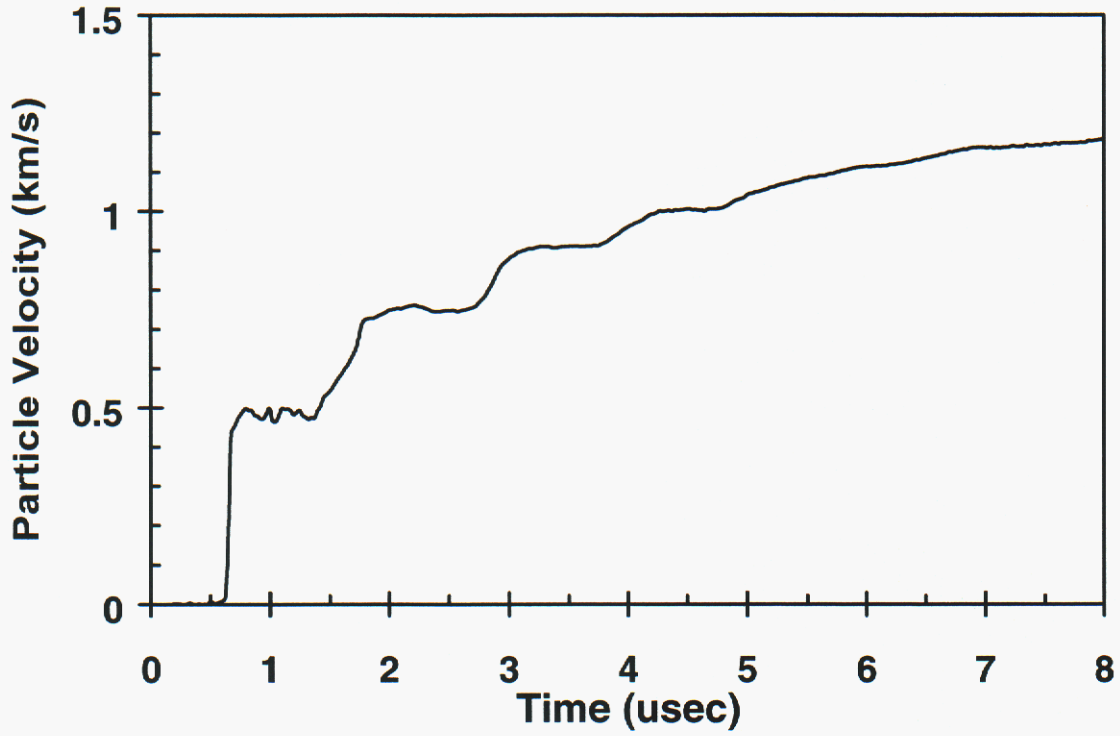

Figure 26. Shot Number: CON5

Shot Number:CON6

Impact Velocity: 1.32 km/s
Concrete Density: 2323 kg/m^3

	Material	Thickness (mm)
Concrete	SAC5	25.4
Target	Copper	2.34

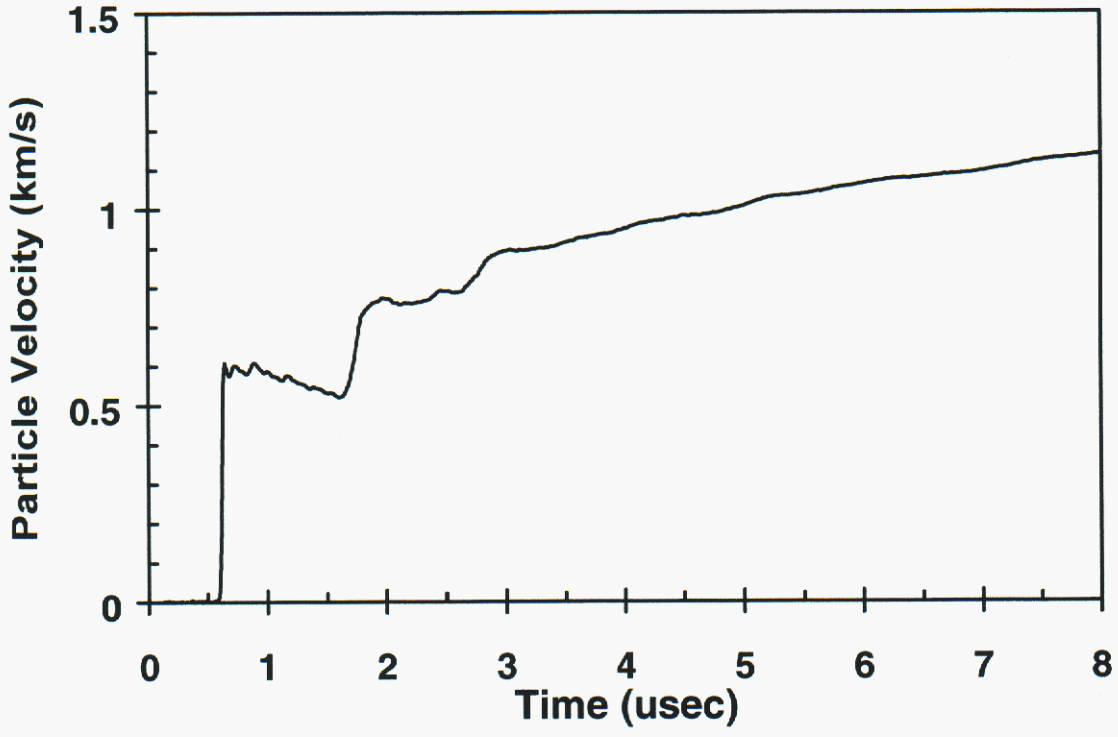

Figure 27. Shot Number: CON6

Shot Number:CON7

Impact Velocity: 2.27 km/s
Concrete Density: 2337 kg/m^3

	Material	Thickness (mm)
Concrete	SAC5	25.4
Target	Tantalum	1.53

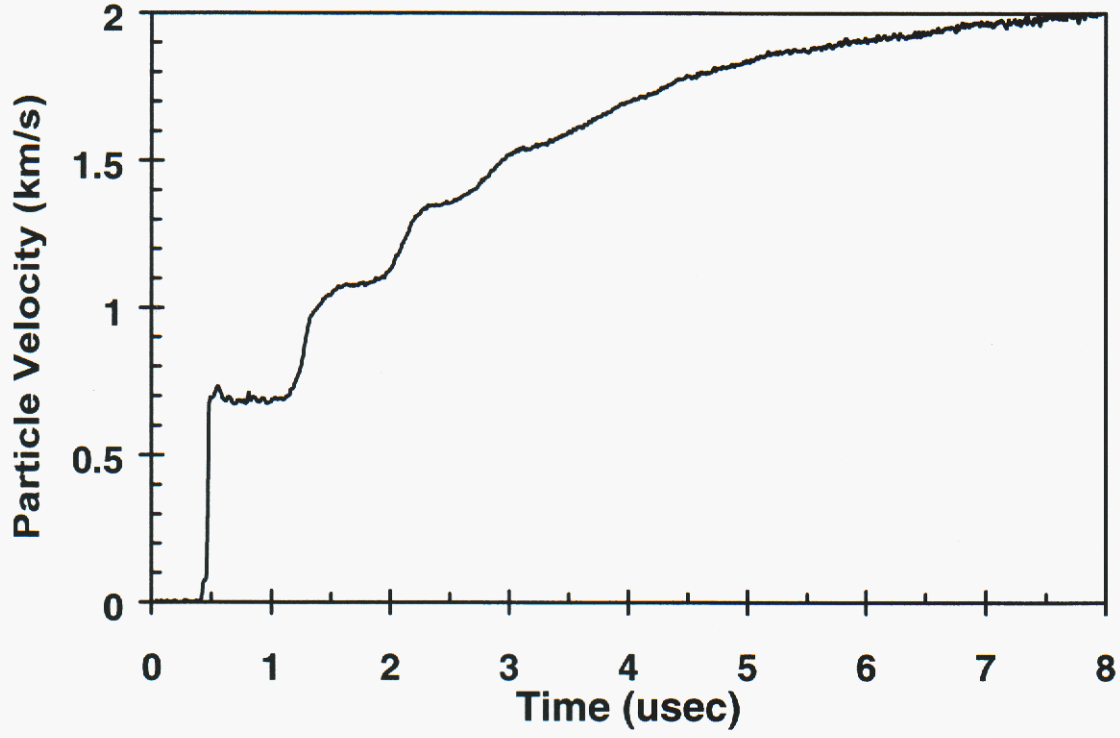

Figure 28. Shot Number: CON7

Shot Number:CON8

Impact Velocity: 2.20 km/s
Concrete Density: 2320 kg/m^3

	Material	Thickness (mm)
Concrete	SAC5	25.4
Target	Tantalum	1.52

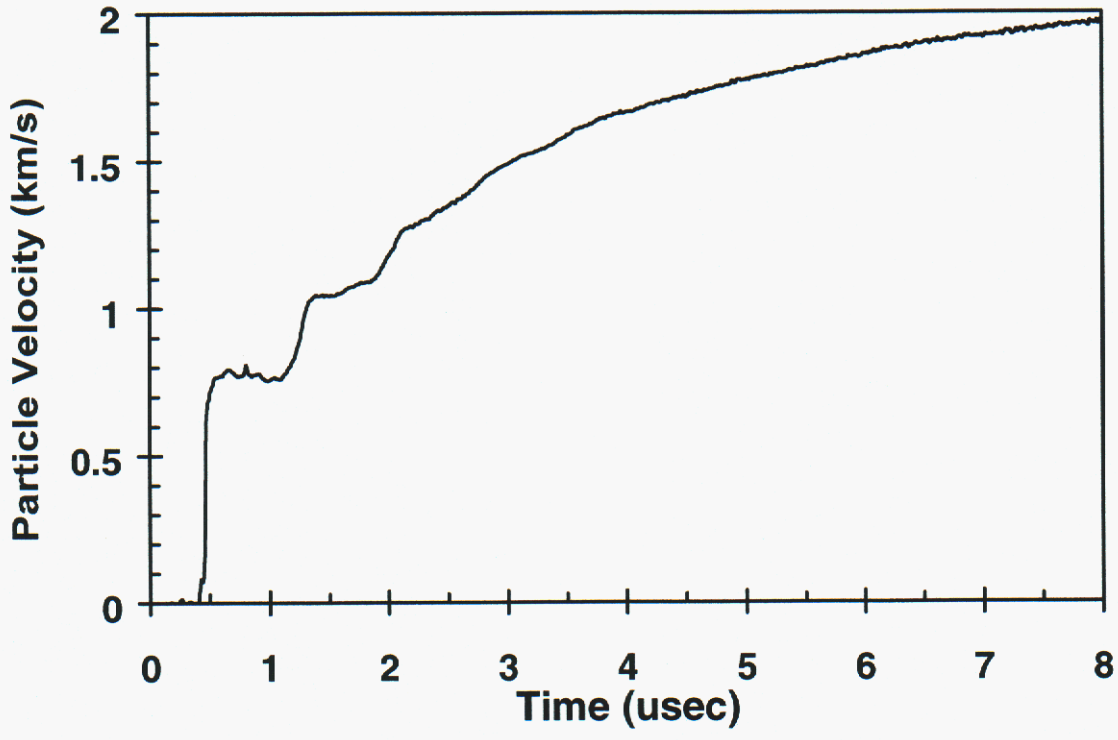

Figure 29. Shot Number: CON8

Shot Number:CON9

Impact Velocity: 2.09 km/s
Concrete Density: 2315 kg/m^3

	Material	Thickness (mm)
Concrete	SAC5	25.4
Target	Copper	2.41

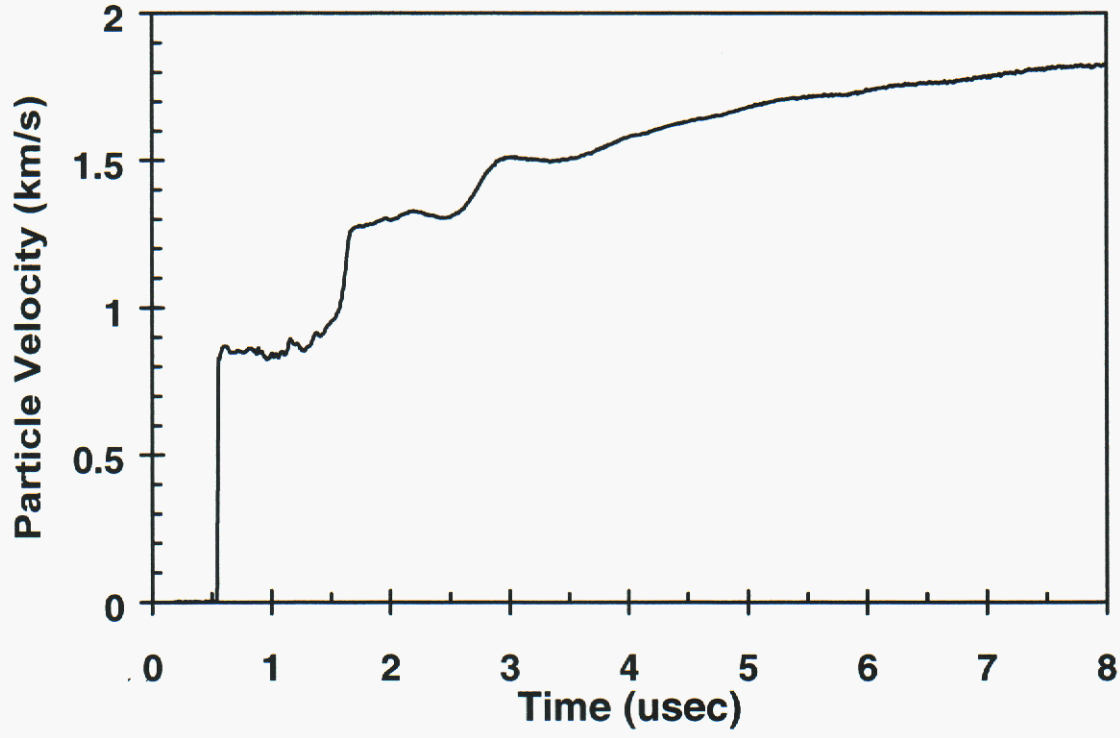

Figure 30. Shot Number: CON9

Shot Number:CON10

Impact Velocity: 1.71 km/s
Concrete Density: 2314 kg/m^3

	Material	Thickness (mm)
Concrete	SAC5	25.4
Target	Copper	2.36

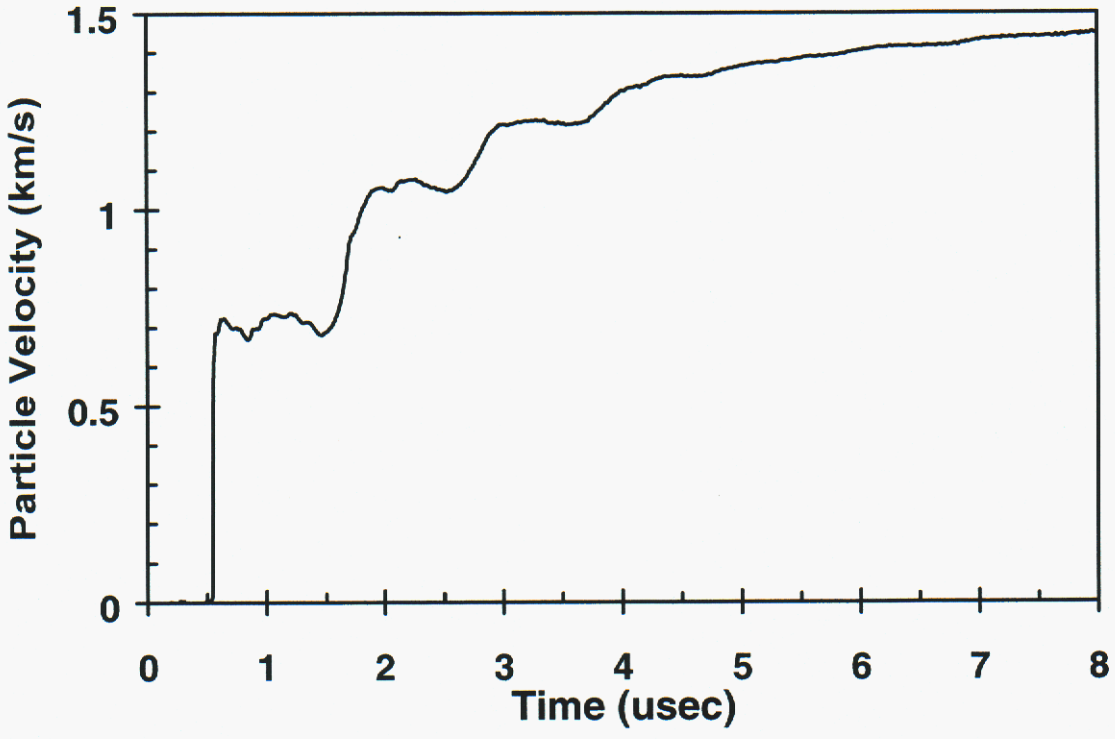

Figure 31. Shot Number: CON10

Shock and Release Properties of Different Aggregate Concretes

1.0 Introduction

A series of controlled impact experiments has been performed to determine the shock loading and release behavior of two types of concrete, differentiated by aggregate size, but, with average densities varying by less than 2 %. Hugoniot stress and subsequent release data was collected over a range of approximately 3 to 25 GPa using a plate reverberation technique with VISAR interferometry. This data was compared in several ways to data previously collected on SAC-5 concrete, which had a different aggregate size, but, similar density. In one comparison, the particle velocity profiles were normalized with respect to plate thickness and overlaid on the same graph. Also, derived quantities such as stress and strain for both the Hugoniot and subsequent release states were plotted and compared. Results indicate that the average loading and release behavior, of the 3 types of concrete discussed here, are grouped within scatter bars derived from particle velocity variations that are caused by the heterogeneous character of the material. Therefore, it appears that concrete does not exhibit a strong dependence upon aggregate size in the 3 to 25 GPa stress range (Hall et al., 1998, Reinhart et al., 1999).

2.0 Material Description

The concrete used in this study had two distinctive aggregate size distributions. The concrete referred to as "large aggregate" (LC in the profiles) had an ASTM aggregate size number of 57. This means that 5 % of the material by weight is between 25 mm and 37.5 mm, 40 % to 75 % is between 19 mm and 25 mm, and the balance is 4.75 mm or smaller. The concrete referred to as "small aggregate" (SC in the profiles) had an ASTM aggregate size number of 7. This means that 10 % of the material by weight is 12.5 mm, 30 % to 60 % is 9.5 mm, and the balance is 4.75 mm or smaller. Cores were taken from large castings in both cases to ensure representative responses. Samples were obtained from each core by grinding to precise dimensions and measurements were made to determine the density of each sample.

3.0 Experimental Method

The plate reverberation technique described in the previous section was also used for this study (see **Figure 17**). Results are shown in the subsequent profiles (see **Figure 32** through **Figure 44**).

4.0 Velocity Profiles

Shot Number: LC1

Impact Velocity: 0.464 km/s
Concrete Density: 2354 kg/m^3

	Material	Thickness (mm)
Concrete	Large Aggregate	30.03
Target	Copper	3.51

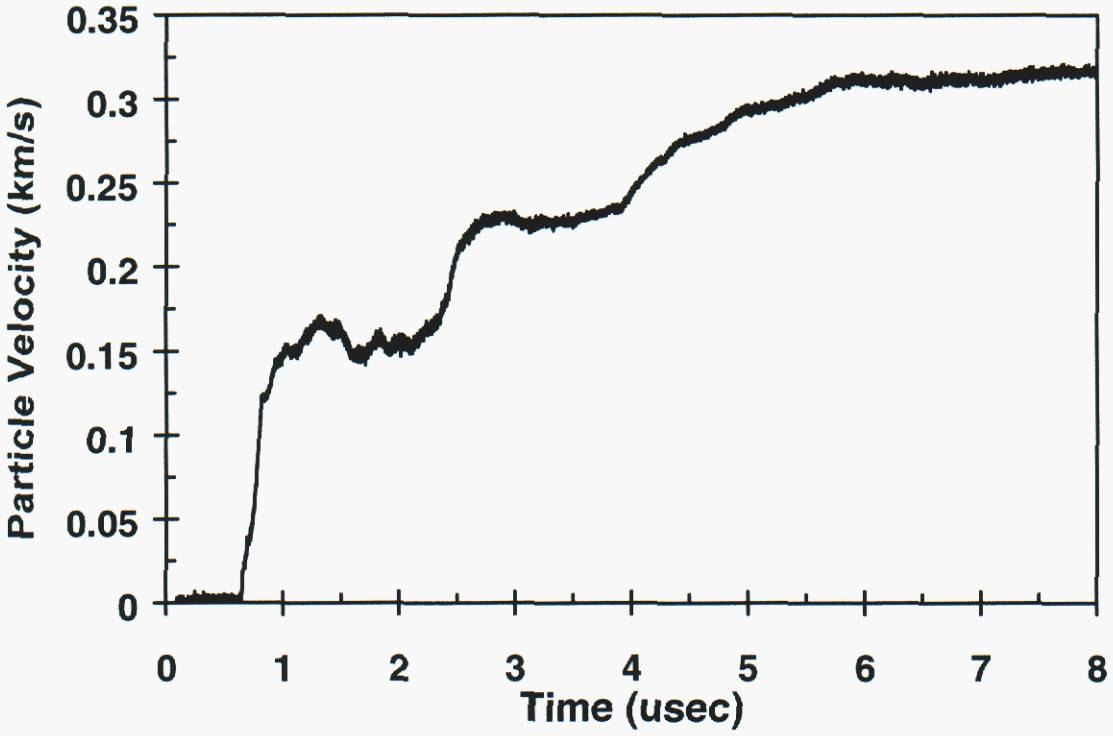

Figure 32. Shot Number: LC1

Shot Number: LC2

Impact Velocity: 0.797 km/s
Concrete Density: 2356 kg/m^3

	Material	Thickness (mm)
Concrete	Large Aggregate	30.03
Target	Copper	3.52

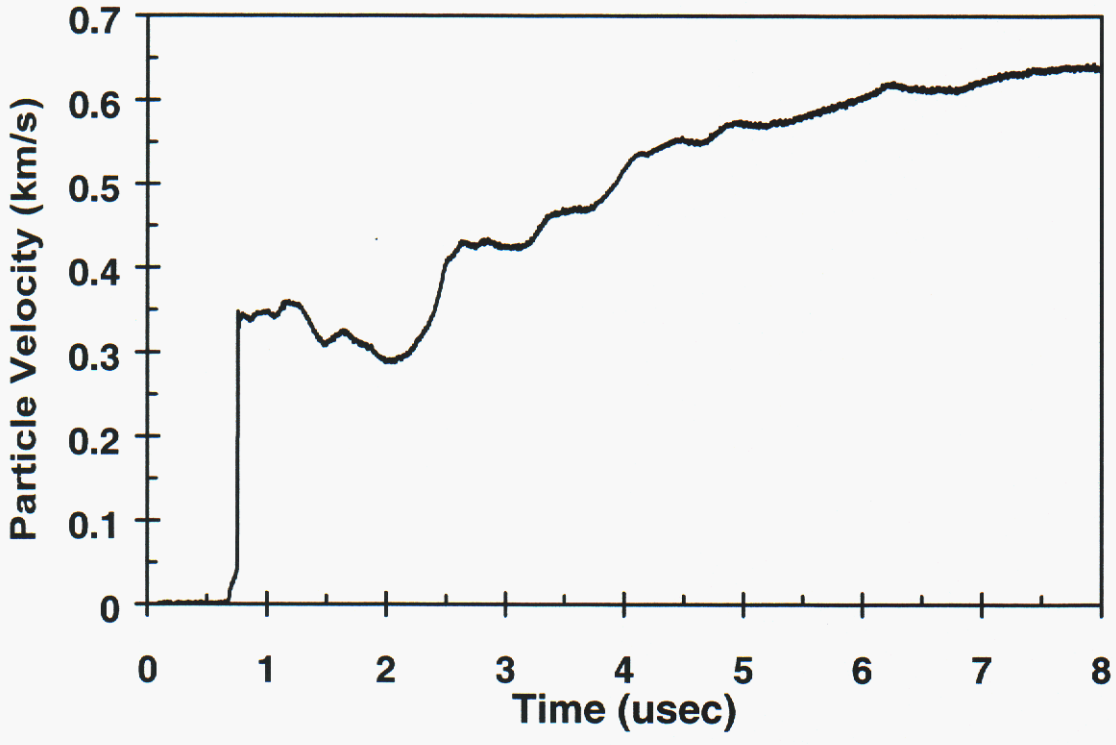

Figure 33. Shot Number: LC2

Shot Number: LC3

Impact Velocity: 1.340 km/s
Concrete Density: 2356 kg/m^3

	Material	Thickness (mm)
Concrete	Large Aggregate	30.01
Target	Copper	3.52

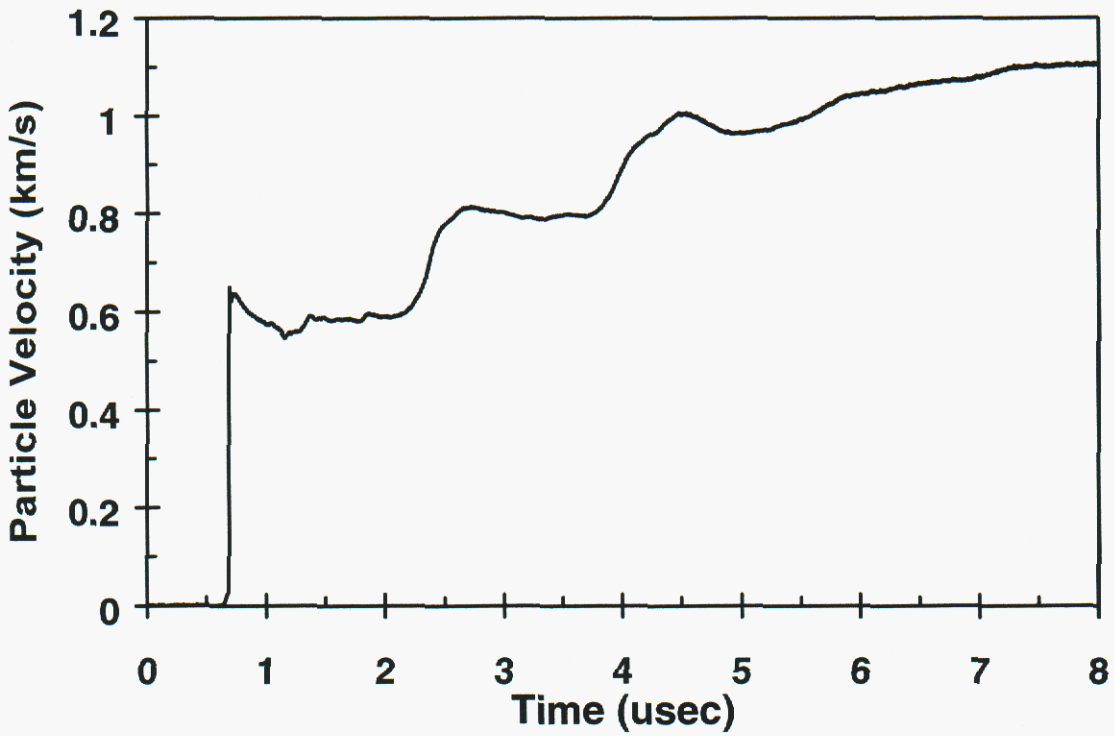

Figure 34. Shot Number: LC3

Shot Number: LC4

Impact Velocity: 1.740 km/s
Concrete Density: 2363 kg/m^3

	Material	Thickness (mm)
Concrete	Large Aggregate	30.00
Target	Copper	3.50

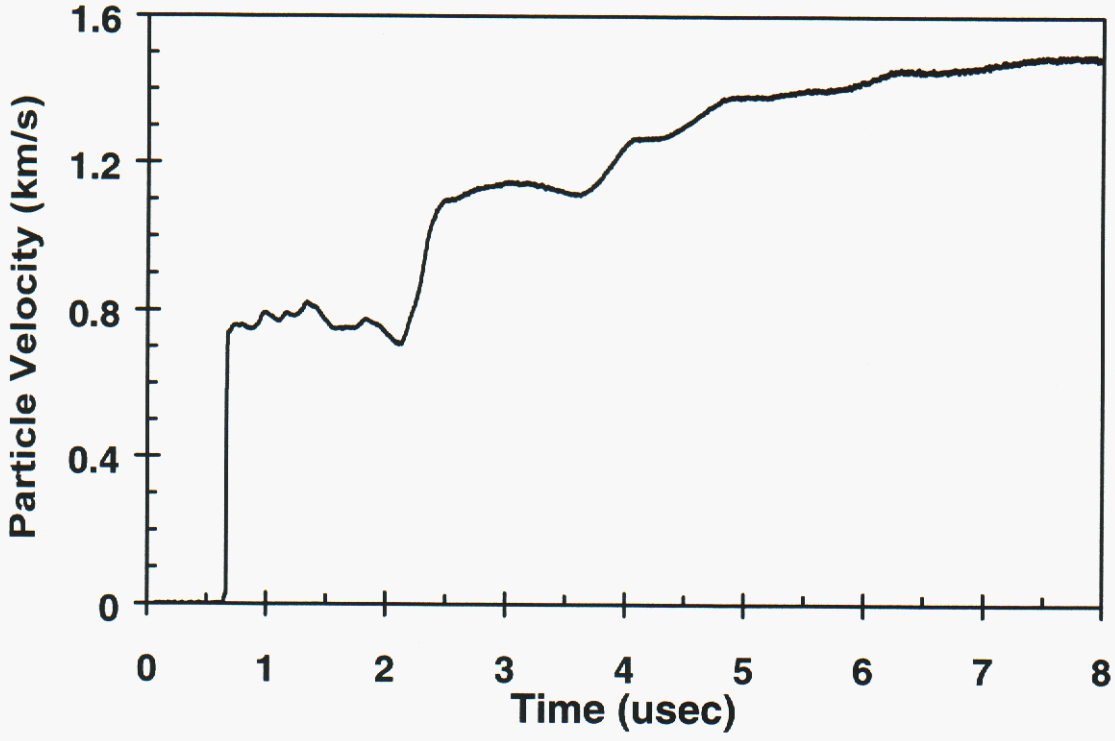

Figure 35. Shot Number: LC4

Shot Number:LC5 On-axis

Impact Velocity: 2.150 km/s
Concrete Density: 2357 kg/m^3

	Material	Thickness (mm)
Concrete	Large Aggregate	30.01
Target	Copper	3.50

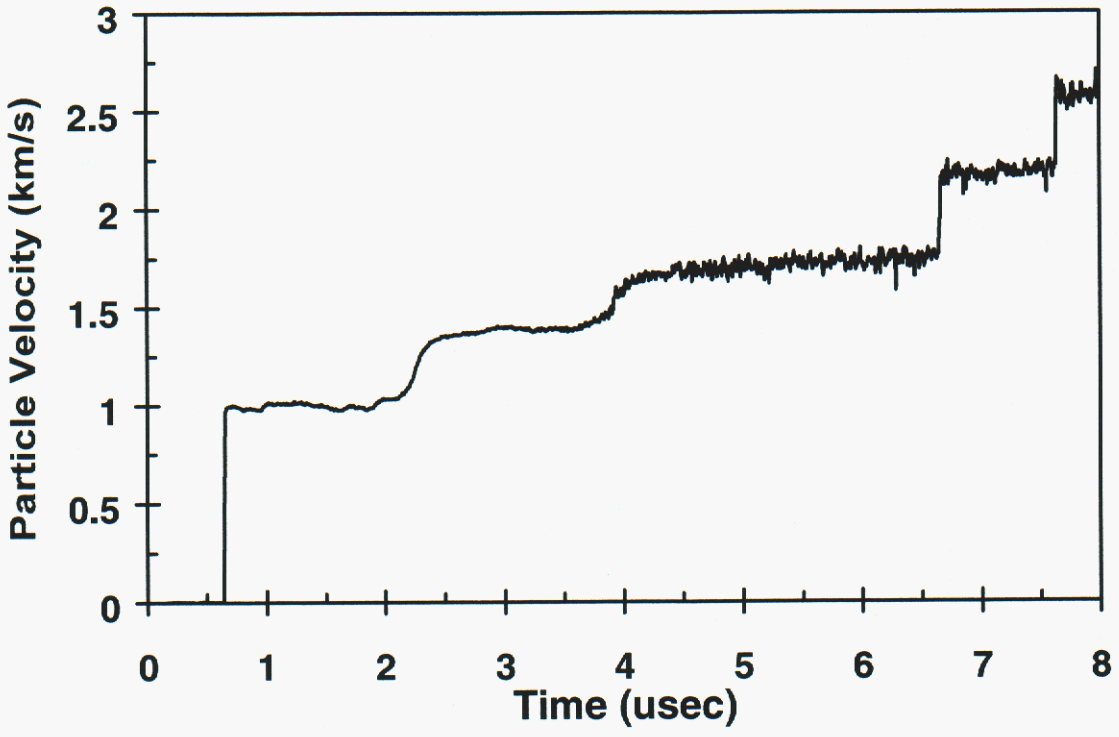

Figure 36. Shot Number: LC5 On-axis

Shot Number:LC5 Off-axis

Impact Velocity: 2.150 km/s
Concrete Density: 2357 kg/m^3

	Material	Thickness (mm)
Concrete	Large Aggregate	30.01
Target	Copper	3.50

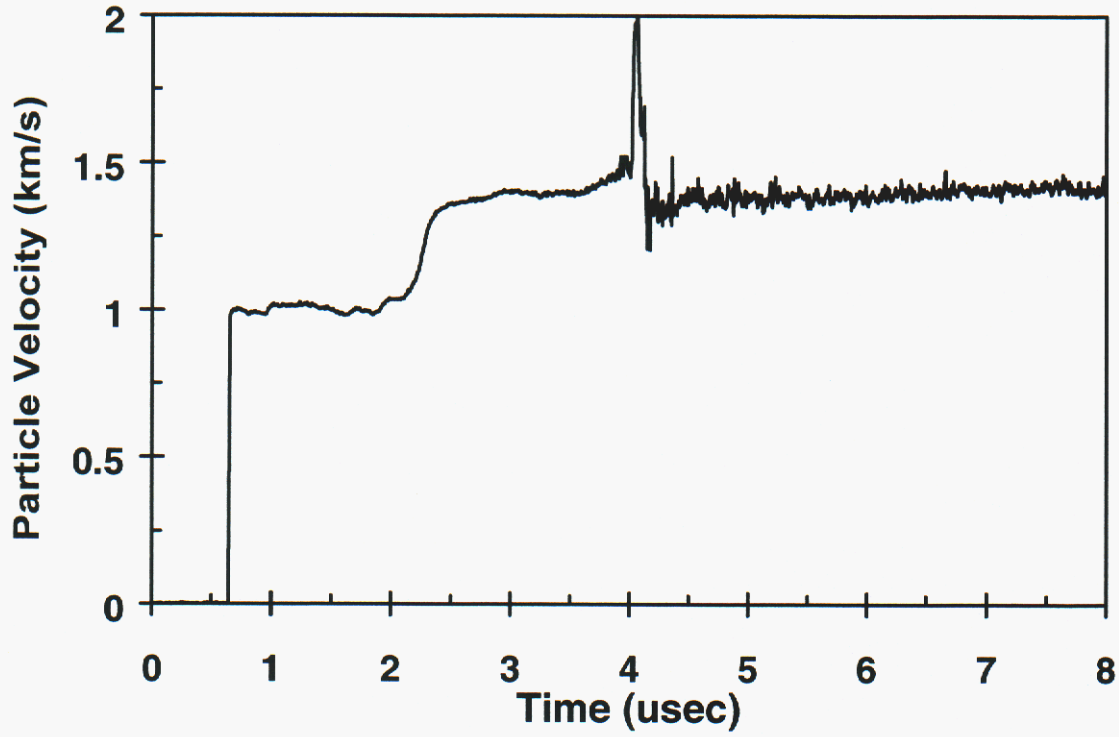

Figure 37. Shot Number: LC5 Off-axis

Shot Number: LC7

Impact Velocity: 2.140 km/s
Concrete Density: 2354 kg/m^3

	Material	Thickness (mm)
Concrete	Large Aggregate	30.02
Target	Tantalum	1.85

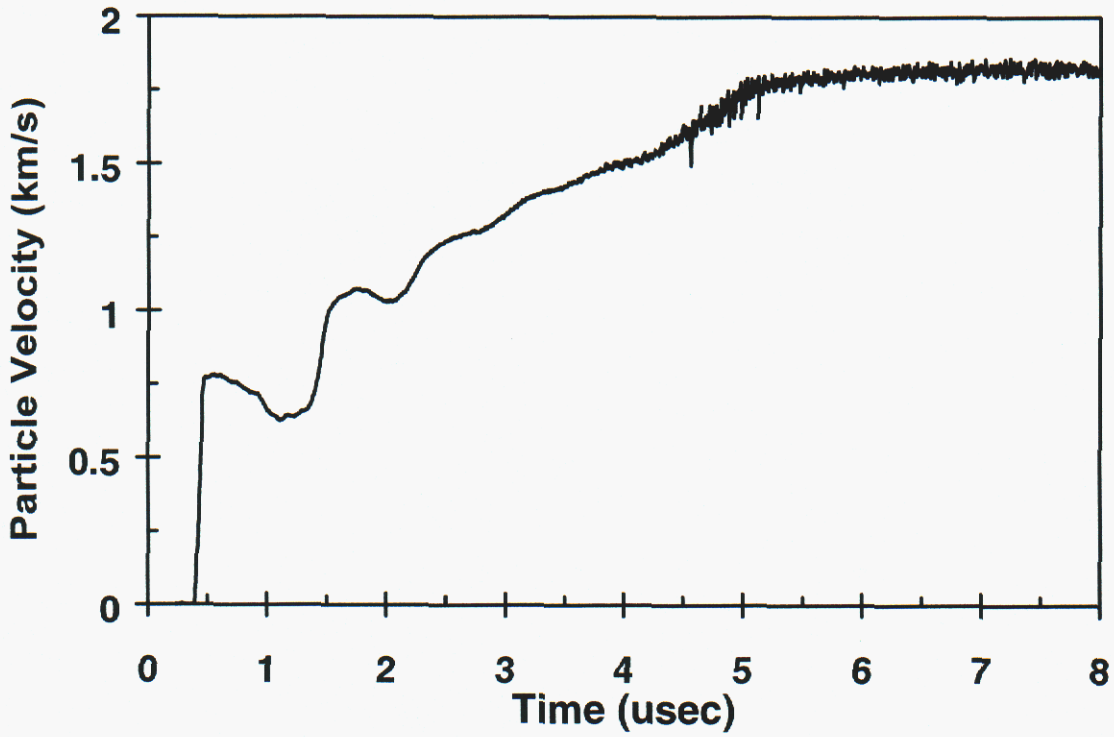

Figure 38. Shot Number: LC7

Shot Number: SC1

Impact Velocity: 2.143 km/s
Concrete Density: 2340 kg/m^3

	Material	Thickness (mm)
Concrete	Small Aggregate	30.00
Target	Copper	3.50

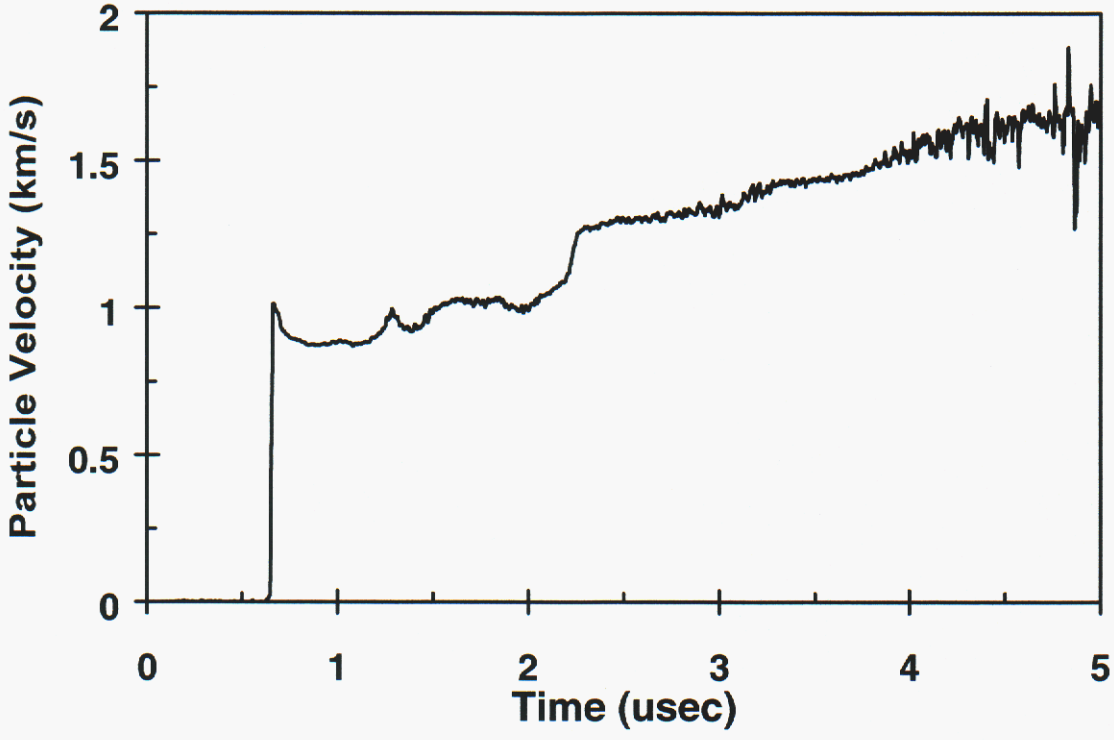

Figure 39. Shot Number: SC1

Shot Number: SC2

Impact Velocity: 1.748 km/s
Concrete Density: 2348 kg/m^3

	Material	Thickness (mm)
Concrete	Small Aggregate	30.01
Target	Copper	3.50

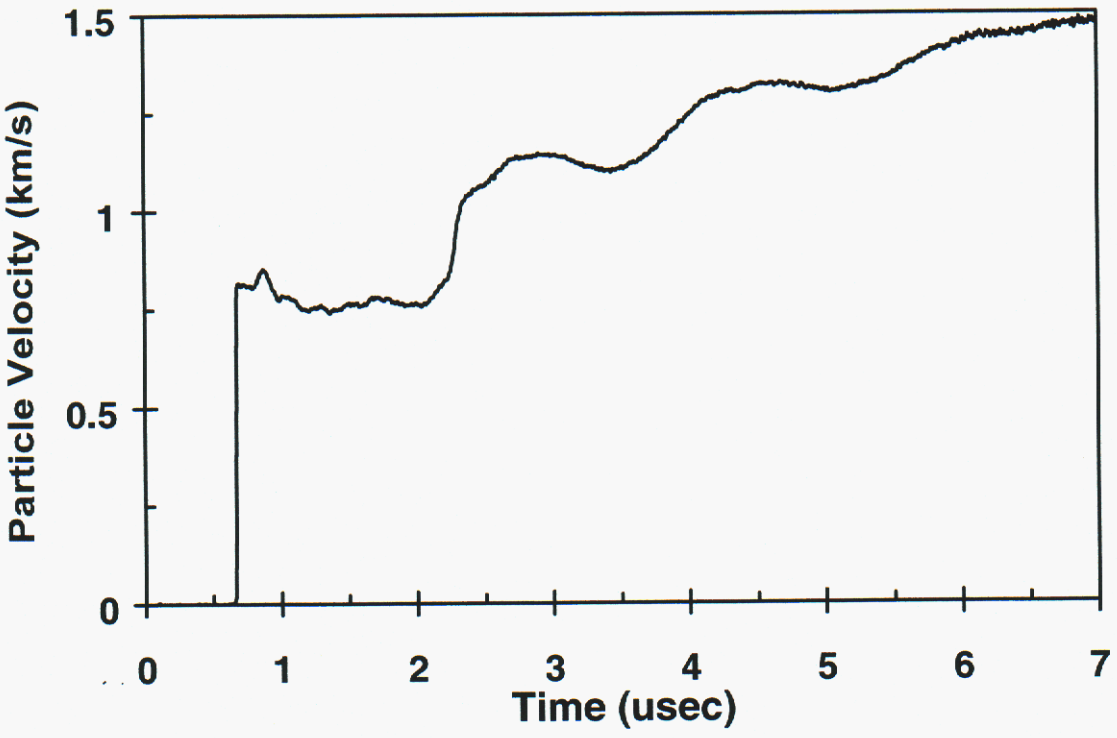

Figure 40. Shot Number: SC2

Shot Number: SC3

Impact Velocity: **1.330 km/s**
Concrete Density: 2322 kg/m^3

	Material	Thickness (mm)
Concrete	Small Aggregate	30.01
Target	Copper	3.50

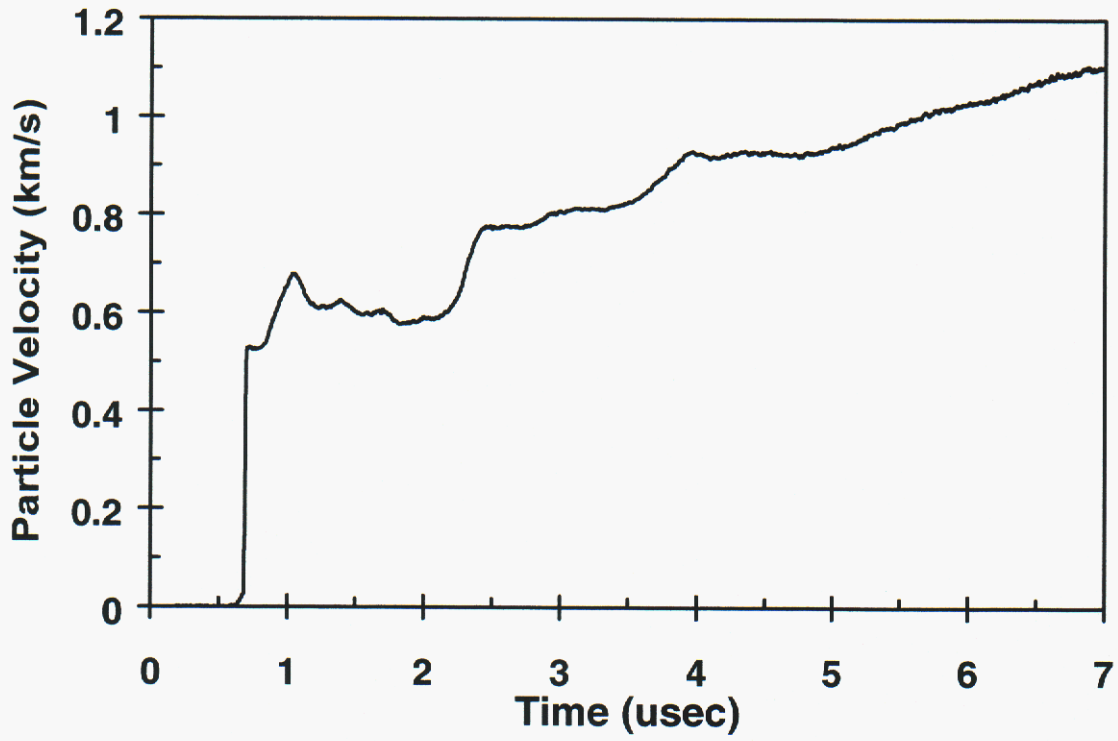

Figure 41. Shot Number: SC3

Shot Number: SC4

Impact Velocity: 2.175 km/s
Concrete Density: 2341 kg/m^3

	Material	Thickness (mm)
Concrete	Small Aggregate	30.01
Target	Tantalum	1.86

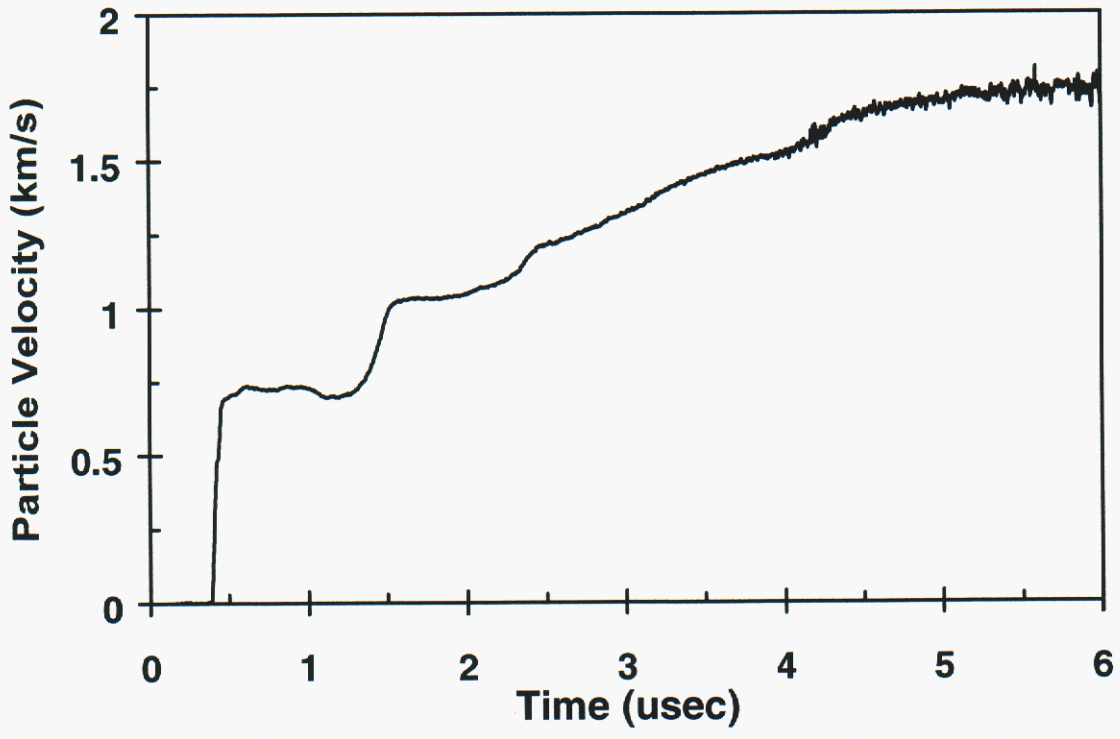

Figure 42. Shot Number: SC4

Shot Number: SC5

Impact Velocity: 0.830 km/s
Concrete Density: 2328 kg/m^3

	Material	Thickness (mm)
Concrete	Small Aggregate	30.01
Target	Copper	3.52

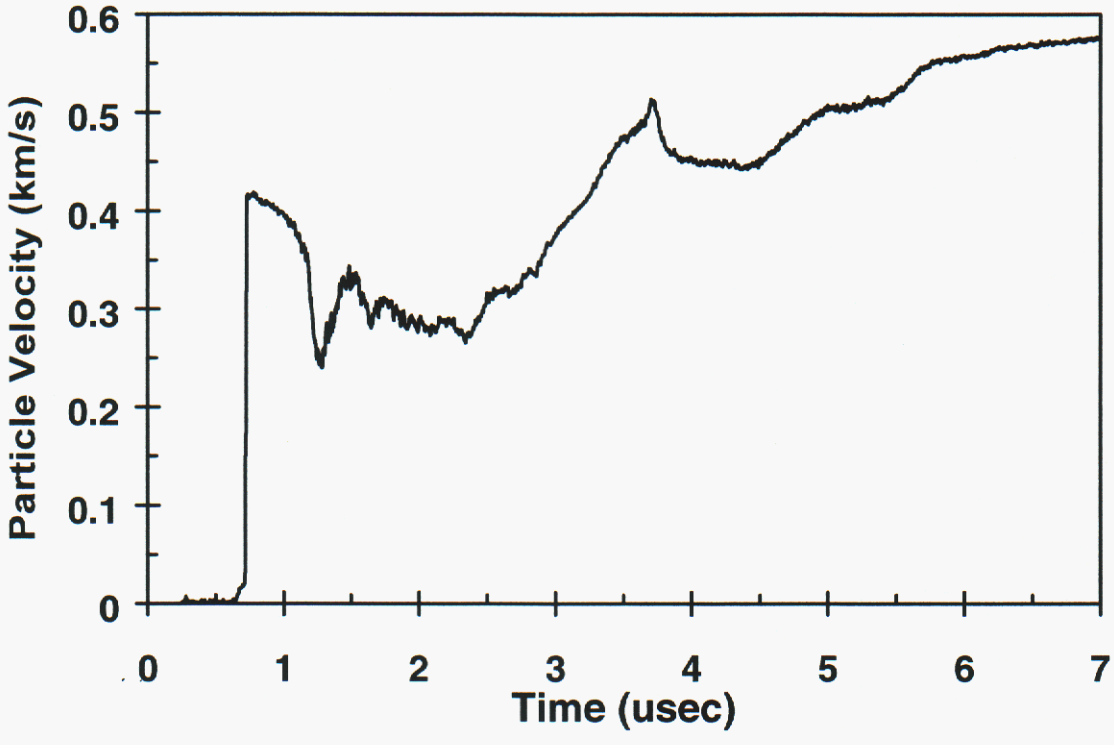

Figure 43. Shot Number: SC5

Shot Number: SC6

Impact Velocity: 0.451 km/s
Concrete Density: 2328 kg/m^3

	Material	Thickness (mm)
Concrete	Small Aggregate	30.00
Target	Copper	3.52

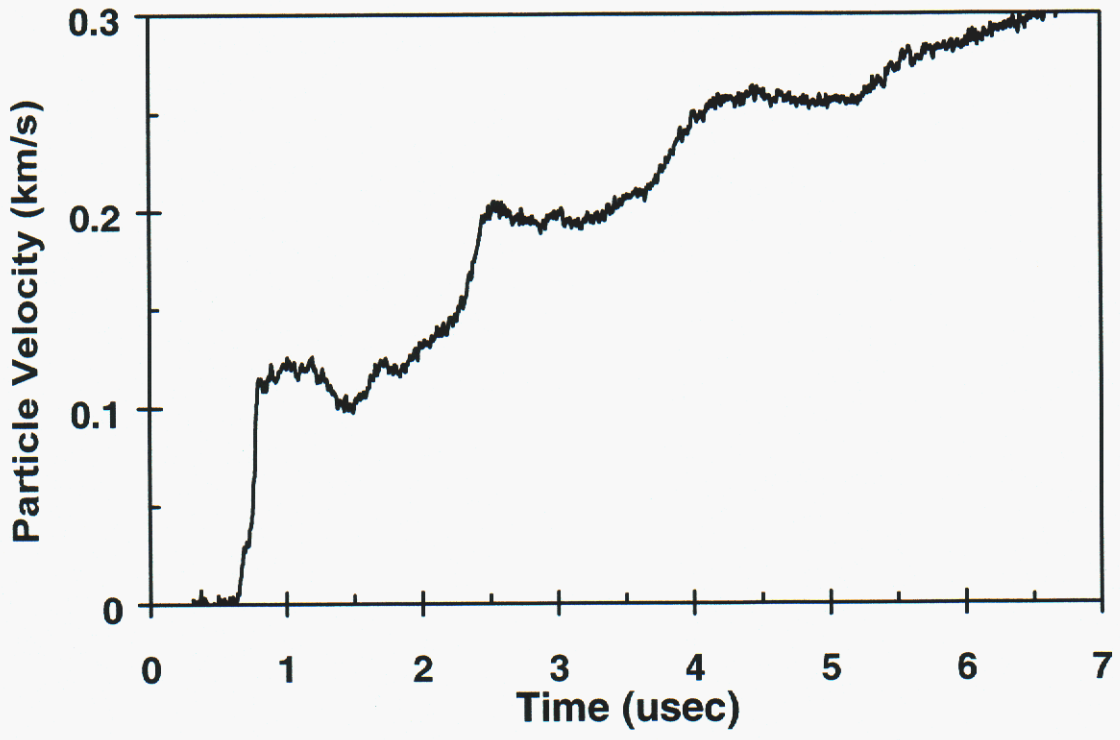

Figure 44. Shot Number: SC6

Spall Properties of Concrete

1.0 Introduction

In the present experiments, two concretes with differing small-scale aggregate were tested under impact conditions to determine their dynamic tensile fracture (or spall) properties. Wave profiles from a suite of experiments using gas gun impact methods achieved compression pressures ranging from 0.08 to 0.55 GPa that remains within the elastic or near-elastic regime. Complex wave structure was observed to develop in the shock transit of these heterogeneous concretes, however, definitive spall pull back profiles were recorded. Spall strengths in the neighborhood of 30 MPa were determined for these concretes and explicit-aggregate simulations of these tests with computer codes and have provided insight into the dynamic tensile failure characteristics of these materials (Reinhart et al., 1999).

2.0 Material Description

Properties pertinent to spall failures are described. The concrete compositions differ in nature of aggregate size. SAC-5 has pea gravel and CSPC has angular gravel with a maximum dimension of 10 mm in both cases, constituting about 40-45% of volume fraction of the concrete, the rest grout. The concrete referred to as large aggregate had an American Society for Testing of Materials (ASTM) aggregate size number of 57. This implies that 5% of the material by weight is between 25 mm and 37.5 mm, 40% to 75% is between 19 mm and 25 mm and the balance is 4.75 mm or smaller. The concrete referred to as small aggregate had an ASTM aggregate size number of 7, which means 10% of the material by weight is 12.5 mm, 30%-60% is 9.5 mm and the balance is 4.75 mm or smaller. Cores were taken from large castings in all cases to ensure representative responses. Samples were obtained from each core by grinding to precise dimensions, and measurements made to determine the density of each sample. The SAC-5 concrete has a nominal density of 2260 kg/m^3 and an ultrasonic longitudinal velocity of 5060 m/s. The CSPC has a nominal density of 2290 kg/m^3 and an ultrasonic longitudinal velocity of 5200 m/s. The large (3/4") has a nominal density of 2352 kg/m^3 and an ultrasonic longitudinal velocity of 4938 m/s; and the small (3/8") has a nominal density of 2346 kg/m^3 and an ultrasonic longitudinal velocity of 4532 m/s.

3.0 Experimental Method

Impact experiments were performed with a single-stage light-gas gun of 64-mm inner-bore diameter capable of achieving controlled velocities over a range of approximately 30 m/s to 220 m/s. The projectile was faced with carbon foam (density = 200 kg/m^3) and a flat polymethyl methacrylate (PMMA) impactor assembly. The PMMA impactor plates had thickness of approximately 4.5 mm and 9.5 mm and a diameter of 57 mm (see individual test profiles). The PMMA impacts directly onto the concrete sample, 12.7 mm thick. A velocity interferometer system for any reflector (VISAR) was used to monitor the free surface velocity motion of the concrete rear surface. A thin (10μm) aluminum foil on the rear surface of the concrete ensured that local surface roughness did not impair the velocity measurement, besides obtaining the reflected optical signals necessary for the interferometric techniques. The heterogeneous nature of concrete gives rise to unique dispersive velocity records whose distinctive features depend upon the location of the monitoring position. Nevertheless, an average shock response for the bulk behavior of the material can still be determined. Schematics of the experimental impact conditions are illustrated in **Figure 45**. The experimental impact conditions are shown in Table 3, as well as with each profile. Aside from four experiments, the rear surface of the concrete remained free. On those four experiments, the concrete was backed with a PMMA window to alter the magnitude of the pullback signal relative to the main shock amplitude, providing a complementary measure of spall strength. The measured particle velocity histories for the series of experiments performed in this study included CSPC, SAC-5, large aggregate (3/4"), and small aggregate (3/8") concrete.

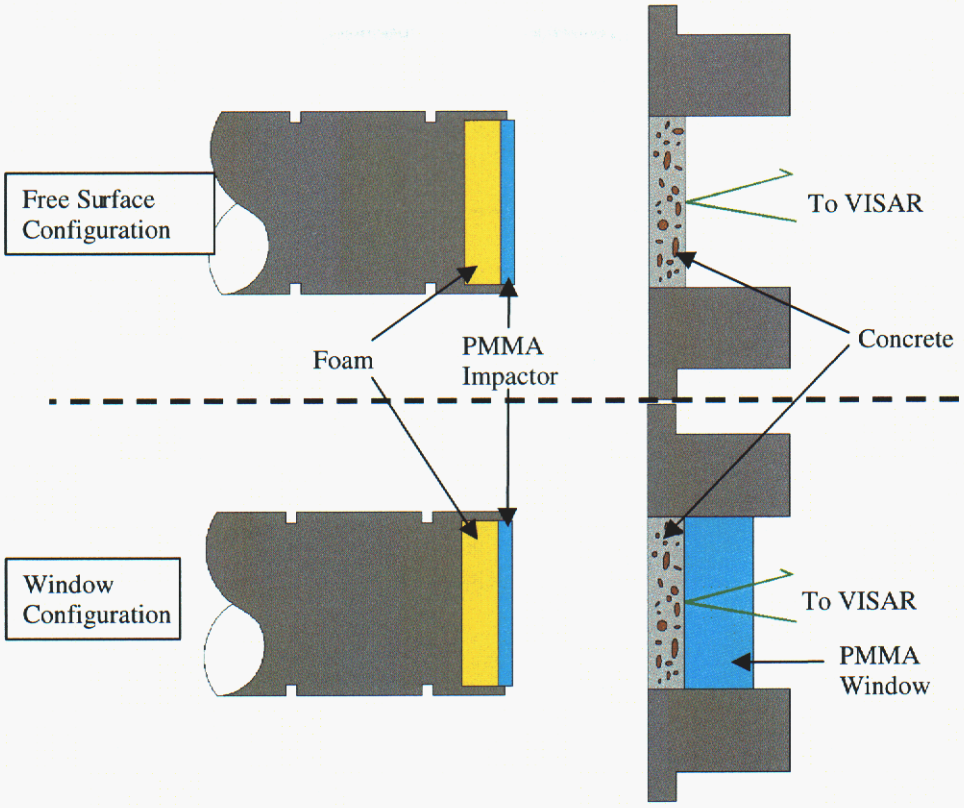

Figure 45. Concrete spall configurations.

SHOT #	Impact Velocity(km/s)	Particle Velocity (km/s)	Impactor Thickness (mm)	Concrete Density (kg/m^3)	Concrete Thickness (mm)	Window Thickness (mm)
CS1 CSPC	0.220	0.136	9.469	2292	12.743	na
CS2 CSPC	0.107	0.068	9.437	2295	12.753	na
CS3 CSPC	0.062	0.041	9.535	2298	12.746	na
CS4 SAC5	0.062	0.040	9.528	2292	12.753	na
CS5 CSPC	0.066	0.035	4.430	2231	12.756	na
CS6 SAC5	0.062	0.036	4.404	2283	12.761	na
CS7 SAC5	0.032	0.019	4.402	2280	12.730	na
CS8 CSPC	0.032	0.015	4.553	2297	12.753	na
CS9 CSPC-w	0.062	0.026	4.630	2301	12.748	24.210
CS10 SAC5-w	0.062	0.029	4.460	2273	12.741	24.247
CS13 small	0.067	0.037	4.481	2360	12.718	na
CS14 large-w	0.068	0.027	4.479	2377	12.733	23.850
CS15 large	0.066	0.041	4.467	2349	12.720	na
CS16 small-w	0.070	0.028	4.467	2356	12.708	23.863
CS18 small	0.030	0.016	4.474	2332	12.728	na
CS19 large	0.029	0.017	4.478	2331	12.728	na

Table 3. Summary of concrete spall experiments

4.0 Velocity Profiles

Shot Number: CS1

Impact Velocity: 0.220 km/s
Concrete Density: 2292 kg/m^3

	Material	Thickness (mm)
Concrete	CSPC	12.74
Impactor	PMMA	9.47

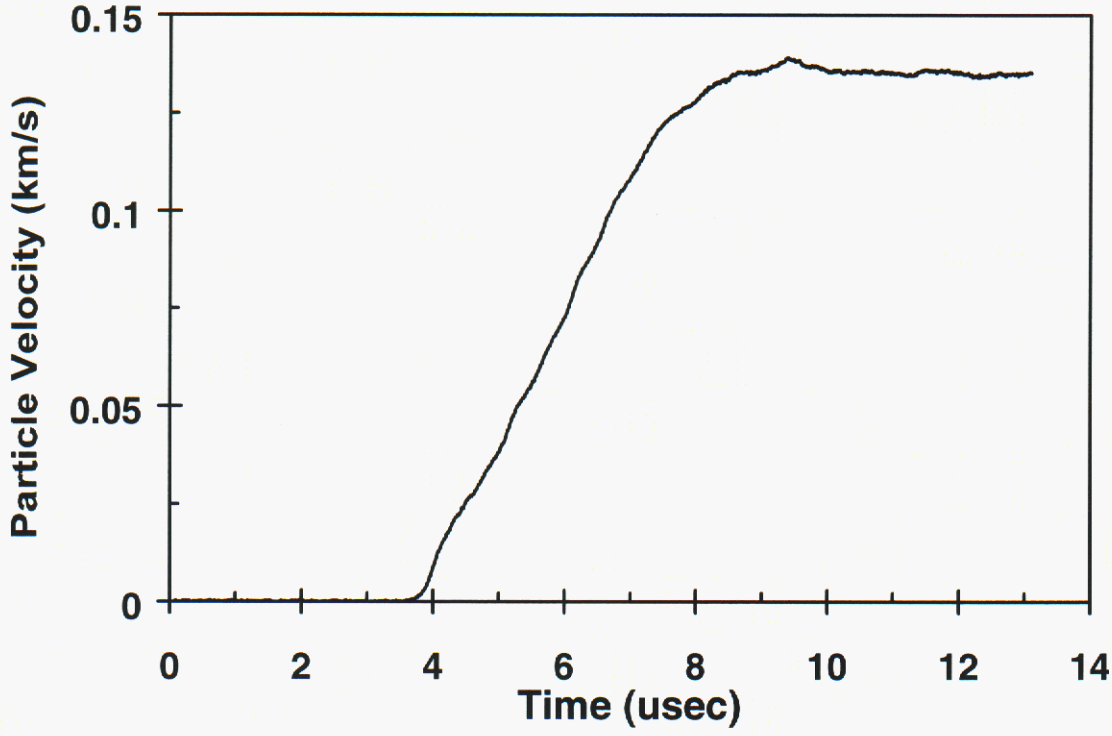

Figure 46. Shot Number: CS1

Shot Number: CS2

Impact Velocity: 0.107 km/s
Concrete Density: 2295 kg/m^3

	Material	Thickness (mm)
Concrete	CSPC	12.75
Impactor	PMMA	9.44

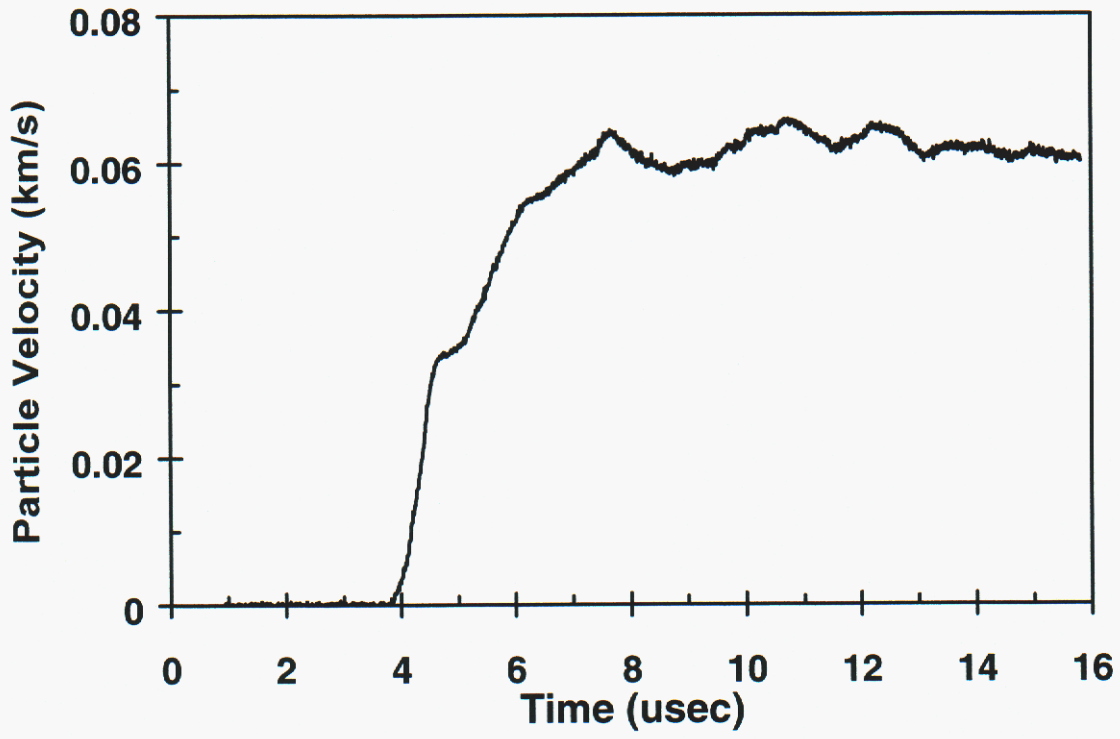

Figure 47. Shot Number: CS2

Shot Number: CS3

Impact Velocity: 0.062 km/s
Concrete Density: 2298 kg/m^3

	Material	Thickness (mm)
Concrete	CSPC	12.75
Impactor	PMMA	9.54

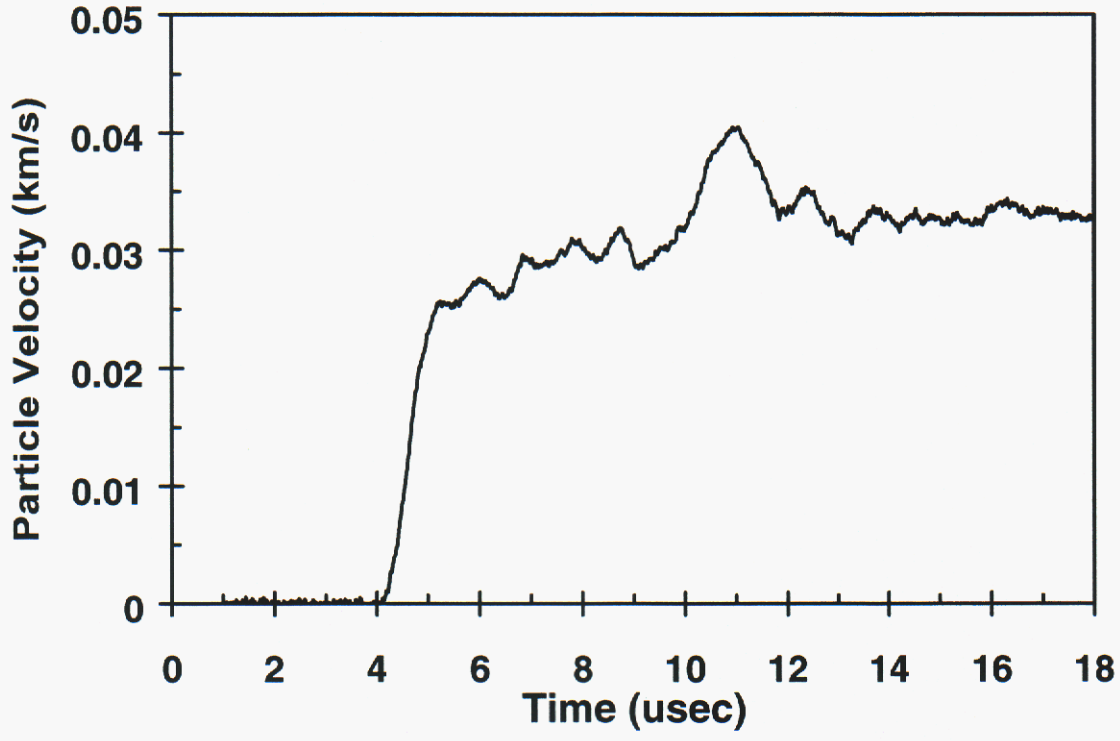

Figure 48. Shot Number: CS3

Shot Number: CS4

Impact Velocity: 0.062 km/s
Concrete Density: 2292 kg/m^3

	Material	Thickness (mm)
Concrete	SAC5	12.75
Impactor	PMMA	9.53

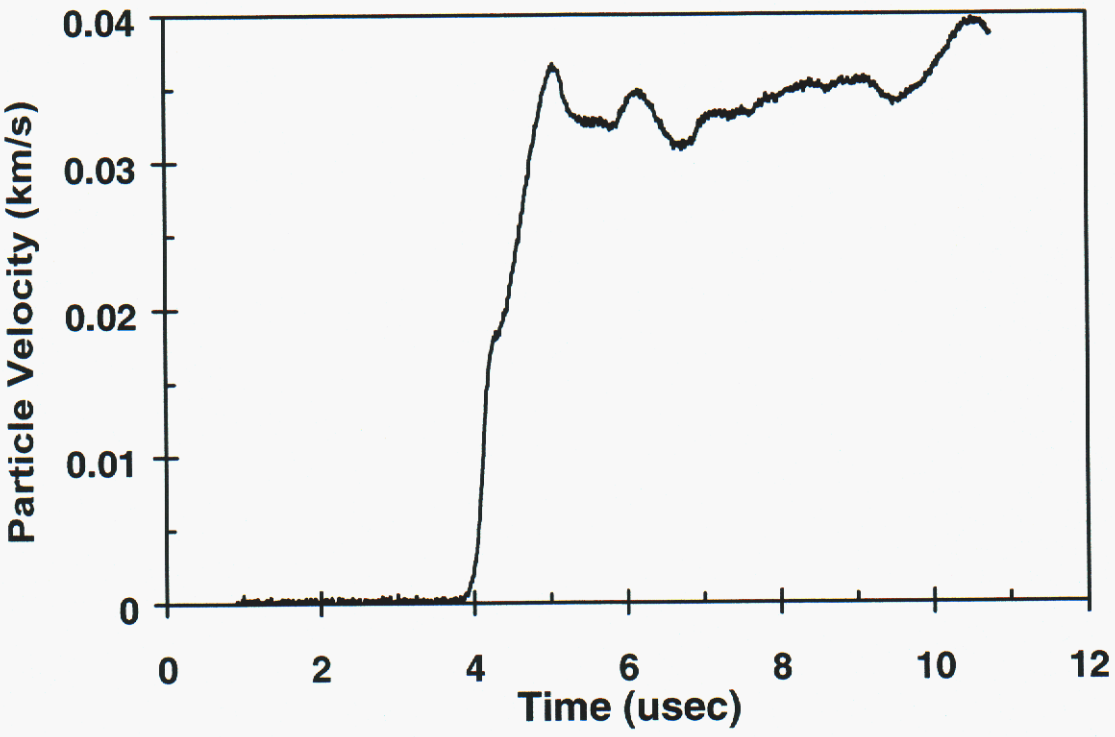

Figure 49. Shot Number: CS4

Shot Number: CS5

Impact Velocity: 0.066 km/s
Concrete Density: 2231 kg/m^3

	Material	Thickness (mm)
Concrete	CSPC	12.76
Impactor	PMMA	4.43

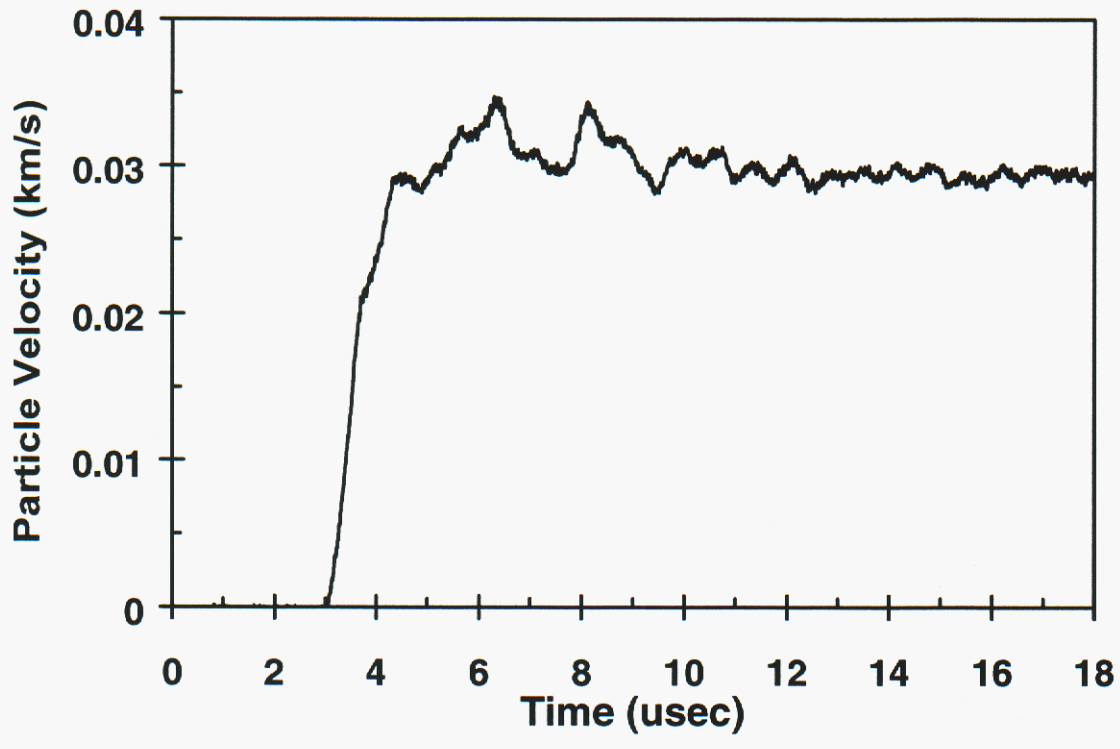

Figure 50. Shot Number: CS5

Shot Number: CS6

Impact Velocity: 0.062 km/s
Concrete Density: 2283 kg/m^3

	Material	Thickness (mm)
Concrete	SAC5	12.76
Impactor	PMMA	4.40

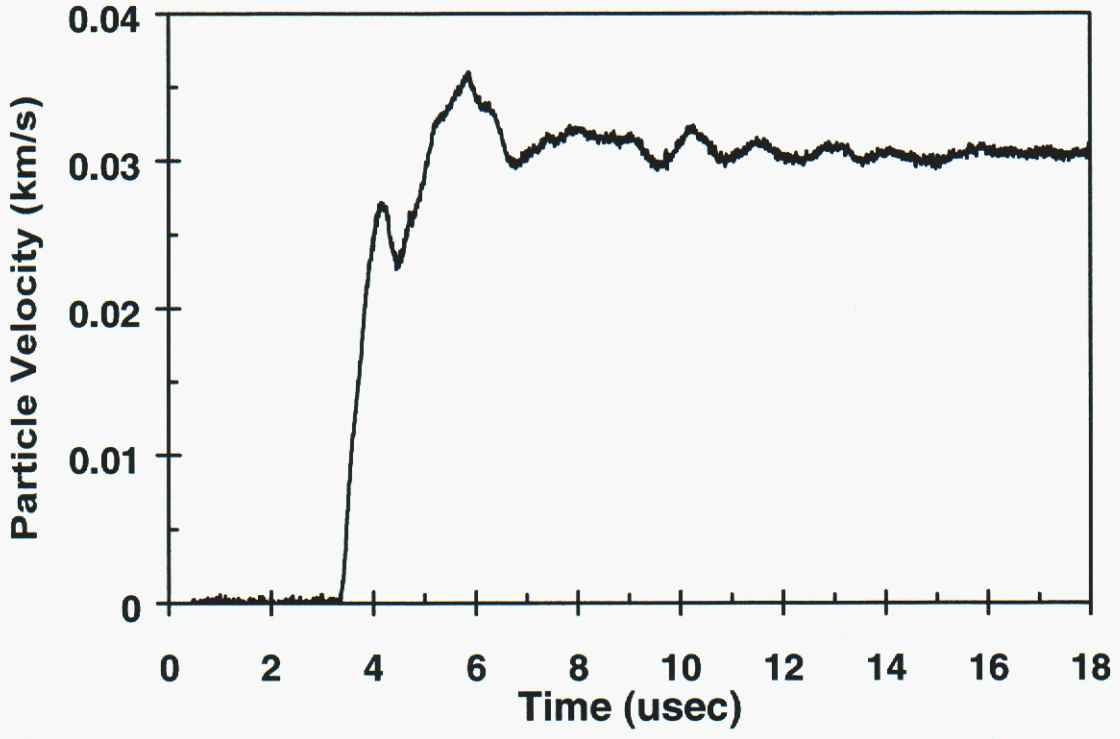

Figure 51. Shot Number: CS6

Shot Number: CS7

Impact Velocity: 0.032 km/s
Concrete Density: 2280 kg/m^3

	Material	Thickness (mm)
Concrete	SAC5	12.73
Impactor	PMMA	4.40

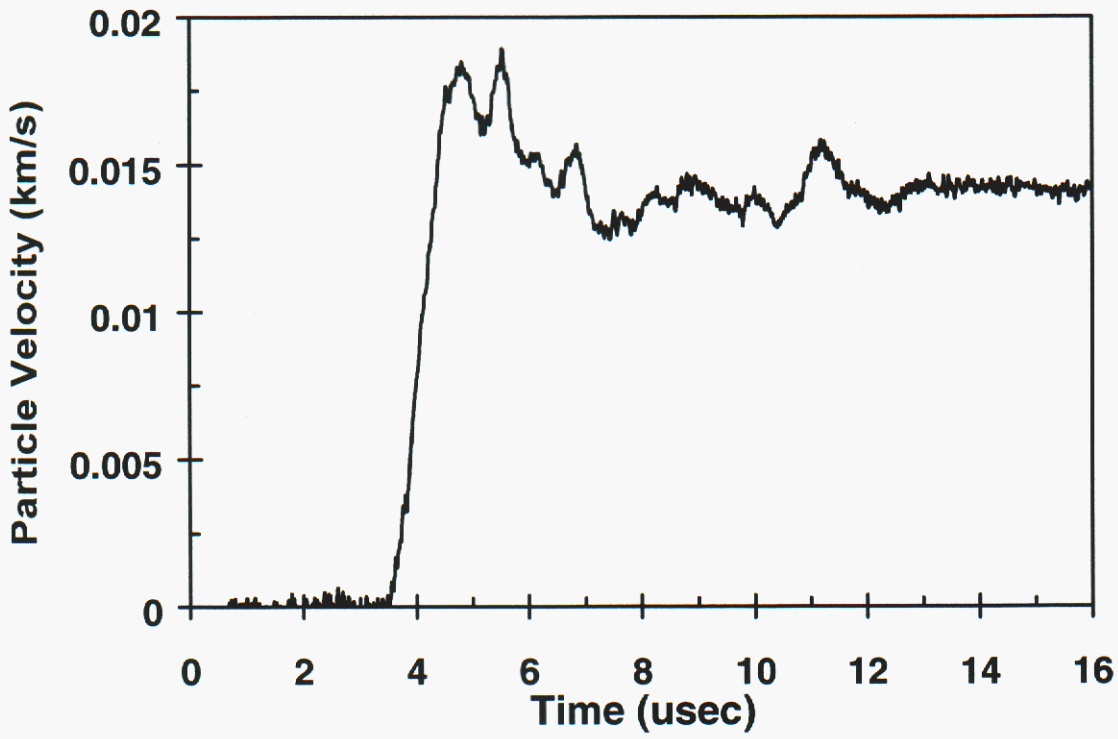

Figure 52. Shot Number: CS7

Shot Number: CS8

Impact Velocity: 0.032 km/s
Concrete Density: 2297 kg/m^3

	Material	Thickness (mm)
Concrete	CSPC	12.75
Impactor	PMMA	4.55

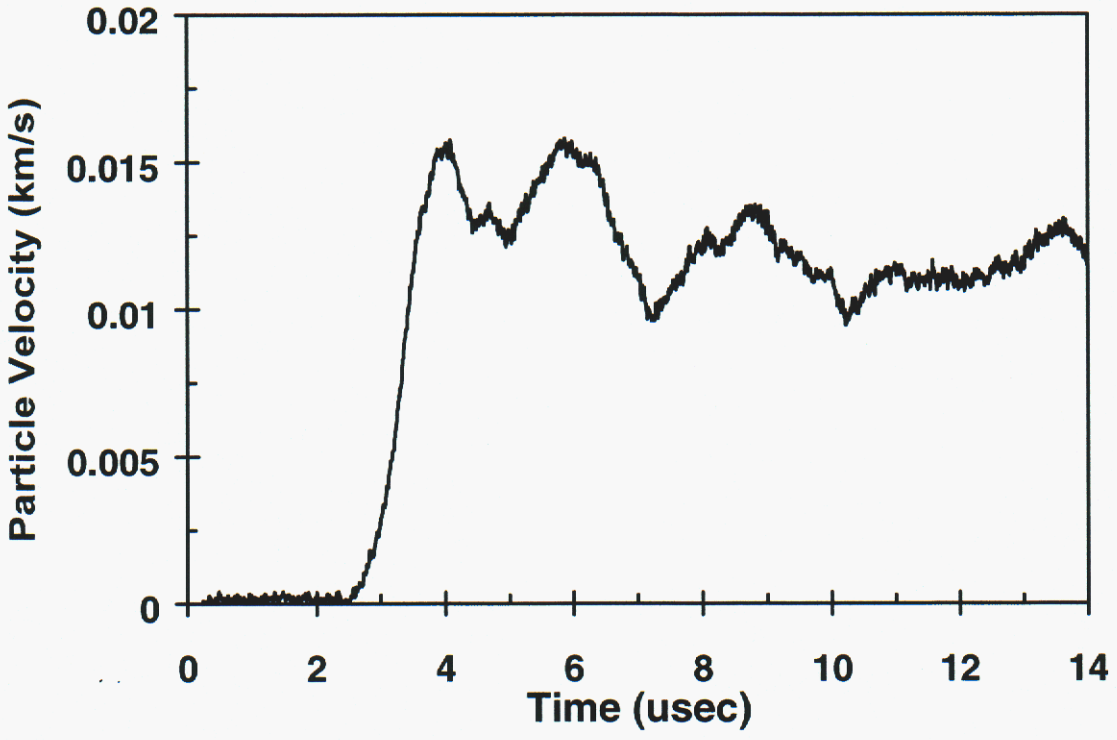

Figure 53. Shot Number: CS8

Shot Number: CS9

Impact Velocity: 0.062 km/s
Concrete Density: 2301 kg/m^3

	Material	Thickness (mm)
Concrete	CSPC	12.75
Impactor	PMMA	4.80
VISAR Window	PMMA	24.21

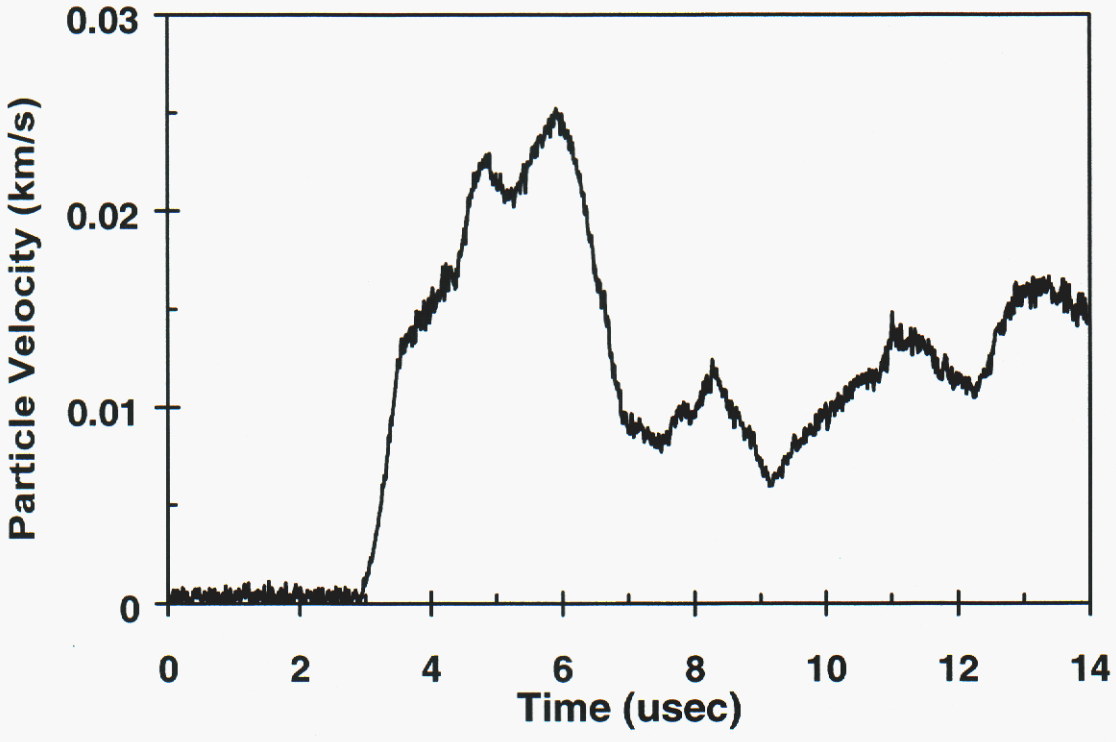

Figure 54. Shot Number: CS9

Shot Number:CS10

Impact Velocity: 0.062 km/s
Concrete Density: 2273 kg/m^3

	Material	Thickness (mm)
Concrete	SAC5	12.74
Impactor	PMMA	4.46
VISAR Window	PMMA	24.25

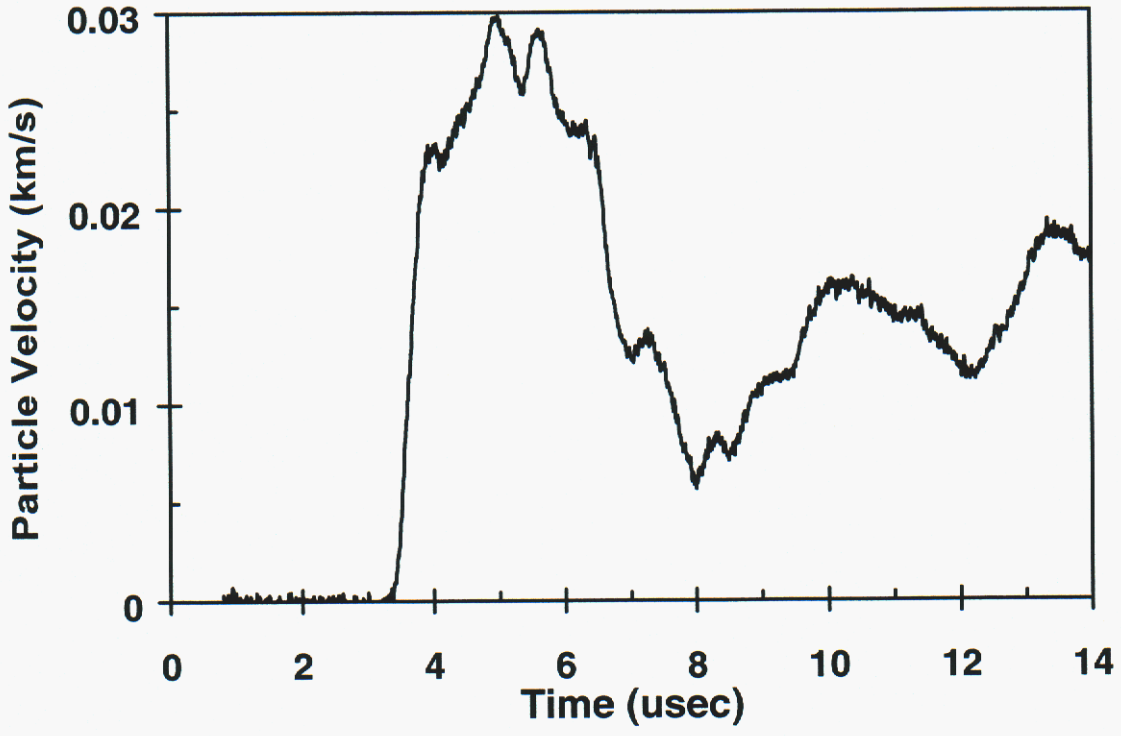

Figure 55. Shot Number: CS10

Shot Number:CS13

Impact Velocity: 0.067 km/s
Concrete Density: 2360 kg/m^3

	Material	Thickness (mm)
Concrete	Small Aggregate	12.72
Impactor	PMMA	4.48

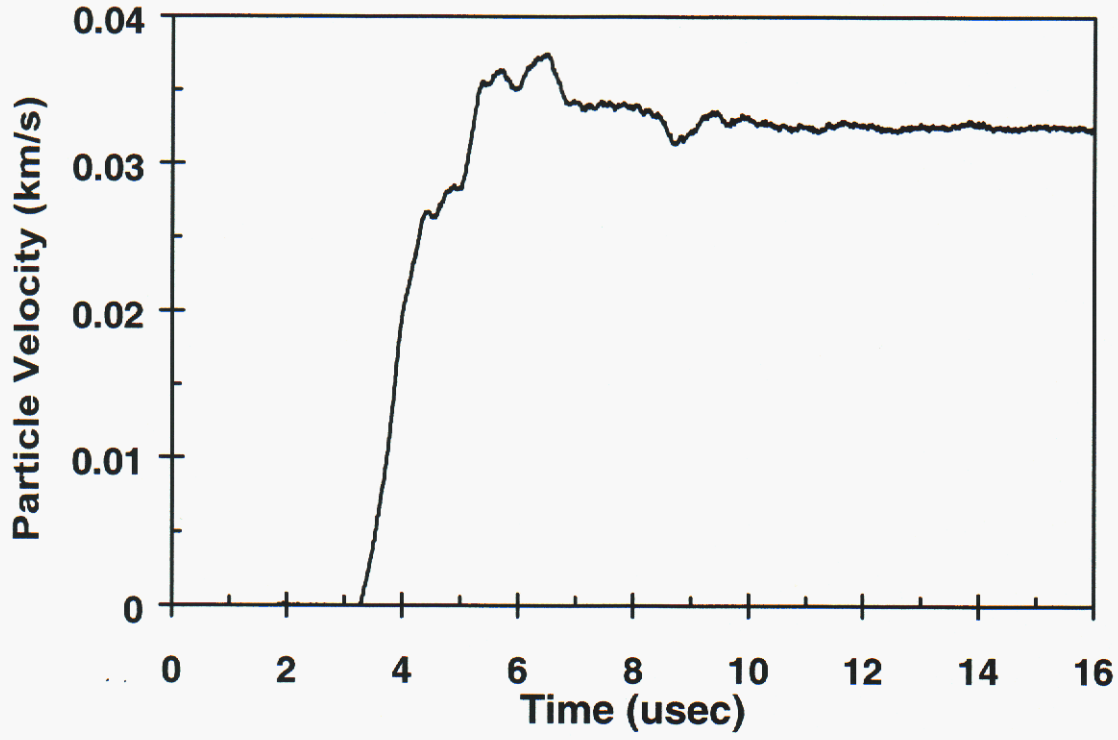

Figure 56. Shot Number: CS13

Shot Number:CS14

Impact Velocity: 0.068 km/s
Concrete Density: 2377 kg/m^3

	Material	Thickness (mm)
Concrete	Large Aggregate	12.73
Impactor	PMMA	4.48

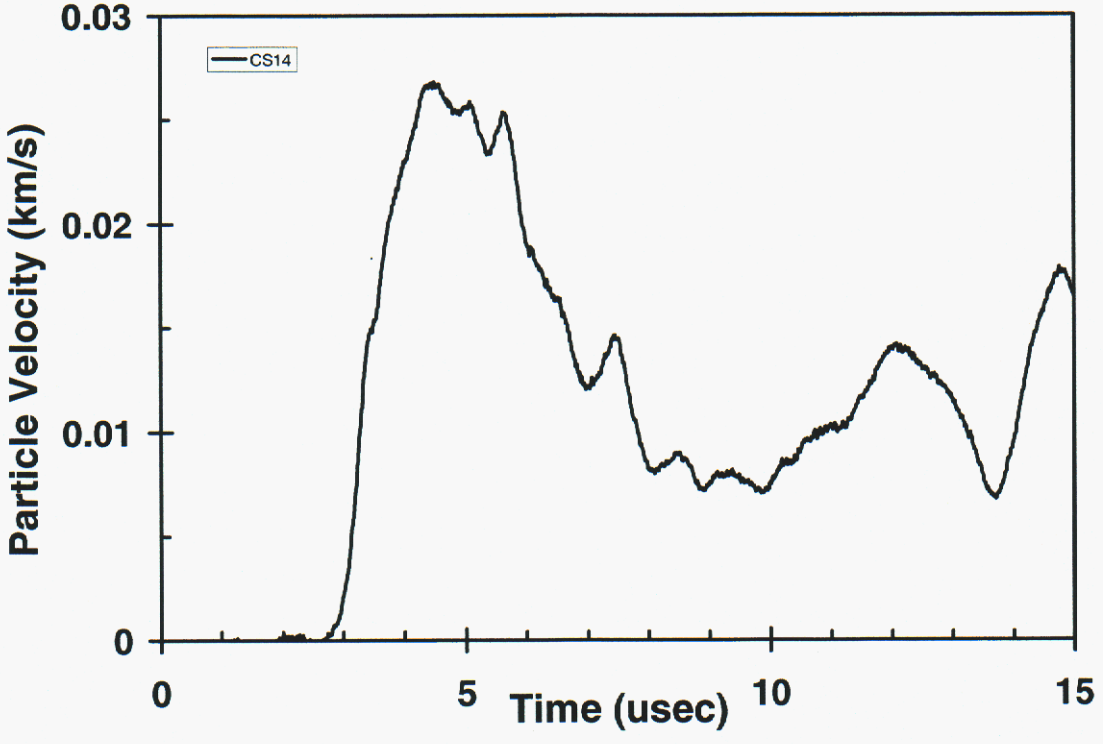

Figure 57. Shot Number: CS14

Shot Number:CS15

Impact Velocity: 0.066 km/s
Concrete Density: 2349 kg/m^3

	Material	Thickness (mm)
Concrete	Large Aggregate	12.72
Impactor	PMMA	4.47

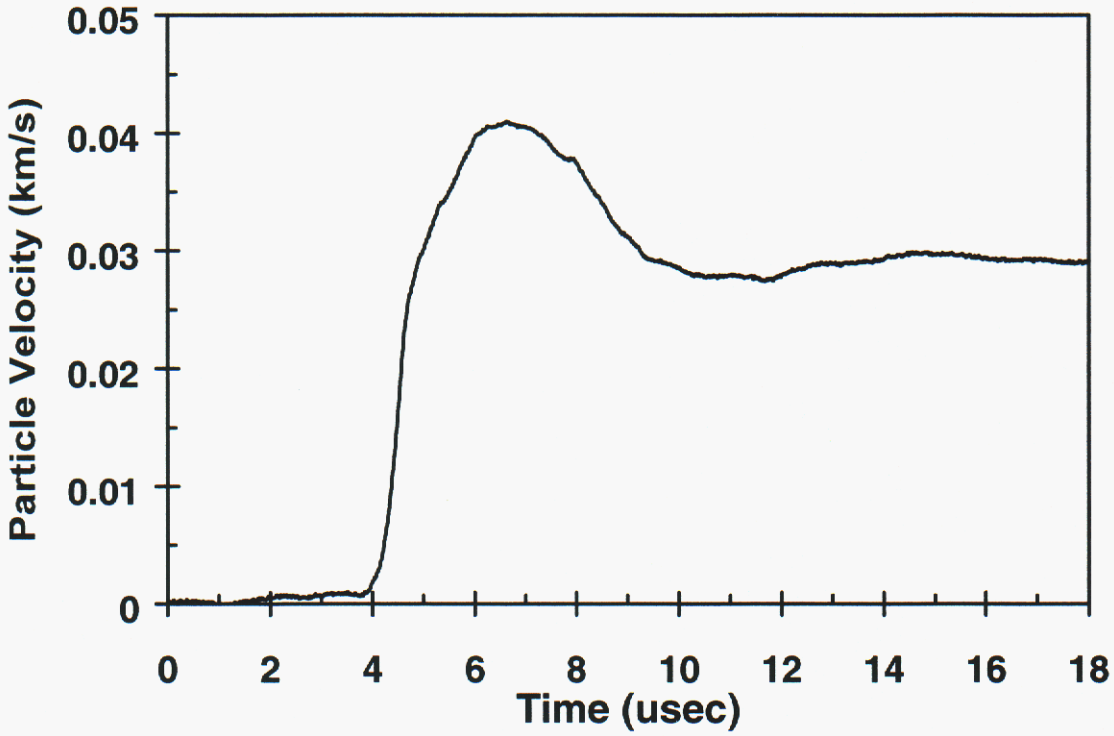

Figure 58. Shot Number: CS15

Shot Number:CS16

Impact Velocity: 0.070 km/s
Concrete Density: 2356 kg/m^3

	Material	Thickness (mm)
Concrete	Small Aggregate	12.71
Impactor	PMMA	4.47
VISAR Window	PMMA	23.86

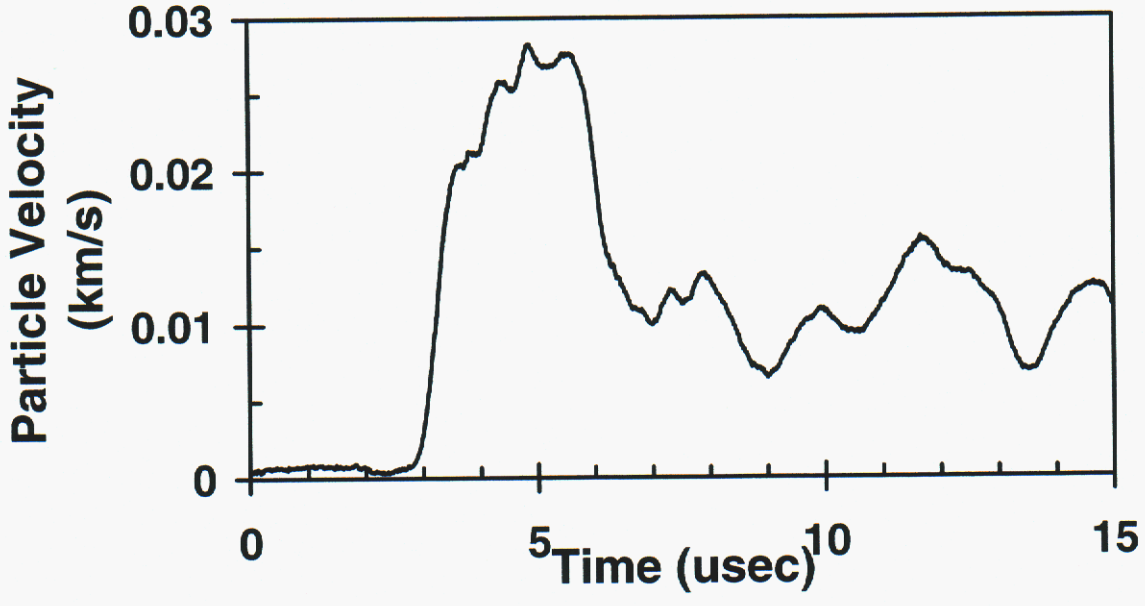

Figure 59. Shot Number: CS16

Shot Number:CS18

Impact Velocity: 0.030 km/s
Concrete Density: 2332 kg/m^3

	Material	Thickness (mm)
Concrete	Small Aggregate	12.73
Impactor	PMMA	4.47

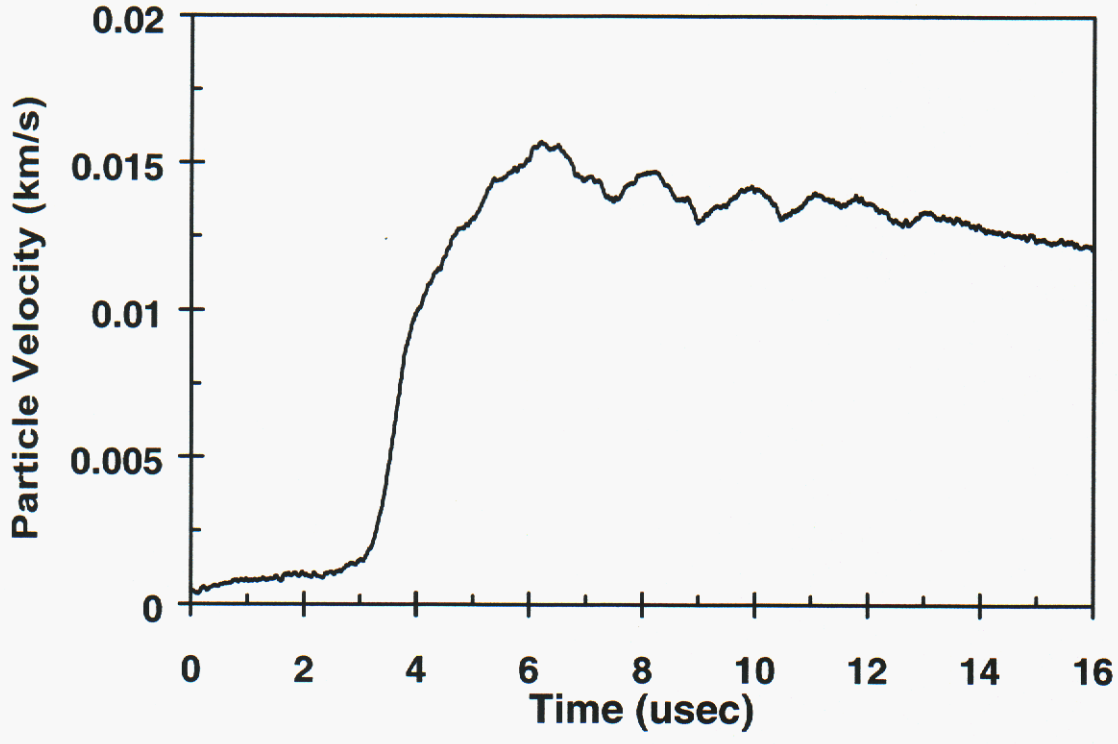

Figure 60. Shot Number: CS18

Shot Number:CS19

Impact Velocity: 0.029 km/s
Concrete Density: 2331 kg/m^3

	Material	Thickness (mm)
Concrete	Large Aggregate	12.73
Impactor	PMMA	4.48

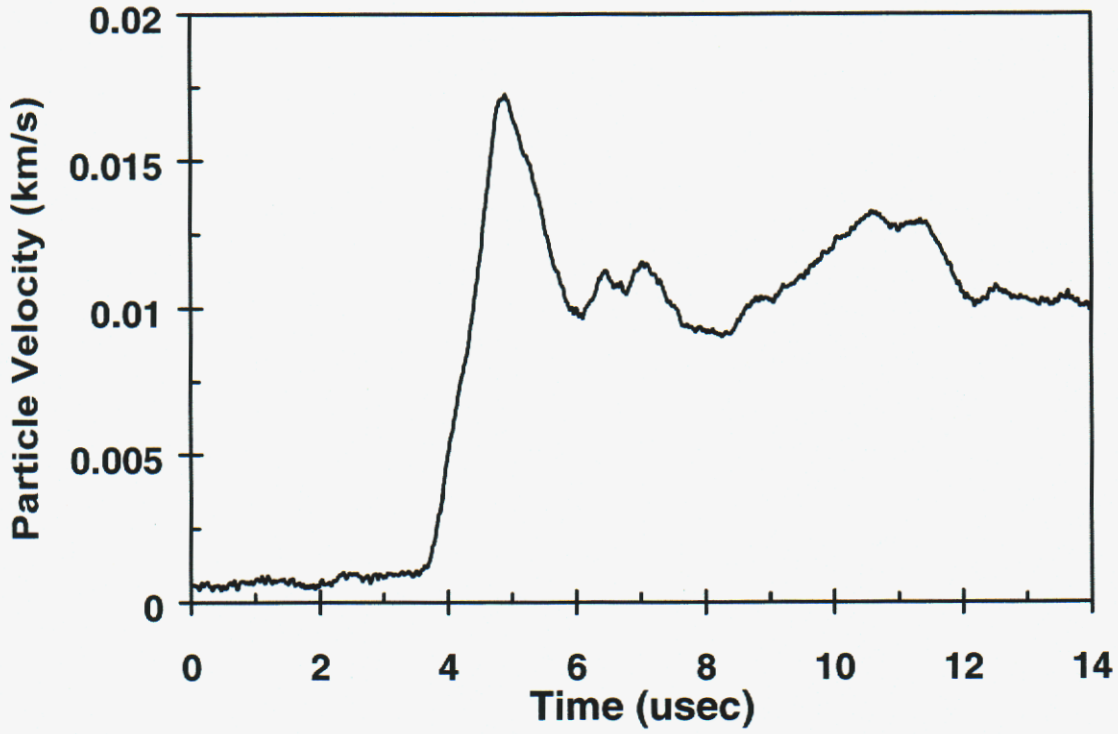

Figure 61. Shot Number: CS19

Intentionally Left Blank

REFERENCES

Barker, L.M., and R.E. Hollenbach, (1970).

Barker, L.M., and R.E. Hollenbach, *Laser Interferometer for Measuring High Velocities of any Reflecting Surface,* J. Appl. Phys., 43, 4669 (1972).

Chhabildas, L.C. and D.E. Grady, *Dynamic Material Response of Quarts at High Strain Rates,* Mat. Res. Symp. Proc., Elsevier, 22, 147-150 (1984).

Crawford, D. A., in Joint DoD/DOE Munitions Technology Development Program Annual Report for FY93, W.K. Tucker, ed., Sandia National Laboratories Report SAND94-1151, June (1994).

Ehrgott, J., *SAC-5 Concrete*, Waterways Experimental Station, Memorandum for Record, CEWES-SP-O, March 12 (1993).

Grady, D.E., *Impact Compression Properties of Concrete*, Proceedings of the Sixth International Symposium on Interaction of Nonnuclear Munitions with Structures, Panama City Beach, Florida, pp. 172-175, May 3-7, (1993a).

Grady, D.E., *Further Shock Compression Data on Concrete*, Sandia Technical Memorandum, unpublished, July (1993b).

Grady, D.E., *Shock Release Experiments on SAC-5 and CSPC Concrete*, Sandia Technical Memorandum, unpublished, September (1993c).

Grady, D.E., *Shock Compression Profiles in SAC-5 Concrete*, Sandia National Laboratories, Interdepartmental Technical Memorandum, TMDG0493. November, 1993 (1993c).

Grady, D.E., *Shock and Release for SAC-5 Concrete 25 GPa*, Sandia Technical Memorandum, TMDG0595, October (1995).

Grady, D.E., R.E. Hollenbach, K.W. Schuler, J.F. Callender, *Strain Rate Dependence in Dolomite Inferred from Impact and Static Compression Studies*, J.Geophys. Res., 82, 1325 (1977).

Grady, D.E. and M.D. Furnish, *Shock and Release Wave Properties of MJ-2 Grout*, Sandia National Laboratories Rept., SAND88-1642, December (1988).

Grady, D.E., *Impact Compression Properties of Concrete*, Proceedings of the Sixth International Symposium on interaction of Nonnuclear Munitions with Structures, Panama City Beach, Florida, pp. 172-175, May 3-7 (1993a).

Grady, D.E., *Further Shock Compression Data on Concrete*, unpublished, Sandia National Laboratories Technical Memo, dated July, 1993 (1993b).

Hall, C.A., L. C. Chhabildas, W. D. Reinhart, *Shock Hugoniot and Release in Concrete with Different Aggregate Sizes from 3 to 23 GPa*, Int. J. Imp. Engng., 23, pp. 341-351 (1999)

Hall, C.A., L. C. Chhabildas, W. D. Reinhart, *Shock Hugoniot and Release States in Concrete Mixtures with Different Aggregate sizes from 3 to 23 GPa. in Shock Compression of Condensed Matter*, edits by Schmidt, Dandekar, Forbes, 1997, (1998)

Kipp, M. E., L. C. Chhabildas, W. D. Reinhart, *Elastic Shock Response and Spall Strength of Concrete, in Shock Compression of Condensed Matter – 1997*, edited by Schmidt, Dandekar, Forbes, Am. Institute Physics (1998).

Lysne, P.C., R.R. Boad, C.M. Percival and O.E. Jones, *Determination of Release Adiabats and Recentered Hugoniot Curves by Shock Reverberation Techniques*, J. Appl. Phys., 40, 3786 (1969).

Grady, D.E. *Shock Equation of State Properties of Concrete*, in Structures Under Shock and Impact IV, N. Jones, C. Brebbia, A. Watson ets., Computational Mechanics Publication pp.405-414 (1996)

Olsson, W.A., *Preliminary Hopkinson Bar Data on SAC-5 and CSPC Concrete*, unpublished (1993).

W. D. Reinhart, L. C. Chhabildas, M. E. Kipp, *Spall Strength Measurements of Concrete for Varying Aggregate Sizes*, published in Proceedings 15th US Army Symposium on Solid MechanicsMyrtle Beach, South Carolina, April 12-14, (1999).

Rosenberg, J.T. and T.J. Ahrens, ASME Paper No. 66-WA-/PT-7, Amer. Soc. Mech. Eng., New York, December (1966).

Silling, S.A., private communication (1995).

Sinz, K., private communication (1995).

DISTRIBUTION

1 102 Stevens Forrest Professional Center
Attn: M.L. Alme
9650 Santiago Road
Columbia, MD 21045

1 46 OG/OGM
Project Engineer
Attn: Ian S. Talbot
205 W. D Ave Suite 241
Eglin AFB, FL 32542-6866

1 ACTA
Attn: Ronald Lambert
Building 7015, Section 3C
Vandenberg AFB, CA 93437

1 Advanced Research Projects Agency
Land Systems Office
Attn: R. W. Kocher
3701 North Fairfax Drive
Arlington, VA 22203-1714

1 Advatech Pacific Inc.
Attn: Jay Ebersohl
PO Box 1376
San Bernardino, CA 92402-1376

1 Aerojet Propulsion Division
Attn: Bounmy Chhouk
Department 5215
P.O. Box 13222
Sacramento, CA 95813-6000

2 Air Force Research Laboratory
Attn: Kenneth B. Milligan, MNAC
Molly Hughes, MNMW
101 West Eglin Blvd.
Eglin AFB, FL 32542-6810

1 Air Force Institute of Technology/ENP
Attn: Kirk A. Mathews
2950 P Street -- Bldg 640
Wright-Patterson AFB, OH 45433-7765

1 Air Force Research Laboratory
Attn: Guy C. Spitale
3550 Aberdeen Ave SE
Kirtland AFB, NM 87117-5776

1 Air Force Wright Aeronautical Labs.
Air Force Systems Command
Materials Laboratory
Attn: T. Nicholas
Wright-Patterson AFB, OH 45433

1 Alliant TechSystems
Attn: Frederick Stecher
600 2nd Street NE (MN11-2720)
Hopkins, MN 55343

1 AlliedSignal
Federal Manufacturing and Technology Group
Attn: Ted Rupp
3500 Trinity Dr., Suite C3
Los Alamos, NM 87544

1 Applied Research Associates
Attn: David J. Stevens
1846 Lockhill-Selma Road, Suite 107
San Antonio, TX 78213

1 Army Missile Command
AMSMI-RD-ST-WF
Attn: D. Lovelace
Redstone Arsenal, AL 35898-5240

1 AZ Technologies
Attn: Craig Schmitz
4901 Corporate Drive, Suite 101
Huntsville, AL 35805

1 Battelle Memorial Institute
Attn: Dale Trott
201-2693
505 King Ave.
Columbus, OH 43201-2693

1 Boeing Corporation
Attn: Kevin Housen
MS 8H-05, 18.03
P. O. Box 3999
Seattle, WA 98124

1 Boeing North America/Rocketdyne Division
Attn: N. A. Louie
Mail Stop EB63
PO Box 7922
Canoga Park, CA 91309-7922

1 Brookhaven National Laboratory
National Synchrotron Light Source
Attn: Paul A. Montanez
Bldg. 725D
Upton, NY 11973-5000

1 Brown University
Division of Engineering
Attn: R. Clifton
Providence, RI 02912

1 California Institute of Technology
Graduate Aeronautical Laboratories
Associate Professor of Aeronautics
Attn: Joseph E. Shepherd
MS 105-50
Pasadena, CA 91125

1 California Institute of Technology
Seismological Laboratory 252-21
Attn: Sarah T. Stewart-Mukhopadhyay
Pasadena, CA 91125

1 CERCOM, Inc.
Attn: R. Palicka
1960 Watson Way
P. O. Box 70
Vista, CA 92083

1 CIA/OSWR
Attn: John Walton
Washington, DC 20505

1 Combustion Research and
Flow Technology, Inc.
Attn: Brian J. York
PO Box 1150
Dublin, PA 18917

1 Commander: U.S. Army TACOM
AMSTA-TR-R MS 263
Attn: Krishan D. Bishnoi
Warren, MI 48397-5000

1 Concurrent Technologies Corp.
Attn: Glenn Nickodemus
1450 Scalp Ave.
Johnston, PA 15904

1 Dominca
Attn: Nancy Winfree
12111 Ranchitos Rd NE
Albuquerque, NM 87122

1 DOW Chemical USA
Attn: K. Epstein
Ordnance Systems, 800 Building
Midland, MI 48667

2 Phillips Laboratory
PL/WSSD
Attn: F. Allahdadi
David F. Medina
Kirtland AFB, NM 87117-6008

1 Plattsburgh State University
Department of Physics
Attn: Paul P. Szydlik
101 Broad Street
Plattsburg, NY 12901-2681

1 Raytheon TI Systems
Warhead/Fuze Systems Manager
Attn: Stoney Stonebraker
PO Box 405 MS 3468
Lewisville, TX 75067

1 Rockwell International Corp.
Rocketdyne Division
Attn: Dennis W. Kneff
6633 Canoga Avenue
Canoga Park, CA 91304

1 Rockwell Science Center
Attn: S. V. Ramakrishnan
1049 Camino Dos Rios
Thousand Oaks, CA 9136

1 SAIC
Attn: Wilford Smith
4901 Olde Towne Parkway, Suite 200
Marietta, GA 30068

1 S-Cubed
Attn: Gerry Gurtman
P.O. Box 1620
La Jolla, Ca.92037

1 Simula Inc.
Attn: J. W. Coltman
10016 South 51st Street
Phoenix, AZ 85044

1 Southwest Research Institute
Attn: James Walker
P. O. Drawer 28510
San Antonio, TX 78228-0510

1 Svedrup Technology
Attn: Nick Yakaboski
Building 260
PO Box 1935
Eglin AFB, FL 32542

1 Brown University
Division of Engineering
Attn: R. Clifton
Providence, RI 02912

1 California Institute of Technology
Graduate Aeronautical Laboratories
Associate Professor of Aeronautics
Attn: Joseph E. Shepherd
MS 105-50
Pasadena, CA 91125

1 California Institute of Technology
Seismological Laboratory 252-21
Attn: Sarah T. Stewart-Mukhopadhyay
Pasadena, CA 91125

1 CERCOM, Inc.
Attn: R. Palicka
1960 Watson Way
P. O. Box 70
Vista, CA 92083

1 CIA/OSWR
Attn: John Walton
Washington, DC 20505

1 Combustion Research and
Flow Technology, Inc.
Attn: Brian J. York
PO Box 1150
Dublin, PA 18917

1 Commander: U.S. Army TACOM
AMSTA-TR-R MS 263
Attn: Krishan D. Bishnoi
Warren, MI 48397-5000

1 Concurrent Technologies Corp.
Attn: Glenn Nickodemus
1450 Scalp Ave.
Johnston, PA 15904

1 Dominca
Attn: Nancy Winfree
12111 Ranchitos Rd NE
Albuquerque, NM 87122

1 DOW Chemical USA
Attn: K. Epstein
Ordnance Systems, 800 Building
Midland, MI 48667

1 DynaEast Corporation
Attn: William Clark
3620 Horizon Drive
King of Prussia, PA 19104

1 Dynetics
Attn: Allen Stults
P.O. Drawer B
1000 Explorer Blvd.
Huntsville, AL 35814-5050

1 Enig Associates, Inc.
Attn: Julius W. Enig
11120 New Hampshire Ave., Suite 500
Silver Spring, MD 20904-2633

1 FMC Corporation
Ground Systems Division
Attn: J. D. Morrow
1107 Coleman Avenue Box 367
San Jose, CA 95103

1 Foils Engineering
Attn: Marshall B. Eck
25731 Ridge Road
Damascus, MD 20872

1 General Dynamics Electric Boat Division
Attn: Chris Abate, MS D5-4
7500 Eastern Point Road
Groton, CT 06340-4989

1 General Dynamics
Attn: James Eridon
Mail Zone 439-01-07
P. O. Box 2094
Warren, MI 48090-2094

1 Hughes Aircraft Company
Radar Systems Group
RE/R2/V524
Attn: T. E. Wong
P.O. Box 92426
Los Angeles, CA 90009-2426

1 Hughes Missile Systems Co.
Attn: David Campbell
Bldg 805 MS C4
PO Box 11337
Tucson AZ, 85734

1 IIT Industries
Attn: Sheldon Jones
P. O. Box 15012
Colorado Springs, CO 80935-5012

1 Institute for Defense Analyses
Attn: Bohdan Balko
1801 North Beauregard Street
Alexandria, VA 22311

1 International Research Associates
Attn: Dennis L. Orphal
4450 Black Ave., Suite E
Pleasanton, CA 94566

1 James L. Thompson
Attn: AMSTA-RSS,
Warren, MI 48397-5000

1 Kaman Sciences Corporation
Attn: Nasit Ari
P. O. Box 7463
Colorado Springs, CO 80933

1 KTech
Attn: Doug Reeder
901 Pennsylvania Ave., N.E.
Albuquerque, NM 87110

1 Lanxide Armor Products, Inc.
Attn: K. T. Leighton
1300 Marrows Road
P. O. Box 6077
Newark, DE 19714-6077

1 LM Aeronautical Systems Company
Department 73-CC2, Zone 0648
Attn: Bharat M. Shah
86 South Cobb Drive
Marrietta, GA 30063

1 Lockheed Martin Idaho Tech - INEL
Attn: Henry Chu
M/S 0206
P.O. Box 1625
Idaho Falls, ID 83415-0206

1 Lockheed Martin Launching Systems
VLS Loading Dock
Attn: Larry Barisciano
103 Chesapeake Park Plaza
Baltimore, MD 21220-0931

1 Lockheed Martin Missiles Space
Attn: Erik Matheson
Organization V2-10 Building 157
P. O. Box 3504
Sunnyvale, CA 94089-3504

1 Lockheed Martin Shunk Works
Department 2512
Attn: Dewey Wong
Building 611
Palmdale, CA 93599

1 Lockheed Martin Tactical Defense
Systems
Attn: Gregg K. Fenton
1210 Massillon Road
Akron, OH 44315-0001

1 Lockheed Martin Vought Systems
Senior Engineering Specialist - Lethality
Attn: Kenneth W. Havens
P.O. Box 650003 M/S EM-36
Dallas, TX 75265-0003

1 Lockheed Martin
Attn: Allen Hagan
MP 544
5600 Sand Lake Road
Orlando, FL 32819-8907

1 Logicon RDA
Attn: William R. Espander
P.O. Box 9377
Albuquerque, NM 87119-9377

1 MEVATEC
Attn: Steve Clark
1525 Perimeter Parkway, Suite 500
Huntsville, AL 35806

1 Military Technology, Inc.
Attn: Mitchell D. White
6767 Old Madison Pike NW
Building 2, Suite 200
Huntsville, AL 35806

2 NASA Johnson Space Center
Attn: Eric L. Christiansen, Mail Code SN3
Justin H. Kerr, Mail Code SN3
Houston, TX 77058

2 NASA Langley Research Center
Attn: Carl Poteet, MS 396
Scott A. Hill, MS 431
Hampton, VA 23681-0001

1 Naval EOD
Technology Division
Code 6021A
Attn: Richard Gold
Indian Head, MD 20640-5070

1 Naval Facilities Service Center
Waterfront Structures Division
Attn: Kevin Hager
560 Center Drive
Port Hueneme, CA 93043

1 Naval Research Laboratory
Attn: F. Zerilli
Washington,DC 20375

1 Naval Surface Warfare Center
Code 614
Attn: John McKirgan
9500 MacArthur Blvd.
West Bethesda, MD 20817-5700

2 Network Computing Services, Inc.
AHPCRC
Attn: Gordon R. Johnson
Tim Holmquist
1200 Washington Avenue South
Minneapolis, MN 55415

1 New Mexico Tech
Attn: Robert Abernathy, EMRTC
Socorro, NM 87801

1 NMSU
Department of Mechanical Engineering
Department 3450
Attn: Ian H. Leslie
Box 30001
Las Cruces, NM 88003

1 NSWC-IH
Code 90
Attn: Thomas P. Russell
101 Strauss
Indian Head, MD 20640

1 Oak Ridge National Laboratory
Attn: Rusi Taleyarkhan
MS 8058
P. O. Box 2009
Oak Ridge, TN 37831-8058

1 Pantex
Attn: Kurtis Kuhrts
Building 11-2
P. O. Box 30020
Amarillo, TX 79177

2 Phillips Laboratory
PL/WSSD
Attn: F. Allahdadi
David F. Medina
Kirtland AFB, NM 87117-6008

1 Plattsburgh State University
Department of Physics
Attn: Paul P. Szydlik
101 Broad Street
Plattsburg, NY 12901-2681

1 Raytheon TI Systems
Warhead/Fuze Systems Manager
Attn: Stoney Stonebraker
PO Box 405 MS 3468
Lewisville, TX 75067

1 Rockwell International Corp.
Rocketdyne Division
Attn: Dennis W. Kneff
6633 Canoga Avenue
Canoga Park, CA 91304

1 Rockwell Science Center
Attn: S. V. Ramakrishnan
1049 Camino Dos Rios
Thousand Oaks, CA 9136

1 SAIC
Attn: Wilford Smith
4901 Olde Towne Parkway, Suite 200
Marietta, GA 30068

1 S-Cubed
Attn: Gerry Gurtman
P.O. Box 1620
La Jolla, Ca.92037

1 Simula Inc.
Attn: J. W. Coltman
10016 South 51st Street
Phoenix, AZ 85044

1 Southwest Research Institute
Attn: James Walker
P. O. Drawer 28510
San Antonio, TX 78228-0510

1 Svedrup Technology
Attn: Nick Yakaboski
Building 260
PO Box 1935
Eglin AFB, FL 32542

1 Sverdrup Technology Inc., AEDC Group
Attn: Mark Smith
740 Fourth Street
Arnold AFB, TN 37389-6001

1 Talley Defense Systems
Attn: Jon Conner
P.O. Box 849
Mesa, Arizona 85211

1 TASC, Inc.
Attn: Charles Drutman
5500 Walkers Brook Drive
Reading, MA 01940

1 Teledyne Brown Engineering
Attn: Burton S. Chambers III
M/S 66
PO Box 070007
Huntsville, AL 35807-7007

1 Texas A&M University
Nuclear Engineering Dept.
Zachry Building, Room 129
Attn: Bruce L. Freeman
Mail Stop 3133
College Station, Texas 77843-3133

1 Texas Tech University
Department of Mechanical Engineering
Attn: Darryl James
Box 41021
Lubbock, TX 79409-1021

1 The Aerospace Corporation
Attn: R. B. Pan
M/S: M4/920
P. O. Box 92957
Los Angeles, CA 90009-2957

1 The Ensign-Bickford Company
Attn: Kevin Duprey
660 Hopmeadow Street
Simsbury, CT 06070-0483

2 The University of Texas at Austin
Institute for Advanced Technology
Attn: Stephan J. Bless
David Littlefield
3925 W. Braker Lane, Suite 400
Austin, TX 78759

2 Thiokol Corporation
Science & Engineering Division
Attn: Dwight Clark, MS 280
Robert L. Hatch, MS 244
P. O. Box 707
Brigham City, Utah 84302-0707

1 Timothy W. Moore
PO Box 12273
Huntsville, AL 35815

1 Tracor Aerospace Inc.
Mine/Countermine Division
Attn: Mark Majerus
1400 Peoples Plaza, Suite 233
Newark, DE 19702

1 U. S. Army ARDEC
SMCAR-AEE-WW - Bldg. 3022
Attn: Chuck Chin
Picatinny Arsenal, NJ 07806-5000

1 U. S. Army ARDEC
AMSTA-AR-WEE-C
US Army TACOM-ARDEC
Attn: Ernest L. Baker, B3022
Picatinny Arsenal, NJ 07806-5000

1 U. S. Army Corps Engineers
CEMRO-ED-SH
Attn: William Seipel
215 North 17th Street
Omaha, NE 68102

1 U. S. Army Engineering Division
CEHND-ED-SY
Attn: John Tipton
P.O. Box 1600
Huntsville, AL 35807-4301

1 U. S. Army MICOM
Attn: Scott Howard
Bldg. 5400, Room B-314
Redstone Arsenal, AL 35898-5247

1 U. S. Army Natick Research and
Development Center
SATNC-IB
Attn: Philip Cunniff
Kansas Street
Natick, MA 01760-5019

1 UDLP MS M443
Attn: Jerome Glaser
4800 East River Road
Minn., MN 55421

1 University of Alabama in Huntsville
University of Missouri-Rolla
CE Department
Attn: William Schonberg
Rolla, MO 65409

1 University of Arizona
Professor of Planetary Science
Attn: H. J. Melosh
Tucson, AZ 85721

1 University of Hawaii
Mineral Physics Group
Attn: M. Manghnani
2525 Correa Rd.
Honolulu, HA 96822

1 University of Illinois
NCSA
Attn: LeRay Dandy
Urbana Champaign, IL

1 University of Notre Dame
Department of Aerospace and Mechanical
Engineering
Attn: Joseph M. Powers
372 Fitzpatrick Hall of Engineering
Notre Dame, Indiana 46556-5637

1 University of Texas
Department of Mechanical Engineering
ETC 5.160
Attn: Eric P. Fahrenthold
Austin, TX 78712

1 University of Washington
Department of Aeronautics and Astronautics
Attn: Keith A. Holsapple, FS10
Seattle, WA 98195

1 US Army Space & Missile Defense Command
Attn: Robert Becker, SMDC-TC-WL
PO Box 1500
Huntsville, AL 35807-3801

1 USA CRREL
Attn: Jerome B. Johnson
PO Box 35170 (Building 4070)
Ft. Wainwright, AK 99701

3 USAE Waterways Experiment Station
Attn: Mark D.Adley
Byron J. Armstrong
Tommy Bevins
3909 Halls Ferry Rd
Vicksburg, MS 39180

1 UTEP
FAST Center for Structural Integrity of
Aerospace Systems
Attn: Roberto A. Osegueda
500 West University Avenue
El Paso, TX 79968

1 Washington State University
Institute for Shock Physics
Attn: Y. M. Gupta
Box 642816
Pullman, WA 99164-2816

3 Wright Laboratory
WL/MNSA
Attn: Dan Brubaker
William Cook
Bruce C. Patterson
Eglin AFB, FL 32542- 5434

1 Army Research Office
Senior Reserach Scientist
Attn: Arunachalam M. Rajendran , , ,
RTP, NC 27709-2211

15 Kerley Technical Services
Attn: Gerald I. Kerley, Consultant
P.O. Box 709
Appomattox, VA 24522-0709

24 Army Research Laboratory
Weapons Technology Directorate
AMSRL-WT
Attn: W. J. Bruchey
G. Bulmash
D. Dandekar
J. Dehn
G. Filbey, Jr.
K. Frank
G. Gazonas
W. Gillich
W. Gooch
F. Gregory
A. D. Gupta
C. Hubbard
K. Kimsey
P. Kingman
R. Lottero
H. W. Meyer
A. Prakash
G. Randers-Pehrson
E. Rapacki
D. Scheffler
M. Scheidler
S. Segletes
J. Starkenberg
T. Wright
P.O. Box 334, Main Station
Aberdeen Proving Ground, MD 21005-5066

2 Naval Surface Warfare Center
Indian Head Division
Attn: J. Burns, 4220
G. T. Sutherland, 9230E
101 Strauss Avenue
Indian Head, MD 20640-5035

2 Southwest Research Institute
Attn: C.E. Anderson
J. Lankford
6220 Culebra Road
San Antonio, TX 78284

2 U.S. Air Force Armament Laboratory
AD/MNW
Attn: J. A. Collins
J. C. Foster, Jr.
Eglin Air Force Base, FL 32542-5434

2 Univ. of Calif. at San Diego
Dept. of Applied Mech. & Eng. Sciences
Attn: M. Meyer
S. Nemat-Nasser
La Jolla, CA 92093

2 U.S. Army Research Office
Attn: J.A. Bailey
K. Iyer
P. O. Box 12211
Research Triangle Park, NC 27709

3 California Institute of Technology
Attn: T. J. Ahrens, MS/252-21
Geophysics Division
G. Ravichandran, MS 105-50
Graduate Aeronautical Laboratories
Pasadena, CA 91125

4 Applied Research Associates
Attn: P. T. Dzwilewski
K. Edquist
L. Brown
G. Recht
5941 South Middlefield Rd., Suite 100
Littleton, CO 80123

9 Applied Research Associates, Inc
Attn: D. E. Grady
B. L. Bingham
C. Scheffield
Craig Dolittle
4300 San Mateo Blvd. NE, Suite A-220
Albuquerque, NM 87110

6 Naval Air Warfare Center
Attn: E. Cykowski, C2746
J. Gill
J. Kandell
A. Lindfors
K. Minnick, C3261
P. J. Miller
1 Administrative Circle
China Lake, CA 93555

8 Naval Surface Warfare Center
Dahlgren Division
Attn: J. R. Cogar, G22
R. K. Garrett, Jr, G24
M. Hobson, G22
W. Holt, G24
W. Mock, Jr., G24
D. F. Robinson, G24
D. Vavrick, G22
L. T. Wilson, G24
R. Gamache, G22
17320 Dahlgren Rd.
Dahlgren, VA 22448

12 University of California
Lawrence Livermore National Laboratory
Attn: D.W. Baum, L-35
Cauble, MS L-041
N. C. Holmes, MS L-050
D. Lassila, L-35
Maiden, MS L-010
B. Moran, MS L-170
R.M. More, MS L-321
W. J. Nellis, MS L-050
P. C. Souers, MS L-282
D. A. Young, MS L-299
Doug Faux, MS L-140
M. Gerassimenko, MS L-183
7000 East Ave.
P.O. Box 808
Livermore, CA 94550

13 Los Alamos National Laboratory
Attn: T.F. Adams, MS F663
J. Boettger, MS B221
G. T. Gray, MS G755
R. Gustavsen, MS P952
R. S. Hixson, MS P952
B. L. Holian, MS J569
J. D. Johnson, MS B221
J. N. Johnson, MS B221
J. E. Kennedy, MS P950
D. Mandell, MS F663
J. Richey, MS B214
S. Sheffield, MS P952
Yasuyuki Horie, MS D413 X-7
Mail Station 5000
P.O. Box 1663
Los Alamos, NM 87545

1 MS 0130 J. Polito, 2800
1 0139 R. K. Thomas, 9904
1 0310 J. A. Ang, 9220
1 0316 S. S. Dosanjh, 9233
1 0318 M. B. Boslough, 9212
1 0318 P. Yarrington, 9320
1 0321 W. J. Camp, 9200
1 0521 S. T. Montgomery, 2561
1 0801 A. L. Hale, 9300
1 0819 E. A. Boucheron, 9231
1 0819 K. G. Budge, 9231
1 0819 D. E. Carroll, 9231
1 0819 C. J. Garasi, 9231
1 0819 A. C. Robinson, 9231
1 0819 T. G. Trucano, 9211
1 0819 M. K. Wong, 9231
1 0820 P. Chavez, 9232
1 0820 R. E. Cole, 9232
1 0820 A. V. Farnsworth, 9232
1 0820 M. E. Kipp, 9232

1	0820	S. A. Silling, 9232
1	0820	R. M. Summers, 9232
1	0820	P. A. Taylor, 9232
1	0820	J. R. Weatherby, 9232
1	0824	A. C. Ratzel, 9110
1	0835	J. M. McGlaun, 9140
1	0835	J. S. Peery, 9142
1	0836	M. R. Baer, 9100
1	0836	D. Crawford, 9116
1	0836	E. S. Hertel, 9116
1	0836	M. Hobbs, 9116
1	0847	H. S. Morgan, 9120
1	0847	J. W. Swegle, 9142
1	0865	D. R. Martinez, 1902
1	0893	R. M. Brannon, 9123
5	1106	G.A. Mann, 15335
1	1027	E. H. Barsis, 3038
1	1033	J. L. Wise, 6211
1	1134	J. Hickerson, 15414
1	1168	C. Deeney, 1612
1	1168	M. D. Furnish, 1612
1	1174	M. J. Forrestal, 15414
1	1178	Doug Bloomquist, 1630
1	1181	J. R. Asay, 1610
20	1181	L.C. Chhabildas, 1610
1	1181	J. P. Davis, 1610
5	1181	C. A. Hall, 1610
1	1181	M. Knudson, 1610
5	1181	W. D. Reinhart, 1610
1	1185	R. Dukart, 15417
1	1185	Dan Kelly, 15417
1	1185	Bob Weir, 15417
1	1186	Jeff Lawrence, 1674
1	1190	J. P. Quintenz, 1600
1	1191	Keith Matzen, 1670
1	1194	D. H. McDaniel, 1640
1	1411	H. E. Fang, 1834
1	9042	J. J. Dike, 8727
1	9042	M. Horstemeyer, 8728
1	9042	L. E. Voelker, 8727
2	0899	Technical Library, 9616
1	0612	Review and Approval Desk, 9612
1	9018	Central Technical Files, 8945-1